In vitro evaluation of synergistic inhibitory effects of neuraminidase inhibitors and Methylglyoxal against Influenza virus infection

A thesis submitted in partial fulfilment towards Doctor of Philosophy

Degree in Medical Sciences

By

Siriwan Charyasriwong

Laboratory of Molecular Biology of Infectious Agents

Graduate School of Biomedical Sciences

Nagasaki University, Nagasaki, Japan

September 2017

Table of Contents

List of Figures

List of Tables

Abbreviations and Acronyms

ATCC	American Tissue Culture collection
BM2	small integral membrane protein
°C	Degrees Celsius
CC_{50}	50% Cytotoxic concentration
CO_2	Carbon Dioxide
CPE	CytoPathic Effect
DMSO	Dimethyl Sulfoxide
EDTA	Ethylenediaminetetraacetic acid
FBS	Fetal Bovine Serum
h	Hour(s)
HA	Hemagglutinin
H_2O	Water
IC_{50}	50% Inhibitory concentration
IFV	influenza virus
M1	matrix 1
M2	matrix 2
MDCK	Mardin-Darby Canine Kidney
MEM	Minimum Essential Medium
mg	Milligrams
mg/ml	Milligrams/millilitre
MGO	Methylglyoxal

min	Minute(s)
ml	Millilitre
mM	Millimolar
NA	Neuraminidase
NB	The second protein product
NCRs	Non-coding regions
NEP	Nuclear export protein
ng/mL	Nanograms/millilitre
NIID	National Institute of Infection Diseases
NP	Nucleoprotein
NSP1	Non-structural protein 1
NSP2	Non-structural protein 2
PA	Polymerase acidic protein
PB1	Polymerase basic protein 1
PB2	Polymerase basic protein 2
PB1-F2	Polymerase basic protein 1 – F2
PBS	Phosphate Buffered Saline
rpm	Revolutions per minute
sec	Second(s)
SI	Selective index
TCID50	50% Tissue Culture Infective Dose
vRNPs	viral ribonucleoproteins

w/v	Weight per Volume
wt	Weight
WST-1	Water-soluble tetrazolium salt
μM	Micromolar
μg/mL	Micrograms/millilitre
μL	Microlitre

CHAPTER 1: INTRODUCTION

Influenza viruses are enveloped, negative, single-stranded RNA viruses with eight segmented genomes belonging to the *Orthomyxoviridae* family. There are three distinct virus types, A, B and C, distinguished according to their antigenicity to internal protein structures, nucleoprotein (NP) and matrix protein. Influenza A and B viruses are important human respiratory pathogens that cause epidemics with significant disease burden. Influenza A virus easily mutates, which often results in the emergence of new antigenic variants of each subtype. Influenza pandemic is a global outbreak of influenza A viruses that is completely different from current circulating human seasonal influenza viruses. The pandemic influenza virus emerges that can infect human, cause serious illness compared to infected with seasonal influenza viruses, and spread easily from human-to-human. In 1918, the 1918 H1N1 influenza pandemic was first identified. It was the most severe pandemic outbreak in recent history. It spread around the world during 1918-1919 reporting that about 500 million people became infected with this virus and approximately 50-100 million people dead. In 1957, a new influenza H2N2 was found in East Asia, called a pandemic "Asian flu". This virus was composed of three different genes from an H2N2 virus that originated from an avian influenza A viruses. The 1968 pandemic influenza H3N2 was first noted in 1968 composing of the new H3 hemagglutinin and the N2 neuraminidase from the 1957 H2N2 influenza virus. After that, the H3N2 influenza virus continues to circulate worldwide as a seasonal influenza A virus and undergo regular antigenic drift. The latest pandemic influenza virus was reported in 2009 as H1N1 pandemic 2009 influenza virus. This pandemic virus composed of a novel combination of influenza genes that were not detected even in animal or people resulting in spread quickly around the world. The H1N1 pandemic

2009 influenza A virus was generated by gene reassortment between a virus present in pig of north America and a virus that circulates in the swine population of Euroasia. It was significantly different from circulating H1N1 influenza A virus in that time, as a result vaccination with seasonal flu vaccine could not completely prevent people for this pandemic H1N1 influenza virus. The threat of a human influenza pandemic has greatly increased over the past 60 years. The highly pathogenic avian influenza viruses, notably the H5N1 virus, emerged in 1997 [1]. The 2009 pandemic virus (H1N1) quickly spread throughout the world [2], and more recently, human infection with avian influenza virus (H7N9) has been reported [3]. These outbreaks should serve as warnings to responsible agencies to prepare for the next pandemic threat. Recombination occurs in RNA viruses resulting in abundant genetic variability. For influenza viruses, which are negative sense RNA viruses, reassortment has been shown to be common and important mechanism for evolution. This process occurs when two or more different viruses infect the same host cell. The reassortment of different gene segments encoding viral surface proteins, especially HA and NA is related to the evasion of host immunity and the pandemic outbreak termed antigenic shift [4, 5]. Homologous recombination is not common in influenza viruses, but recombination by template switching or copy choice recombination has been reported that it caused changing the virulence of influenza viruses. This process occurs when the RNA polymerase that initiates viral replication switches from one RNA molecule to another molecule, thereby generating viral RNA with mixed ancestry. Although concern regarding influenza B virus infection relative to influenza A in humans has been neglected in the past, Several studies have recently shown that influenza B infection causes similar rates of mortality in some epidemic seasons, especially in children [6, 7]. Clinical reports also have shown that infection by

influenza B viruses tends to induce lethal secondary bacterial infections and myocardial or neurological complications [8-11]. Although influenza B viruses share similar fundamental structural features of this family, these have different characteristics from those of influenza A viruses; for example, the enveloped influenza A viruses have three membrane proteins (HA, NA, M2). On the other hand, influenza B viruses present four proteins in the envelope: HA, NA, NB, and BM2. The NB and BM2 are unique to influenza B viruses. In the same manner to the M2 of influenza A viruses, the BM2 protein is a proton channel that is essential for the uncoating process. The NB is believed to be an ion channel but not be required for viral replication in cell culture but promotes efficient growth *in vivo* such as in mice model [12]. Moreover, the influenza A viruses show a more rapid rate of evolution than that of the influenza B viruses [13]. Thus, it is essential to invent ways to control influenza spreading.

1.1 Influenza A viruses

The Influenza A viruses have eight segments that encode for the 11 viral genes as described below:

Genome segment	Gene length (bp)	Viral protein	Location	Function
1	2341	PB2	Internal	Transcription/capping/replication
2	2341	PB1	Internal	Transcription/replication
		PB1-F2	Nonstructural	Apoptosis
3	2233	PA	Internal	Transcription/replication
4	1778	HA	Transmembrane	Receptor/uncoating
5	1565	NP	Internal	RNA synthesis
6	1414	NA	Transmembrane	Release new virion
7	1027	M1	Internal	Assembly/regulation
		M2	Transmembrane	uncoating
8	890	NS1	Nonstructural	IFN antagonist
		NS2 (NEP)	Internal	Nuclear export

Table 1 Influenza A virus genome structure and function.
[a]PB2 (polymerase basic protein 2); PB1 (polymerase basic protein 1); PB1-F2 (polymerase basic protein 1 – frame2); PA (polymerase acidic protein); HA (hemagglutinin); NP (nucleoprotein); NA (neuraminidase); M1 (matrix protein 1); M2 (matrix protein 2); NSP1 (non-structural protein 1); NS2 (non-structural protein 2, also known as nuclear export protein, NEP)

Influenza A viruses are categorized into subtypes based on two proteins appearing on the viral surface; HA and NA. The major influenza A subtypes that have harmed humans during seasonal epidemics are H1N1 and H3N2. Centers for disease control and prevention, CDC reported that there are 18 known HA subtypes and 11 known NA identified so far. All known subtypes can infect birds except recently found subtypes H17N10 and H18N11, which have been found in bats (updated 20 April 2017).

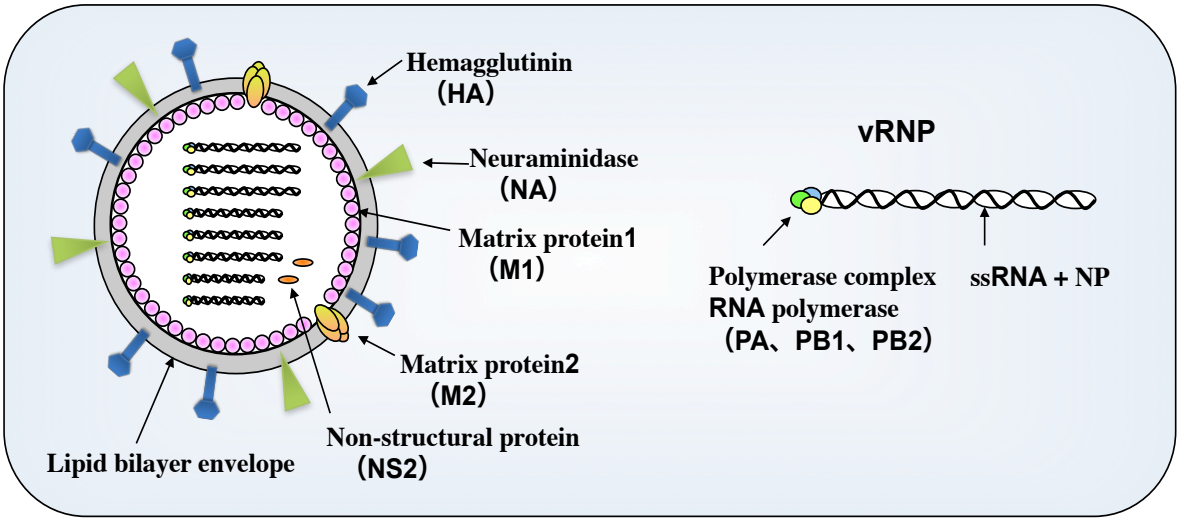

Figure 1 The structure of influenza A virus

The life cycle of influenza viruses can be divided into the following stages [14, 15]:

1) Entry into the host cell; The spikes of HA on the viral membrane bind to sialic acid receptor found on host cell surface. After binding to sialic acid on the host cell, receptor-mediated endocytosis occurs and the virus enters the host cell using endosome called endocytosis.

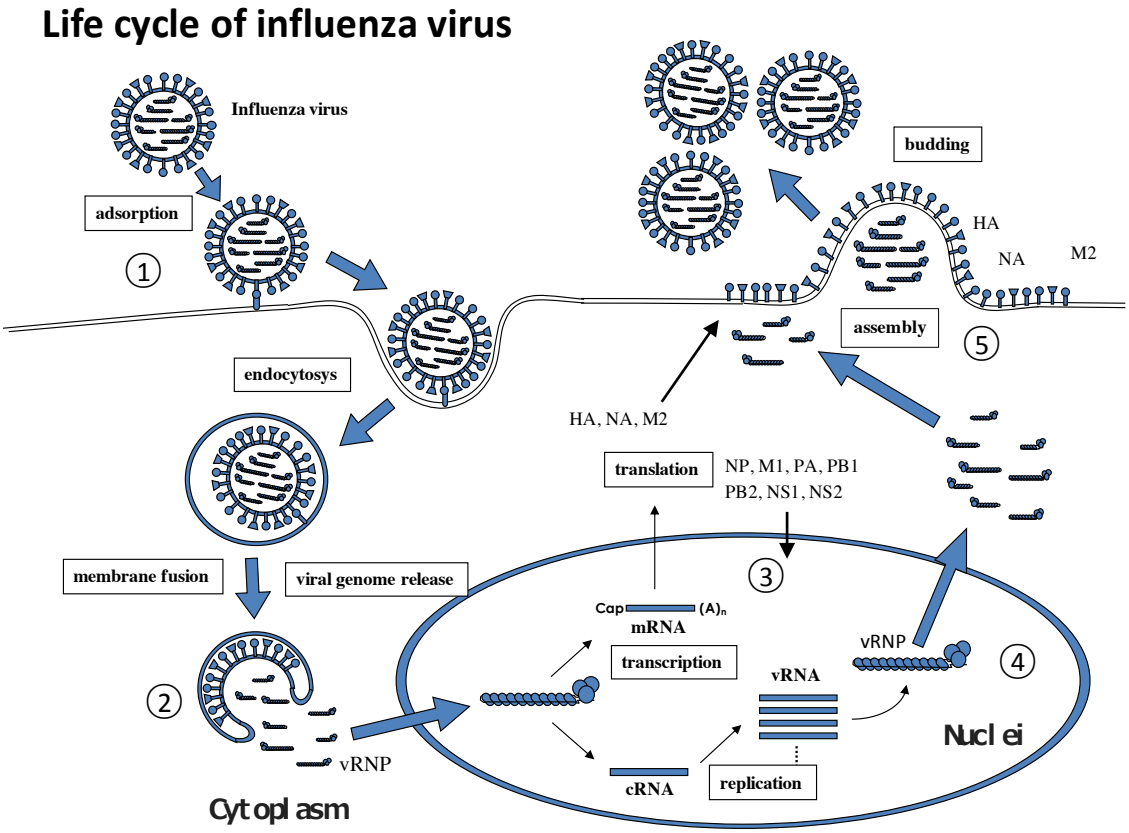

Figure 2 Life cycle of influenza virus

Influenza viruses can enter cells via clathrin-mediated endocytosis. They are internalized mainly in clathrin-coated vesicles (CCVs), but also in non-coated vesicles, suggesting that influenza viruses may utilize many endocytosis pathway, not only chathrin-mediated endocytosis, but also non-chathrin entry route in parallel [16, 17]. After internalization, influenza virus is thought to be trafficked to late endosome, where the acidic environment (pH5) occurs. Rab proteins (cellular GTPases that are recruited

to vesical membranes) and other factors regulate these endocytic compartments, which play an essential role in viral infection. Late endosomes (LEs) are formed from early endosomes (EEs) during their microtubule-dependent transport into the perinuclear region. LEs contain integral membrane proteins such as lysosomal membrane protein and then the pH drops to 4.8-6.0. The switch from EEs to LEs step is regulated by "Rab switch", which Rab5 for EEs is changed to Rab7 for LEs [18].

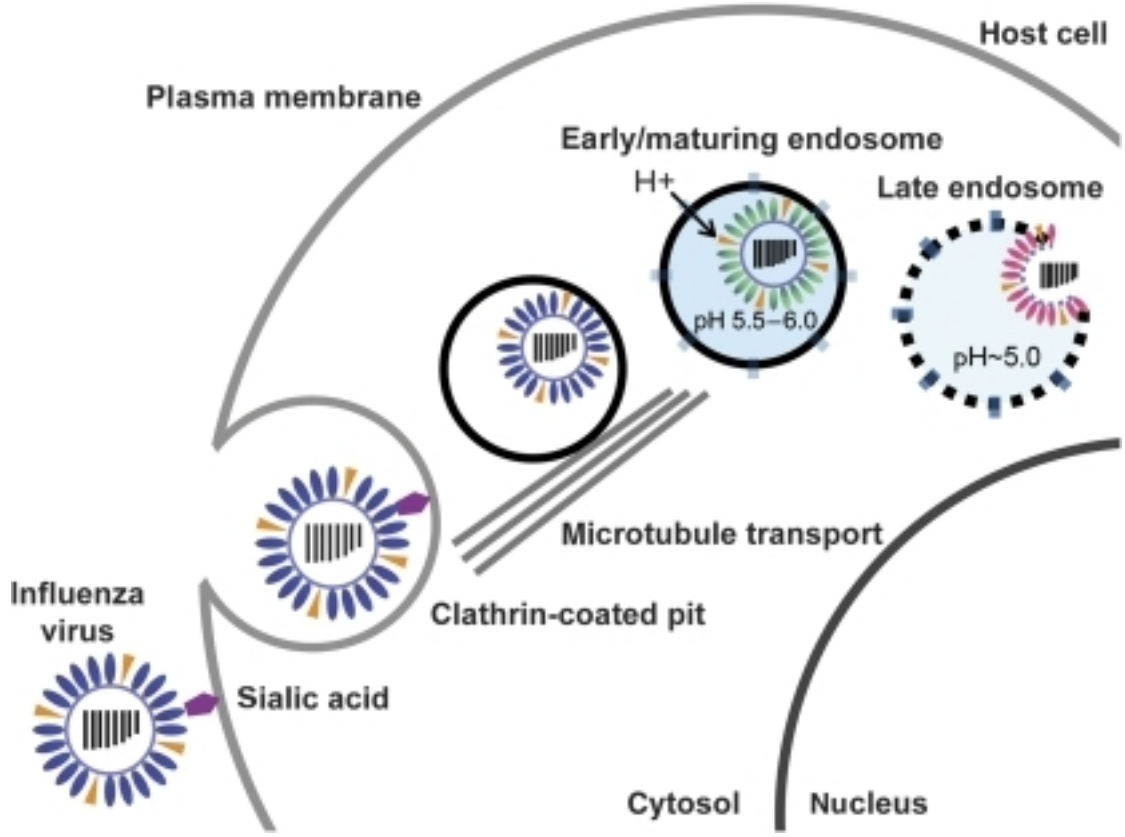

Figure 3 Endocytosis of influenza virus [19]

The endosome has a low pH condition around 5 to 6 due to the activity of the ATP-dependent proton pumps presenting in the membrane of endosome [20], which induces the fusion of the viral and endosome membrane. The low pH initiates change of HA conformation, leading exposing of the HA2 fusion peptide, which insert itself into endosome membrane and start to connect the viral and endosome membrane together. Moreover, the acidic environment of the endosome also is required for open up the M2

ion channel, triggering the release of vRNP from M1 and be prompt to enter the host cell's nucleus.

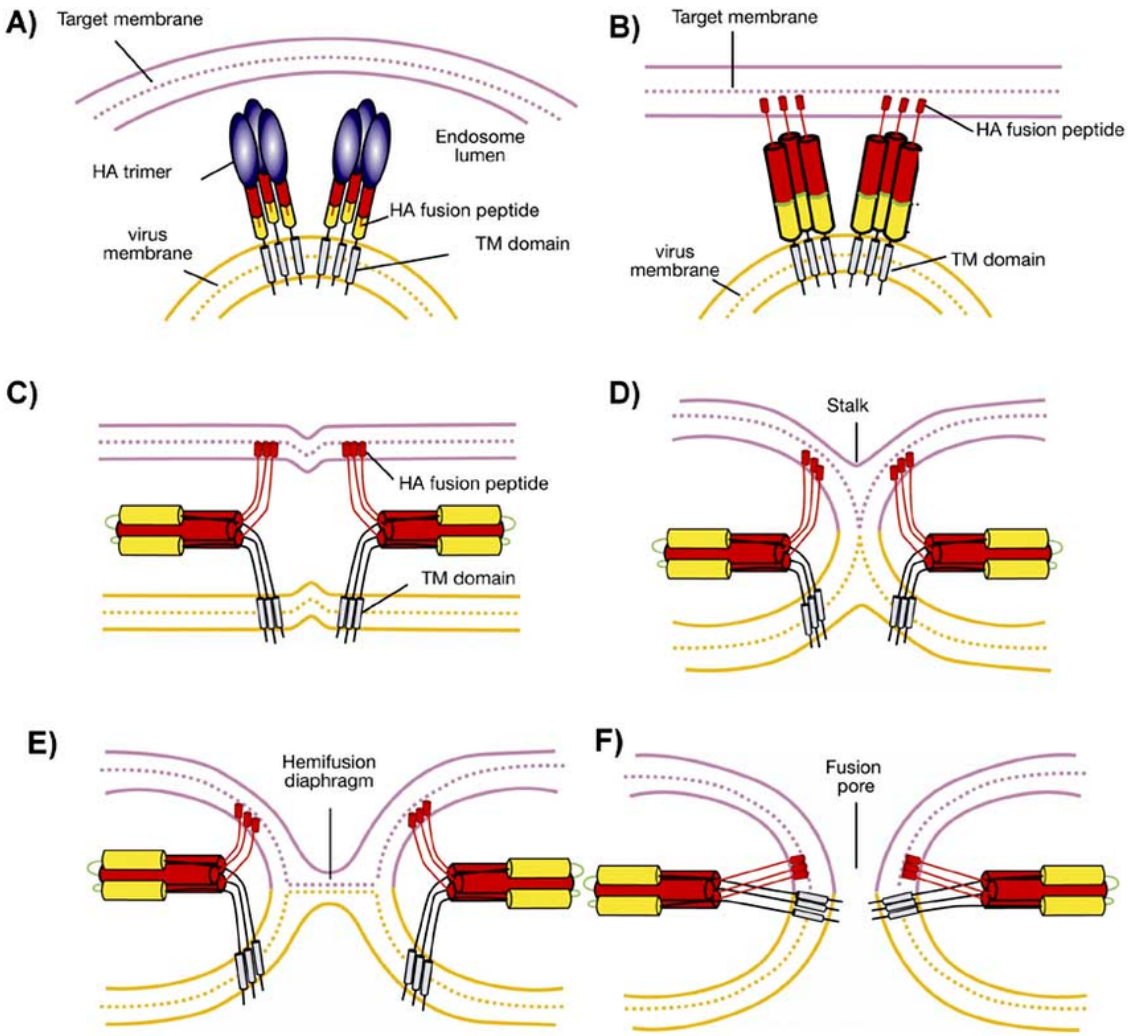

Figure 4 Scheme of a process of membrane fusion between influenza and endosome. (B) Acid-induced HA conformation that allow fusion protein insert into target membrane.[21]

2) Entry of vRNPs into the nucleus; Influenza virus transcription and translation occurs in the nucleus, after being released from M1, the vRNP enter the nucleus. The vRNP composes of a group of viral proteins; NP, PA, PB1, and PB2, having known nuclear localization signal (NLSs) that can bind to the cellular nuclear import machinery (importin), then enter the nucleus through nuclear pore complexes (NPCs). The nuclear pore complexes regulate the exchange of molecules between the nucleus and the

cytoplasm. The active transport of macromolecule between nucleus and cytoplasm is regulated by specific soluble carrier proteins called karyopherins, with those involved in import and export termed importin and exporin, respectively [22, 23]. Importin plays essential role for transporting vRNP into nucleus after binging to NLS signals. Exportin on the other hand plays roles to export molecules from nucleus to cytoplasm by binding NES signals.

3) Transcription and replication of the viral genome; Firstly, negative sense strands of RNA must be conversed into a positive strand for a template for the production of viral RNAs. Interestingly, the viral RNA dependent RNA polymerase (RdRp) is required for initiation RNA synthesis internally on viral viral RNA. The viral RdRp is made up of PB1, PB2, and PA. PB2 has endonuclease activity and bind to 5'methylated caps of cellular mRNA and cleaves the cellular mRNA to acquire the cap structure. This cellular capped RNA fragment is then used to prime viral transcription. Viral mRNA transcription is initiated from the cleaved capped RNA segment at 3'end. Importantly, the NS1 protein play a critical role in suppressing the production of host mRNAs by inhibiting the 3'end processing of host pre-mRNA. The viral RdRp is also responsible for unprimed replication of vRNAs; (-) vRNA –> (+) cRNA –> (-) vRNA.

4) Export of the vRNPs from the nucleus; Viral mRNAs are transported to the cytoplasm and undergo translation. Newly synthesized M1 is transported from the cytoplasm into the nucleus via NLS located in its N-terminal domain (residues 101 to 105). M1 plays an important role for nuclear export of vRNPS. Although M1 does not contain the leucine-rich NES, the N-terminal of M1 binds to C-terminal of NS2 (NEP), which contains the NES. This binding is essential for the nuclear export of vRNP in infected cell[24]. The transport of vRNPs from the nucleus regulated by a M1-NS2

complex that is bound to the vRNPs. It is known that only negative sense vRNPs are exported from nucleus. M1 is found to interact directly with the vRNPs through C-terminal end of the protein. It has been reported that the N-terminal of M1 can bind to NS2 (or NEP), thus masking the NLS, involving in the import of the vRNPs. NS2 also has been shown to interact with human CRM1 protein with the accompanying GTP hydrolysis that exports the vRNPs from the nucleus. It is hypothesized that M1 binds to the negative sense vRNPs, as well as binding to NS2 [24]. It's also reported that heat shock cognate protein 70 (Hsc70) directly bind to M1 at C terminal half of M1 and work for nuclear export of vRNP [25]. The binding of M1 and vRNPs in the cytoplasm also blocks the reentry of vRNPs into the nucleus, which is essential for efficient viral assembly in the next step [26].

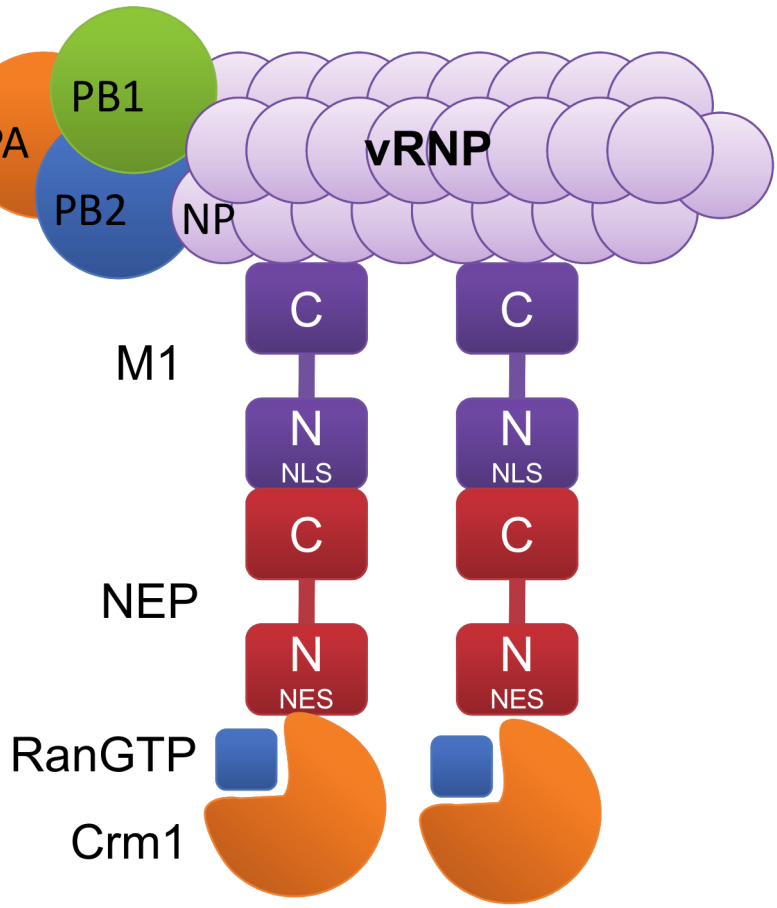

Figure 5 Schematic of the daisy chain model for NEP-mediated nuclear export of vRNP [27]

5) Assembly and budding at the host cell plasma membrane. Since influenza is an enveloped virus, it uses the host cell's membrane to from the viral particles before leave the cell and start infect neighboring cells. Because virus particles bud from apical side, HA, NA, and M2 are transported to the apical plasma membrane. M1, locating underneath the lipid bilayer, is required for the final step of closing and budding out of new virion. The other important step before release new virus particles from infected cell is the cleavage of sialic acid residue from glycoproteins and glycolipids. The HA and NA proteins in new viruses contain sialic acid that would cause the viruses to clump together and stick to the cell surface. The NA cleaves this sialic acid, thereby releasing the virus particle from the host cell surface.

1.2 Influenza B viruses

Influenza B virus found in 1940 was distinct from previous identified influenza A virus. It was isolated from a pediatric patient and named as influenza B/Lee/40[28]. Influenza B viruses also belong to the family of *Orthomyxoviridae*. However, influenza B viruses obtain some features completely different from influenza A viruses so that influenza B viruses were grouped into a different genus. First, the HA and NA surface proteins are antigenically distinct from those of influenza A viruses. Second, both of them contain equal number of gene segments, but they produce different amounts of the protein products and non-coding regions (NCRs). NB is encoded by RNA segment 6, which also encodes NA. The NB is an 11 kDa transmembrane protein with ion channel activity. The influenza B virus RNA segment 7 encodes the BM2 protein. The influenza B virus BM2 protein contains 109 amino acids residues, which contains a hydrophobic region at residue 7-25. The BM2 protein could act as a transmembrane (TM) anchor.

The ion channel protein M2 of influenza A viruses are replaced with the matrix BM2 protein for influenza B viruses so influenza B viruses are resistant to adamantine class of antiviral drugs. The resistance is structurally innate, because adamantine could not bind to the ion pore of BM2 [29]. The rate of evolution and ecology of influenza A and B viruses are also different. The evolution rate of influenza A viruses are found faster than that of influenza B viruses due to a broad host range including a wild aquatic bird reservoir of influenza A viruses[13, 30].

Genome segment	Gene length (bp)	Viral protein	Location	Function
1	2348	PB2	Internal	Transcription/capping/replication
2	2319	PB1	Internal	Transcription/replication
3	2269	PA	Internal	Transcription/replication
4	1833	HA	Transmembrane	Receptor/uncoating
5	1806	NP	Internal	RNA synthesis
6	1515	NA	Transmembrane	Release new virion
		NB	Transmembrane	Ion channel
7	1149	M1	Internal	Assembly/regulation
		BM2	Transmembrane	Ion channel
8	1055	NS1	Nonstructural	IFN antagonist
		NS2 (NEP)	Internal	Nuclear export

Table 2 Influenza B virus genome structure and function.

1.3 Influenza virus hemagglutinin (HA)

Influenza virus hemagglutinin (HA) is a homotrimer that form spikes on the viral lipid membrane about 500 HA on each virion [31]. HA is coded by RNA segment 4. The translation of HA occurs in the rough endoplasmic reticulum (RER) and a precursor protein (HA0) form non-covalent homotrimer. Each monomer has a molecular weight of approximately 60 kDa for the unglycosylated form, and its molecular weight increases depend on the number or complexity of N-glycans, which is

occurred in the Golgi apparatus [32]. HA0 is transported to plasma membrane and cleaved by cellular protease to produce the active forms, HA1 receptor binding domain (327 amino acid) and HA2 the fusion peptide (222 amino acid). These units are combined together with disulphide bonds [33]. *N*-linked oligosaccharides, which affect HA function, are found both in globular and stem domain. The glycosylation results in the variation in the globular head domain of HA1 but to be more conserve in the stem domain of HA1 and HA2.

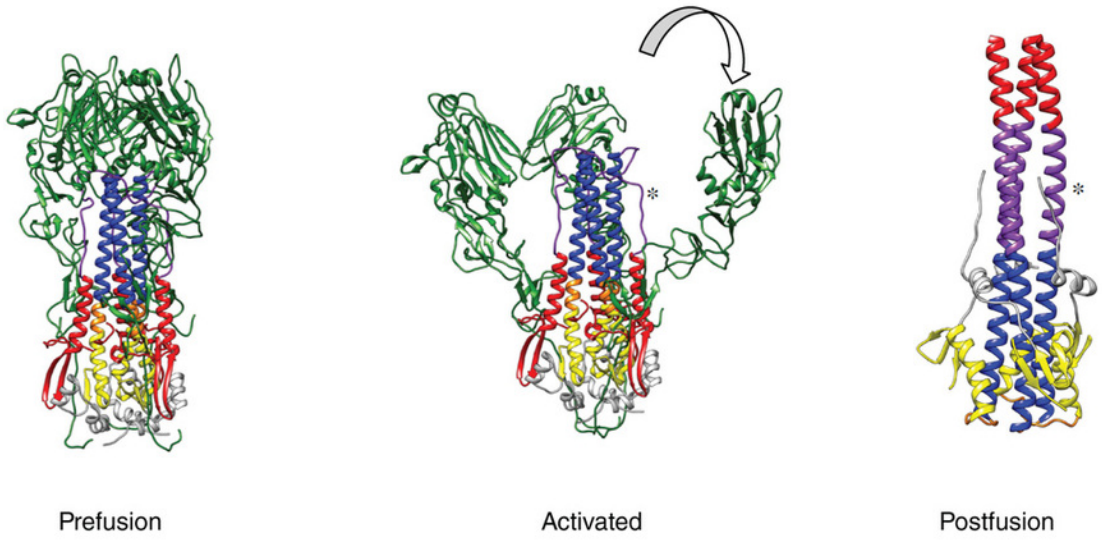

Figure 6 The structure of trimer HA at different state (modified from [34]).

These spikes of HA bind to sialic acid appeared on the surface of host cell's membrane [35]. Two major linkages are found between sialic acid and the carbohydrates they are bound to in glycoproteins: α(2,3) and α(2,6). These are significantly important for the specificity of the HA molecules in binding to cell surface sialic acid receptors in different species. For example, viruses from humans recognize the α(2,6) linkage, whereas those from avians and equines recognize the α(2,3) linkage. In case of swine virus, they can recognize both [35]. Thus, swine accept both human and avian influenza

virus that explains the important of swine being a good mixing vessel for avian and human influenza viruses, therefore producing mutant variants.

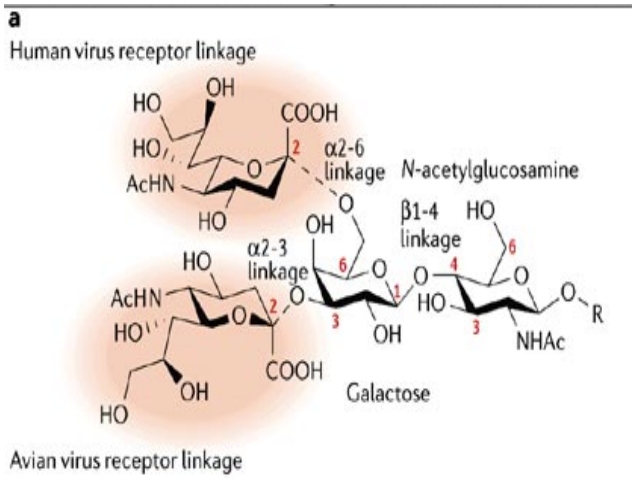

Figure 7 The two positions of the sialic acid linkage, which are crucial for recognition by the haemagglutinin protein of avian and human viruses.

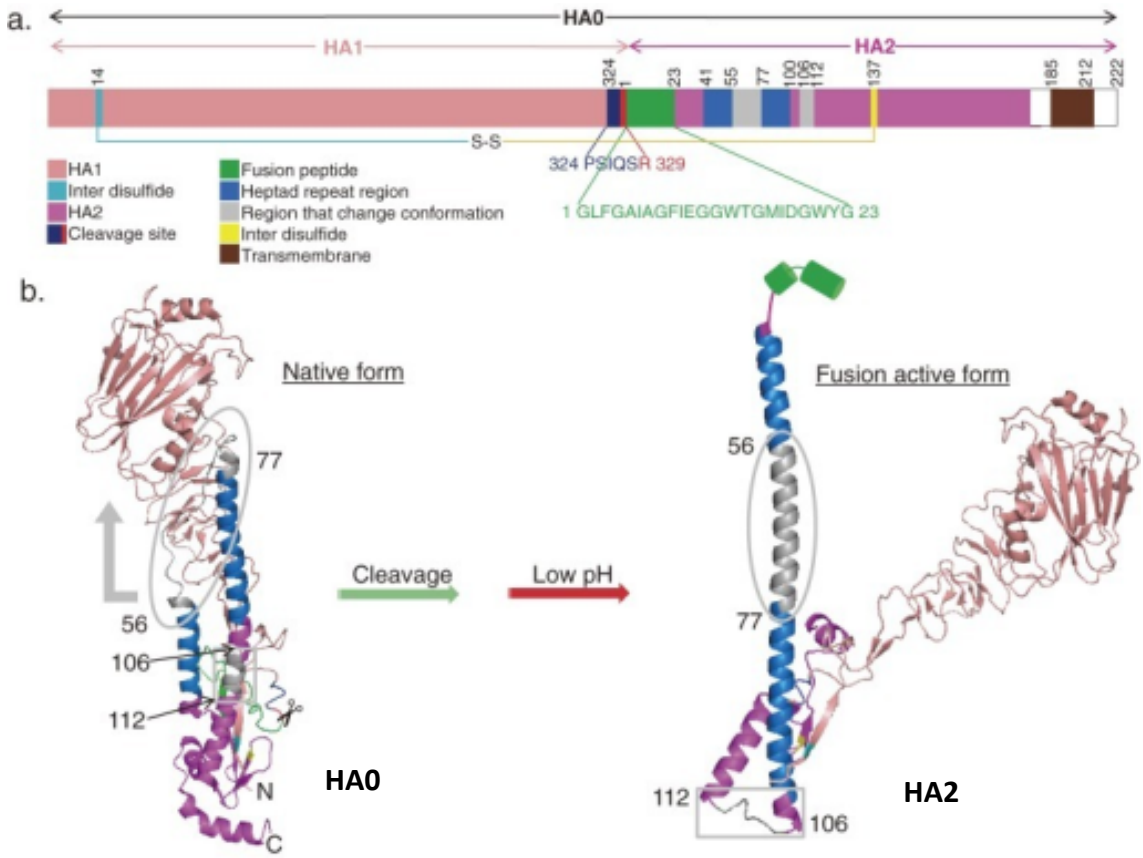

Figure 8 Structural arrangement of HA at the pH of membrane fusion. [32].

Upon binding to the host cell's sialic acid residues, receptor-mediated endocytosis occurs and the virus enters the host cell in an endosome. The proteolytic cleavage of the HA molecule is prerequisite for initiation of influenza virus infection. A trypsin-like host proteases found in respiratory tract cleaves the HA proteins [36]. The low pH, around 5-6, inside an endosome triggers the fusion of the viral and endosome membrane. The low pH induces a conformation change in HA, leading to maintenance of the HA1 receptor-binding domain but exposing the fusion peptide which disclose N-terminal domain in HA2. This fusion peptide inserted itself into the endosome membrane, carrying both the viral and endosome membrane connects to each other.

Acidic environment in endosome

↓

Conformation change in HA

↓

Reveal the fusion peptide in HA2

↓

The fusion peptide inserts itself
into endosome membrane

↓

The fusion of viral and endosome membrane

The acidic environment of the endosome is not only important for inducing the conformation in HA leading the fusion of the viral and endosome membrane but also opens up the M2 ion channel. Opening the M2 ion channel acidifies the viral core. This acidic environment in the virion release the vRNP from M1 such that vRNP is free to enter the host cell's cytoplasm [37] as well as nuclear pore.

1.4 Influenza virus neuraminidase (NA)

One of the surface influenza virus glycoproteins, neuraminidase (NA) is a tetramer (~240kDa) composed of four identical monomers (~60kDa), each of which contains a single peptide chain coded by RNA segment 6. An average of 100 NA spikes on the surface of virion. NA composes of cytoplasmic tail, a transmembrane domain, a stalk region, and a globular head. The NA is anchored in the lipid bilayer of the viral membrane by a series of hydrophobic amino acids near the N-terminal end of polypeptide, which is totally conserved in all influenza A neuraminidase subtypes (but not in influenza B).

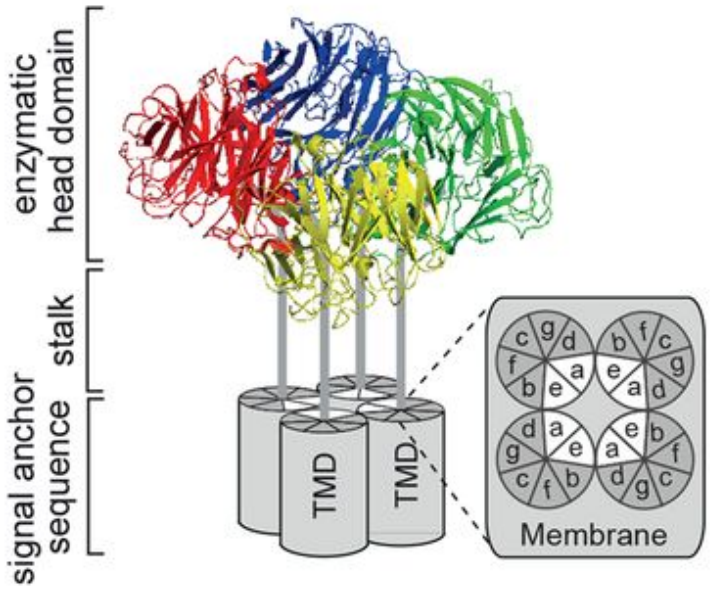

Figure 9 Scheme of influenza NA tetramer (TMD = transmembrane domain) [38]

The active site lies in a large depression on the surface of the head and the residues. Some of them directly contact bound substrate, neuraminic acid, whereas others provide a structural framework for the functional residues. NA destroys receptors recognised by HA by cleaving the α-ketosidic bond. This cleavage promotes movement of the virus from sites of infection in the respiratory tract. Respiratory mucus contains neuraminic

acid residues, so the receptor destruction is important for virus. Progeny virions bud out from the cell surface. Cleavage of HA receptors on the cell membrane is a prerequisite for virus release. Another obstacle on the way of virion liberation is the presence of the neuraminic acid residues on oligosaccharide chains of the newly synthesised HA and NA.

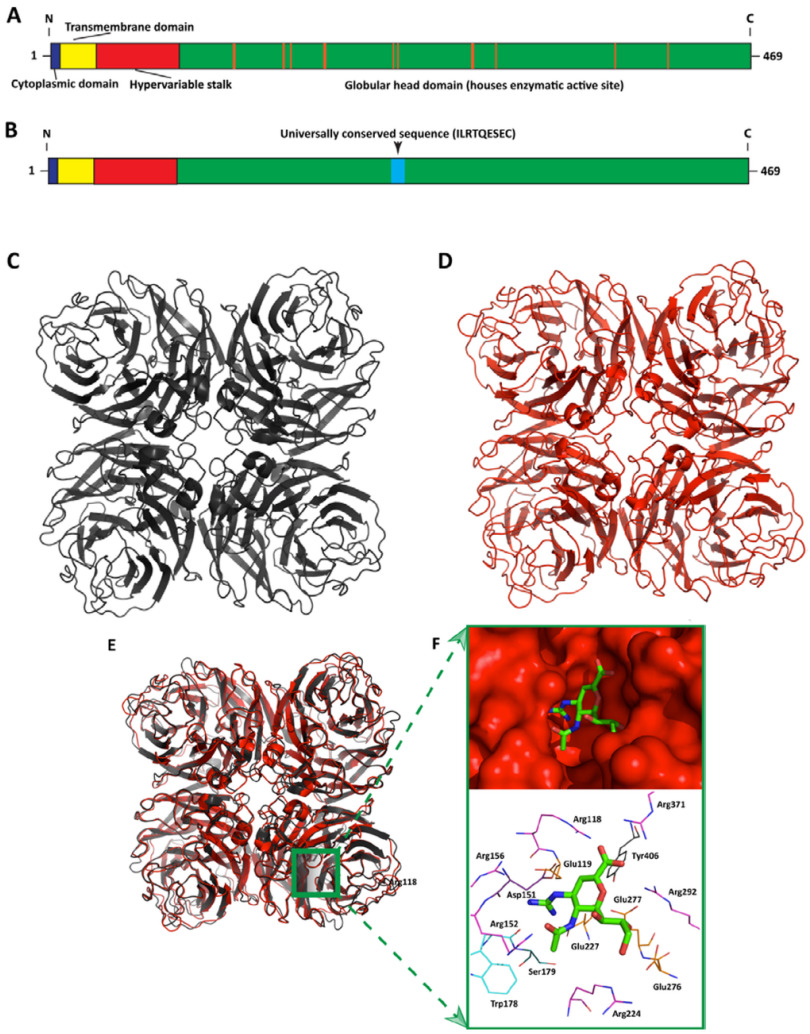

Figure 10 The 3D structure of influenza NA. (A) and (B) Schematic of the NA protein representing the cytoplasmic, transmembrane, hypervariable stalk, and globular head. Orange line represented on (A) showed the positions of active site of zanamivir. Highlighted in blue on (B) is universally conserved region among all known NA subtypes. (C) Despite amino acid sequence differences across NA subtypes, 3D structure tends to be conserved. (D) Zoom in view of one of identical active site NA tetramer when forms complex with zanamivir [39]

The HAs of the neighbouring virions bind to these neuraminic acid residues and cause self-aggregation of progeny virions. Virion liberation therefore requires the receptor-destroying activity in the NA on both viral surface glycoproteins and cellular membrane. In the presence of the NA inhibitors, virions stay attached to the membrane of infected cell and bind to each other and virus spread is inhibited [40, 41].

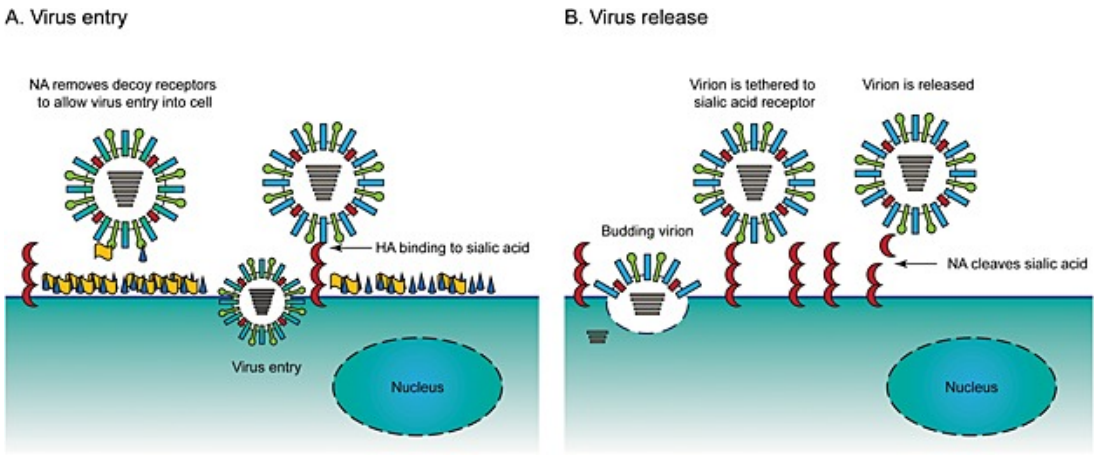

Figure 11 Function of the influenza virus neuraminidase, NA. The NA is a glycoprotein that is an enzyme sialidase. The influenza NA possesses several important functions during viral replication process. (A) In the early step, NA destroys the binding of HA and sialic acid receptor on host cell surface containing neuraminic acid. (B) At the releasing stage, NA is required to cleavage glycosidic linkages on the host cell surface, thereby releasing a new virus particle from the host cell surface [42].

1.5 M2 ion-channel protein

The influenza A virus M2 protein, which is encoded by a spliced mRNA derived from genome RNA segment7, is orientated in membranes with 23 N-terminal extracellular residues, a 19-residue transmembrane domain, and a 54 residue C-terminal cytoplasmic domain [43]. The M2 integral membrane protein (97 aa) is abundantly expressed at the plasma membrane of virus infected cells but is greatly underrepresented in virions, as only a few (on average 23-60) molecules are incorporated into virus particles. The native form of the M2 protein is minimally a homotetramer consisting of either a pair of disulfide-linked dimers or disulfide-linked

tetramers, the disulfide bonds acting to stabilize the oligomer [44]. Highly conserved residues His37 and Try41 are located in the proton channel and critical in the proton transportation. His37 is activated at low pH, which allows the flow of proton. Trp41 residues, located adjacent to His37, are clustered at high pH, building a channel gate that inhibits the flow of proton. The M2 protein, specific to influenza A, is known that the target for the adamantane derivative drugs, amantadine and rimantadine [14].

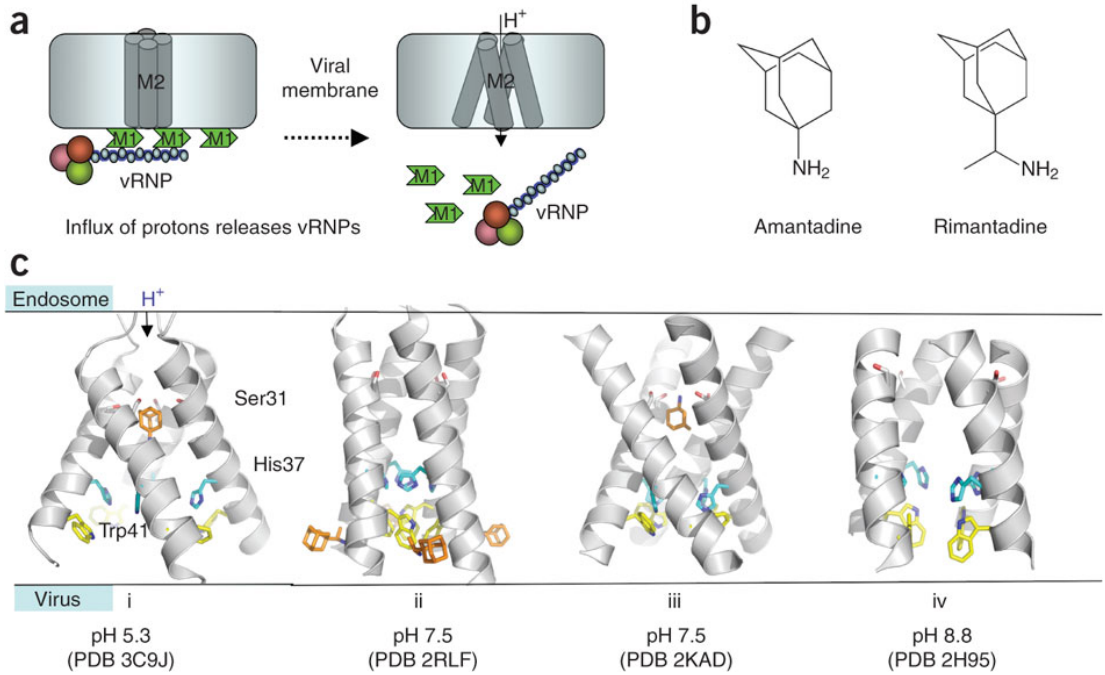

Figure 12 Structure, function and inhibitor of the M2 protein of influenza A virus [14]. (a) The vRNPs attach to the lipid bilayer via M1 viral protein. The influx of proton through M2 channel releases the vRNPs. (b) The chemical structure of adamatane derivative, amantadine and rimantadine. (c) X-ray and NMR structure of M2 channel binding with M2 inhibitor drug under different pH condition. (i) The transmembrane structure of M2-amantadine complex at pH 5.3 when amantadine (orange) binds M2 near Ser31. (ii) The binding of M2-rimantadine at pH7.5 shows that the drug bind individual M2 TM domain near Trp41. (iii) The solid state NMR structure of M2-amantadine complex at pH 7.5 shows that the drug binds to the proton channel similar to (i). However, the arrangement of the TM helices are different depend on pH condition. (iv) The arrangement of M2 TM helices of amantadine-bound M2 TM helix at pH 8.8.

1.6 M2 ion-channel protein blocker

The influenza A virus M2 integral membrane protein has ion channel activity which can be blocked by the antiviral drug amantadine approved in U.S. in 1976 and rimantadine approved in U.S. in 1994. The M2 protein transmembrane domain is highly conserved in amino acid sequence for all the human, swine, equine, and avian strains of influenza A virus, and thus, known amino acid differences could lead to altered properties of the M2 ionchannel. The M2 protein was implicated in having an essential role in the life cycle of influenza virus during studies of the anti-influenza drug amantadine hydrochloride (1-aminoada- mantane hydrochloride). The adamantanes (amantadine and rimantadine) inhibit the proton flow through the tetrameric M2 channel. The resulting acidification of the virus is necessary for viral uncoating at the infection stage. The vRNPs, which are attached to the lipid membrane via M1 matrix protein, could not be released without opening the M2 ion channel. Consequently, the vRNPs could not be transported into the nucleus and thus stops the viral replication process. However, adamantanes are only effective for influenza A viruses, but not influenza B viruses, because influenza B viruses do not have an M2 protein. Influenza B viruses have NB protein instead of M2 protein, which is not affected by adamantanes.

Drug-resistant mutants were isolated, and nucleotide-sequencing studies indicated that these mutants contained changes that mapped predominantly to the M2 transmembrane domain [45]. The most prevalent adamantine-resistant M2 mutation, S31N, is located along the inside rim of the pore (Figure 10c). For all type A influenza viruses, the amantadine block virus replication occurs at an early stage between the step of virus penetration and uncoating [46, 47]. In the presence of amantadine, the M1 proteins fail to release from vRNPs resulting in transfer of vRNPs to nucleus also has been inhibited.

In addition to the early effect of amantadine, the drug has a second late effect on some subtypes of avian influenza virus which have an HA that is cleaved intracellular and have a high pH optimum of fusion. However, these M2 ion-channel blockers were not used for therapeutic now because the side effects of adamantanes have been a potential to limit its use. The common side effects are nausea, dizziness, and insomnia. Moreover, almost all of seasonal type A influenza viruses have already gotten the drug resistance.

1.7 Neuraminidase inhibitors

During the last step of the virus life cycle, neuraminidase (NA) plays an important role in removal of sialic acid from cellular receptors recognised by hemagglutinin (HA), which results in the release of new progeny virions from infected cells. Because the HAs of neighbouring virions recognise and bind to neuraminic acid residues, which cause self-aggregation of new progeny virions, release of new virions, therefore, requires the receptor-destroying activity of NA to cleave glycoconjugates between viral glycoproteins and host cell molecules [48, 49]. From above reasons, NA was chosen as a suitable drug target because it has a critical role in the influenza life cycle. Moreover, amino acid residues of the catalytic site or the framework of the enzyme are highly conserved in both influenzas type A and B [50, 51].

NA inhibitors (NAIs) were designed to be sialic acid analogues that potently and specifically inhibit influenza virus replication by competitively binding to the NA active site, which results in inhibition of cleavage of the cell surface and prevention of the release of newly formed virions [52]. In 1942, G K Hirst found an enzyme activity on the influenza virus surface that removed virus receptors from erythrocytes. F M Burnet and colleagues continue to study about this receptor-destroying mechanism and

predicted that an inhibitor for this enzyme might be a candidate effective antiviral agent. After that, Chemical structure of neuraminic acid residuals (Neu5Ac), its linkage to glycoconjugates, and the specificity of the enzyme for terminal neuraminic acid residues were characterized by A Gottschalk. Finally, the first NA inhibitor was developed by P Meindl and H Tuppy in 1969, which inhibited viral replication but had low efficacy and specificity because it did not inhibit agglutination of red blood cell by all influenza viruses [53]. According to the finding of the crystal structure of influenza virus NA and its complex with neuraminia acid, found by P M Colman in 1980s, together with an improved understanding of synthesis of neuraminic acid derivatives with enhanced affinity for NA, In 1993 Von Itzstein and co-workers demonstrated that 4-guanidino-Neu5Ac2en, zanamivir was a potent and highly specific inhibitor of influenza NA activity. Food and drug Administration, FDA approved zanamivir for the treatment of both influenza A and B viruses in 1999. Kim and colleagues described the first orally active inhibitor called oseltamivir in 1997. FDA has approved it in 1999. There are currently three FDA-approved drugs effective for influenza virus worldwide, zanamivir (Relenza®, GlaxoSmithKline), oseltamivir (Tamiflu®, Roche), and peramivir (Rapivab®, Biocryst), approved in 2014. Inhaled laninamivir (Inavir®, Daiichi-sankyo) is also approved only in Japan in 2010 for treatment of influenza A and B viruses, and for prophylaxis in 2013.

Zanamivir, a dehydrated neuraminic acid derivative, mimics the geometry of the transition state during the enzymatic reaction. To increase interaction between zanamivir and the amino acid residues forming the enzyme active site, a guanidinyl group was substituted for a hydroxyl on carbon atom 4 [54]. The frequent side effects are headache, dizziness, nausea, vomiting, and diarrhea.

The most disadvantage aspect of zanamivir, however, is its administration route. Zanamivir is administrated through oral inhalation but is difficult for patients and children. To increase achievement the proper dose, another oral route compound, using a cyclohexene ring and replacement of a polar glycerol with lipophilic side chains, called oseltamivir was developed. The bioavailable prodrug oseltamivir is an ethyl ester that is converted into the active carboxylate by hepatic esterases. Oseltamivir is water-soluble and could be administered by oral. Common side effects of oseltamivir include vomiting, nosebleed, nausea, diarrhea, dizziness, headache, and sleep problems.

Oseltamivir is used worldwide for the treatment of influenza, however the generation and circulation of oseltamivir-resistant seasonal influenza viruses have become major concerns. The prevalence of oseltamivir-resistant pandemic (H1N1) influenza virus, carrying the H257Y substitution on neuraminidase, was 0.5% during the 2009-2010. Of the patients with oseltamivir-resistant influenza infection, 89% had been exposed to oseltamivir treatment before specimen collection. However, during the 2010-2011 influenza season, even the prevalence of oseltamivir-resistant pandemic (H1N1) 2009 viruses remained low, but most people, who infected with this virus, had no experience to treat with oseltamivir. The increase in the proportion of the patients infected with pandemic (H1N1) 2009 influenza virus without prior oseltamivir exposure caused seriously concern. The prevalence of oseltamivir-resistant seasonal influenza viruses (H1N1) increased to 12% during the 2007-2008 season, and resistance significantly increased to >99% by the 2008-2009 season [55]. Unlike seasonal influenza A (H1N1) viruses, which susceptible to the M2-blocking adamantanes, 99% of circulating pandemic (H1N1) pandemic 2009 are inherently resistant to oseltamivir. To solve this problem, the new compound was developed. The inhaled laninamivir was

approved for use in Japan in 2010. Laninamivir octanoate, the octanoyl ester prodrug of laninamivir, which is chemically similar to zanamivir, has been shown to inhibit neuraminidase activity of various influenza A and B viruses, including oseltamivir-resistant viruses, and also to be effective against A (H5N1) virus in vitro. The most important characteristic of laninamivir octanoate is its long-lasting antiviral activity, such that it is effective when administered as a single inhalation on the first day of treatment. The intranasal administration of a single dose of laninamivir showed efficacy superior to the efficacies of zanamivir and oseltamivir in mouse models of infection with influenza A virus and seasonal and current pandemic strains [56, 57]. Common reported adverse drug reaction (ADRs) of laninamivir were psychiatric disorders, gastrointestinal disorders, and nervous system disorders [58].

Although a single inhalation of laninamivir is effective for the treatment of influenza, including that caused by the oseltamivir-resistant viruses, in adults, seriously ill and pediatric patients need a parenteral formulation because the injectable drug is much easier to administer in such cases than oral oseltamivir, inhaled zanamivir, or laninamivir. In Japan, peramivir has recently been approved for use not only in adults but also in children over 1 month of age. Peramivir is a cyclopentane derivative with a guanidinyl group and lipophilic chains [59, 60]. Common side effects of peramivir are decreasing neutrophils A type of white blood cell and diarrhea.

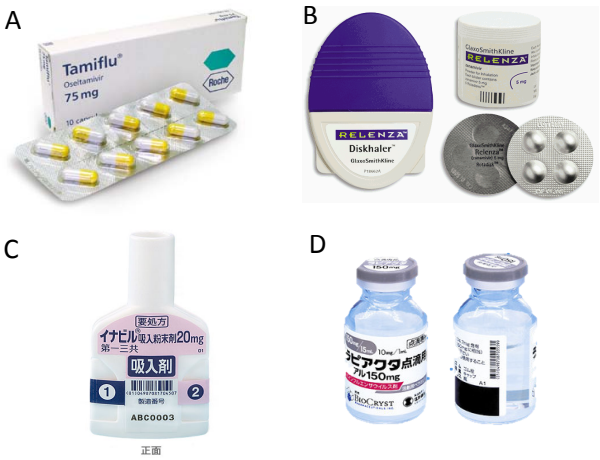

Figure 13 The available NA inhibitor drugs. (A)Tamiflu®, oseltamivir, (B)Relenza®, zanamivir, (C)Inavir®, laninamivir, and (D)Rapiacta®, peramivir

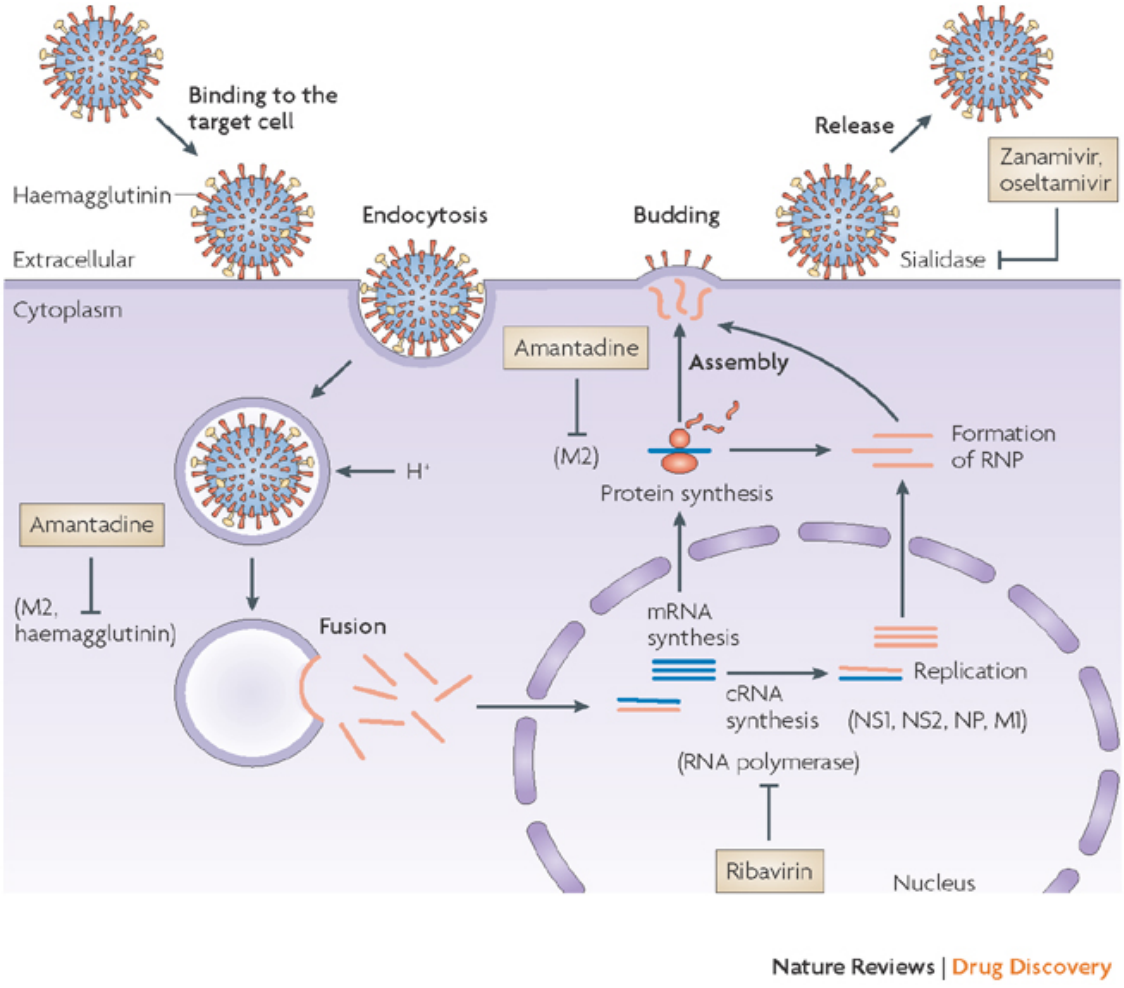

Figure 14 Life cycle of influenza virus and target of therapeutic development. (image obtained form [61])

Although virus replication of both influenza A and B viruses were inhibited by NAIs, several studies have reported that NAIs may have a lower efficacy against influenza B viruses than against influenza A [48, 62-64]. *In vitro* studies also have shown that the 50% inhibitory concentrations (IC_{50}) of oseltamivir were dramatically higher for influenza B than for influenza A viruses [65]. The elevated IC_{50} of oseltamivir for influenza B may result from the structure of NA protein that is less flexible than that of influenza A, which causes incomplete binding to the hydrophobic pocket of oseltamivir [66]. The susceptibilities of NAIs have been considered to be dependent on the B lineage in the same manner as observed for different influenza A neuraminidase subtypes [62].

1.8 Viral RNA-dependent RNA polymerase inhibitor

As influenza viruses have mutated and became resistant to current drugs, many researchers focus on finding novel drug from different inhibitory mechanism. During transcription and translation process, the viral RNA dependent RNA polymerase is required to initiate RNA synthesis. Favipiravir, (6-fluoro-3-hydroxy-2-pyrazinecarboxamide), originally known as T-705, was developed by Toyama chemical Co., Ltd, Japan and approved in 2014. It is a novel anti influenza compound that selectively and potently inhibits the RNA-dependent RNA polymerase not only influenza virus but also other RNA viruses. Favipiravir is phosphoribosylated by cellular enzyme to its active form. The function of this drug is to act as a pseudo purine, indicating the viral RNA polymerase mistakenly recognizes favipiravir-RTP as a purine nucleotide. The mode of action of favipiravir through direct inhibition of viral replication and transcription is unique among anti influenza drugs. Moreover, RNA-

dependent RNA polymerase domains are not present in human cells and are conserved among RNA viruses, making faviparavir a promising drug candidate. Interestingly, favipiravir shows the antiviral activity against all types of influenza viruses, A, B, and C. These includes large amount of strains resistant to currently used drugs including amantadine, oseltamivir, and zanamivir [67]. Several studies reported that abuse use of NA inhibitors might be one reason, which cause emergence of resistant influenza viruses, especially in Japan, where the amount of use of NA inhibitors is higher than everywhere. Importantly, faviparavir should not be used in regular seasonal flu season, but should be prescribed only for treatment of pandemic influenza virus or resistant influenza viruses.

1.9 Description of anti-influenza agent

The anti-IFV drugs used in this experiment were summarize in following table.

Generic name	Trade name	Chemical name	Chemical structure	Molecular weight	Mode of action
Oseltamivir phosphate	Tamiflu®	(3R,4R,5S)-4-acetylamino-5-amino3(1-ethylpropoxy)-1-cyclohexene-1-carboxylic acid, ethyl ester, phosphate	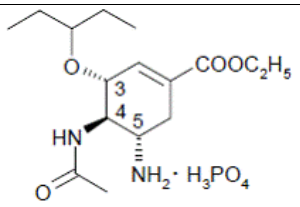	410.4	NA inhibitor
Zanamivir	Relenza®	5- (acetylamino)-4-[(aminoiminomethyl)-amino]-2,6-anhydro-3,4,5-trideoxy-D-glycero-D-galacto non-2-enonic acid	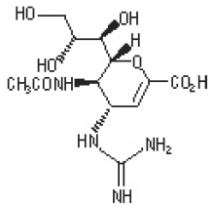	332.3	NA inhibitor
Laninamivir octanoate	Inavir®	(4S,5R,6R)-5-acetamido-4-carbamimidamido-6-[(1R,2R)-3-hydroxy-2-methoxypropyl]-5,6-dihydro-4H-pyran-2-carboxylic acid	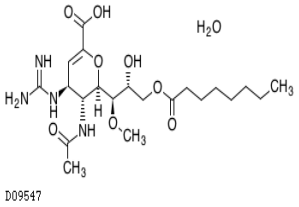	490.55	NA inhibitor
Peramivir	Rapiacta®	(1S,2S,3S,4R)-3-[(1S)-1-acetamido-2-ethylbutyl]-4-(diaminomethylideneamino)-2-hydroxycyclopentane-1-carboxylic acid	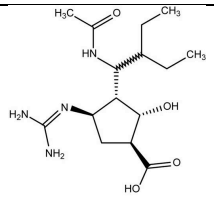	328.41	NA inhibitor
Amantadine hydrochloride	-	adamantan-1-amine	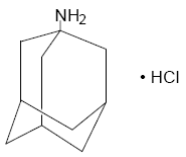	151.25	M2 inhibitor
Favipiravir	Avigan®	6-fluoro-3-hydroxy-2-pyrazinecarboxamide	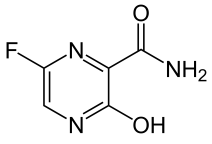	157.1	RNA polymerase inhibitor

Table 3 The summarize of anti-IFV drugs.

1.10 Methylglyoxal (MGO)

Honey has a very long history of safe use and an equally long history as a traditional medicine for its antimicrobial activity, including protection from pathogens and external wound healing. Other beneficial functions that have been attributed to honey include antioxidant, anti tumor, anti inflammatory, antimutagenic and antiviral properties, with the observed physiological effects dependent on the nutritional composition of the honey consumed [68].

Honey contains varying amounts of 1,2-dicarbonyl compounds such as glyoxal (GO), methylglyoxal (MGO), and 3-deoxygluco- sulose (3-DG) besides 5-hydroxymethylfurfural [69]. We reported that honeys have anti-influenza activity and manuka honey, a monofloral honey produced from the nectar of the manuka tree indigeneous to New Zealand and Australia, exhibited the highest anti-influenza activity among tested honey samples [70]. Interestingly, manuka honey contains high amount of MGO compared to other honeys so MGO might be an important component resulting in a high potent inhibitory activity against influenza of manuka honey.

Methylglyoxal (MGO) is clear yellow to yellow-brown solution with the chemical name 2-oxopropanal. It has a molecular formula of $C_3H_4O_2$ and a molecular weight of 72.06. It has the following structural formula:

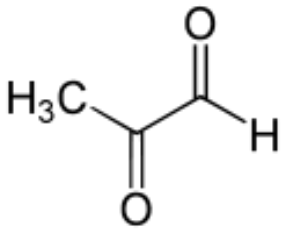

MGO is the major determinant of the antibacterial activities of manuka honey [71, 72]. Previous studies indicated that MGO has antiviral activities against the foot-

and-mouth disease virus [73] and Newcastle disease virus [74]. Moreover, our preliminary results showed that MGO concentration was approximately 20–160 fold higher in manuka honey than that in other honey samples. Therefore, it is possible that MGO contributes to its anti-influenza viral activity.

The antiviral activity against influenza virus of MGO was also reported in 1957, which was performed in embryonated eggs [75]. However, infection of embryonated eggs is a complicated process and the mechanism of anti-influenza activity of MGO remains unclear. In our experiments, Madin–Darby Canine Kidney (MDCK) cells were selected for evaluation of antiviral activity of MGO and also cytotoxicity of MGO.

1.11 Influenza vaccine

The anti influenza drugs, M2 inhibitors, NA inhibitors, vRdRp inhibitor, are found to be effective in order to reduce the disease severity. However, they cannot be prescribed as a first choice for prophylaxis. In general, vaccine is effective and good strategy for prevention of viral infection. Vaccination remains the most effective way to prevent infection and severe outcomes caused by influenza viruses. These vaccines are primarily targeted to induce immunity to the variable major target antigen, hemagglutinin (HA) of influenza virus. The influenza vaccines are effective to preventing and inhibiting the spread of influenza epidemics when the strains contain in the vaccine formulation are closely matched with the circulated virus strains. The current vaccines also are not effective in preventing the emergence of new pandemic or highly virulent influenza viruses.

Because of lack of proofreading enzyme, influenza viruses are continuously evolving, resulting in changes of amino substitutions in the HA and NA proteins. These

changes occur from point mutations in the viral genome RNA. When mutation points accumulate, emergences of new strains responsible for seasonal epidemics occur with both influenza A and B viruses [76, 77]. These substitutions occur more commonly in five antigenic regions (A-E) on the globular domain of HA1 [78], which are crucial for binding with viral neutralizing antibodies. According to these antigenic variations, the mutant influenza viruses can escape recognition by the host immunity produced by previously given vaccination. From these reasons, vaccine manufacturers have to reformulate their vaccine products every year to ensure that HA and NA molecules that contained in their formulation exactly matched to currently circulating influenza strains. Otherwise, the protection efficacy of vaccine decreases.

The first commercial vaccine approved in USA in 1945 was a whole-inactivated influenza virus. The inactivated vaccines contain purified influenza viruses that have been chemically inactivated with formalin or β-propiolactone. Epidemics of influenza viruses currently are caused by 2 subtypes of influenza A (H1N1 and H3N2) and one variant of influenza B. Thus, the trivalent vaccine is determined based on the strain of viruses expected to be circulating in human. The development of high-growth influenza virus in embryonated eggs is a one of critical process in vaccine production. The growth characteristics of reassortant viruses vary because HA and NA also affect the adaptation and replication capabilities of the viruses.

Based on the knowledge that an intact viral membrane is essential for infectivity of enveloped viruses, detergent-treated disruption of influenza viruses to produce subvirion preparations has been most commonly prepared in recent vaccine formulations. These vaccines remain the immunogenic properties of the viral proteins but they have lower reactogenicity compared to the whole virus vaccines.

One of major factor that affect the efficacy of vaccines is the antigenic similarity between the circulating strains and vaccine strains. The most important limitation of current vaccines is that the antigenic domains of HA are highly susceptible to mutation in circulating epidemic virus strains [79]. Thus, the current available vaccines have to be updated every year to match antigenicity of the virus stains that are predicted to circulate in the next season. However, commercial vaccine would not be effective in preventing the spread of novel pandemic strains. From these reasons, novel approaches are being developed to create broadly protective vaccines called universal influenza vaccines, which focus on conserved regions of the viral M2 protein and the HA protein.

New technologies to develop novel influenza vaccines can be divides into general categories as 1) those designed to elicit antibodies response to conserved region of HA and M2e, the extracellular membrane of M2 protein, which consists of N-terminal 24 residual, and 2) those that induce cross-protection T-cell response against internal protein such as NP and M1 protein inducing the reduction of disease severity [77, 80].

Although HA proteins show high variation, novel approaches have been focused the immune responses against the HA stalk that contains some conserved sequences, especially in HA2 subunit. The N-terminal fusion peptide of HA2, especially the first 11 residues, is found that conserved across all known subtypes with only minor substitutions. Broadly neutralizing human mAb CR6261 recognized the conserved stalk region of HA1/HA2, inhibited virus infection by blocking the conformation of influenza viruses associated with membrane fusion [81] and cross protection mice from lethal H5N1 or H1N1 challenge [82].

Other influenza protein that can be used to develop universal vaccine is M2 protein. The M2 protein has a small, non-glycosylated 24 amino acid ectodomain (M2e) that is highly conserved among influenza A viruses both human and avian viruses. The low immunogenicity against natural M2e can be overcome by fusion M2e with some components to facilitate the formation and maintenance of tetrameric structure. Development of M2e-base vaccines requires the use of adjuvant to induce high antibody titers. Adjuvants suitable for human use improve protection, which relate to higher titers responses to defined subtypes [83]. Unfortunately, an M2e-base vaccine is unlikely to cover influenza B viruses.

Non-neutralizing antibodies are also the targets of universal vaccine development. The highly conserved internal proteins such as NP, M1, may contribute to clearance influenza-infected cell. Although cell mediated immunity (CMI) to influenza virus infections does not prevent infection, it can significantly reduces disease severity, decrease viral shedding, and mortality. As T-lymphocytes ($CD4^+$ and $CD8^+$) tend to recognize the more conserved internal proteins, there is a promising potential for broad responses. Several studies reported that $CD8^+$ is important for viral clearance. On the other hand, $CD4^+$ may plays a essential role for the generation and maintenance of memory cells and for antibody production [84].

To enhance immunity and improve cross-protection against seasonal and pandemic strains, some novel candidate vaccines are developed by combination of the conserved epitopes from different viral proteins. Not only their potential ability to elicit cross protection against divergent subtypes, These candidate vaccines also exhibit more advantages such as reduce the production time and costs [85].

The current available vaccines are determined by hemagglutination inhibition titer (HAI) for vaccine efficacy testing. However, the correlate of protection for universal vaccine might not be linked with hemagglutination inhibition antibodies. This factor is a higher regulatory barrier of universal vaccine development. Moreover, human trails are also required to prove the efficacy of vaccines. Wild-type influenza viruses have been used for challenge studies in adults, while attenuated vaccines strains have been used to perform challenge in children. In many studies showed that the interpretation of these results is difficult [80].

1.12 Aim of study

Up to the present, US FDA approves drug prescription strategy of anti IFV drugs for prophylaxis and treatment: M2 ion channel blocker (amantadine, rimantadine) and NA inhibitors. Also a novel anti influenza drug, favipiravir (Avigan®), was approved in Japan in 2014. M2 channel blockers block the hydrogen ion channel activity of the M2 protein of influenza A virus, inhibiting virus replication by blocking virus into the cell. The main drawbacks of M2 blockers are the rapid development of drug-resistant variants and inefficacy against influenza B virus. To solve this reason, NA inhibitors were developed. Because of the genetic stability of the NA enzymatic active centre among IFV, NA inhibitors became a promising target for the development of antiviral drugs.

However, some of NA inhibitors were found that IFV have been mutated to become drug-resisted IFV, resulting in decrease of efficacy for IFV treatment. Drug-resisted IFV triggered a serious problem worldwide because if emergence of IFV occurs, no drug can be used for treatment. Moreover, influenza A viruses rapidly mutate so that

NA inhibitors so far just weaken the influence of influenza virus. For this reason, many researchers focus on development of new anti IFV or combination therapy enhancing the efficacy of anti-IFV drugs.

Until now, our laboratory found the efficacy of MGO, main component in honey derived from natural product, in terms of anti IFV compound. It suggested that MGO might inhibit IFV by directly affect on IFV prior to adsorption. On the other hand, to improve the treatment by using NA inhibitors, it's known that the simultaneously treatment of combination drugs for which are different mechanisms of action might enhance the efficacy, meanwhile might reduce the effect of resistance to a single drug [86].

In this study, we investigated whether MGO has a possibility as concomitant drug for NA inhibitors. We evaluated the synergistic effect of neuraminidase inhibitors and methylglyoxal against influenza virus infection in vitro assay using MDCK cells.

CHAPTER 2: MATERIALS AND METHODOLOGY

2.1 Reagents, Materials and Equipments

2.1.1 Reagents

10xMEM	- Nissui Pharmaceutical
100xMEM vitamin	- GIBCO
A/Duck/Pennsylvania/84	NIID
A/Hong Kong/8/68	NIID
Agarose	Wako
Amido black 10b	Nacalai Tesque
A/Nagasaki/HA-58	Nagasaki University
A/Puerto Rico/8	Tsukuba University
A/WSN/33	NIID
A/2009/6	Nagasaki University
A/200/16	Nagasaki University
A/2009/33	Nagasaki University
Agarose S	- Wako
Amantadine	- Sigma
B/Lee/40	ATCC
B/Brisbane/60/2008	NIID
B/2014/1	Nagasaki University
B/2014/4	Nagasaki University

B/2014/6	Nagasaki University
B/2014/7	Nagasaki University
B/2014/8	Nagasaki University
BSA	
Crystal violet	- Nacalai tesque
Disodium phosphate (Na_2HPO_4)	- Wako
DMSO	- Wako
Ethylenediaminetetraacetic acid (EDTA)	- Dojin
E-MEM	- Wako
Ethanol	- Nacalai tesque
FBS	- Biowest
Laninamivir	- Daiichi-Sankyo
L-glutamine	- Wako
Methylglyoxal 40% in H_2O	- Sigma
MDCK cell	- ATCC
Oseltamivir tablet	- Roche
Penicillin G potassium	- Nacalai tesque
Peramivir solution	- Biocryst
Potassium Chloride (KCl)	- Nacalai tesque
Potassium phosphate monobasic (KH_2PO_4)	- Wako

Sodium chloride (NaCl)	- Nacalai tesque
Streptomycin sulphate	- Nacalai tesque
Trypan blue	- Wako
Trypsin	- Sigma
WST-1 solution	- Dojindo laboratories
Zanamivir tablet	- Glaxo Smith

2.1.2 Materials and Equipments

Axiocam MRm camera microscope	- Carl Zeiss
Axiovert 25 Inverted Fluorescence microscope	- Carl Zeiss
Bacteria culture dishes	- Atect
Cell culture dishes (35, 60, 90mm)	- NEST
Cell culture plates (6,12, 48, 96-wells)	- Nunclon
Centrifuge KS-8000	- KUBOTA
Centrifuge MRX-150	- TOMY
Centrifuge tubes (15,50 ml)	- NUNC
Class II A/B3 Biological safety Cabinet ASC-198	- ASTEC
Glass pipettes (1, 5, 10ml), Pyrex®	- Iwaki
Infinite M200 Tecan plate reader	- Wako

Microcentrifuge tubes (1.5ml)	- NUNC
Microplate genie	- Scientific industries
Micro well plate	- Azuwan
Milli-Q Water Purification System	- Millipore
Multichannel pipette (P20, P200)	- PipettePAL®
Nanospin NS-060	- NIPPON genetics
pH meter	- BECKMAN
PVDF membrane (Immobilon-P, 0.45 μm)	- Millipore
Pipette dispenser, Fastpette^{v-2}	- Labnet
Pipette man (P20, P200, P1000)	- GILSON
Pipette tips (200μl, 1000μl)	- Greiner bio-one
TC10™ automated cell counter	- Biorad
TC10™ system counting slides, Dual chamber	- Biorad
Thermo mate BF200	- Yamato
Vortex genie 2	- Scientific industries
Weighing machine, PM460	- Mettler

2.2 Methodology

2.2.1 MDCK cell culture

2.2.1.1 Subculture of MDCK cell

MDCK cells were grown in 90mm dish with E-MEM medium supplemented containing 5% fetal bovine serum (FBS) and subculture every 3 days. MDCK cells were washed with 10ml of PBS (-) and then treated with 10ml of 0.05%EDTA/PBS(-) to remove traces of medium or divalent cations [87]. After treated with 0.05%EDTA, MDCK cells were treated with 1ml of 0.05%trypsin/0.02%EDTA and incubated in 37°C, 5%CO_2 incubator for 10-15 minutes. The disaggregated MDCK cells were collected by adding 10ml of E-MEM containing 5%FBS and centrifuge with 800 rpm for 3 minutes. After that, the supernatant was aspirated before re-suspend with 10 ml of fresh medium and cell counting was performed. The MDCK cells were seeded on a new 90mm dish to obtain 3.0×10^5 cell/dish of MDCK cells.

2.2.1.2 Seeding MDCK cells on 96-well plate

E-MEM medium supplemented containing 10% fetal bovine serum (FBS) was used for seeding cell instead of E-MEM containing 5%FBS, which was used for subculture cell. MDCK cells were stained with trypan blue in equal amount of cell suspension (1:1). After counting the cell using TC-10, Biorad™, MDCK cells were diluted to obtain 3.0×10^5 cell/ml and 100µl/well of diluted MDCK cells were added to 96-well plate using multichannel pipette. The 96-well plate seeded with MDCK cells were kept in 37°C, 5%CO_2 incubator for 24 hours.

2.2.1.3 Seeding MDCK cells on 24-well plate

E-MEM containing 10%FBS was used to seed MDCK cells. After re-suspend MDCK cell suspension, cell counting was performed. MDCK cells were stained with an equal amount of trypan blue. After counting the cell using TC-10, Biorad™, MDCK cells were diluted to obtain 1.78×10^5 cell/ml and 1ml/well of diluted MDCK cells were added to 24-well plate using. The 24-well plate seeded with MDCK cells were kept in 37°C, 5%CO_2 incubator for 24 hours.

2.2.1.4 Seeding MDCK cells on 6-well plate

E-MEM containing 10% FBS was used to seed MDCK cells. After re-suspend MDCK cell suspension, cell counting was performed. MDCK cells were stained with an equal amount of trypan blue. After counting the cell using TC-10, Biorad™, MDCK cells were diluted to obtain 1.0×10^6 cell/ml and 2ml/well of diluted MDCK cells were added to 24-well plate using. The 24-well plate seeded with MDCK cells were kept in 37°C, 5%CO_2 incubator for 24 hours.

2.2.2 Sample preparation

2.2.2.1 Oseltamivir stock solution

Tamiflu® capsule, 75mg was transferred to 15ml tube and 10ml of PBS (-) was added to dissolve. Mixing is required until homogeneous suspension was obtained. The final concentration of Oseltamivir stock solution was 24mM and kept in -80°C freezer. This stock solution was used for both IC50 and CC_{50} determination.

2.2.2.2 Zanamivir stock solution

For IC_{50}determination, Relenza® 5 mg was unwrapped and transferred to 1.5ml tube. 0.6ml of DMSO was added to dissolve completely. The final concentration of Zanamivir stock solution was 25mM and kept in -80°C freezer. For CC_{50} determination, Relenza® was unwrapped and transferred to 1.5ml tube. 150µl of DMSO was added to dissolve completely. The final concentration of Zanamivir stock solution was 100mM and kept in -80°C freezer.

2.2.2.3 Peramivir stock solution

Rapiacta® 30.5 mM solution was used directly and allocated to 1.5 ml tube kept in -80°C freezer.

2.2.2.4 Laninamivir stock solution

Inavir® 40mg bottle was cut and powder inside was transferred to 1.5ml tube. 150µl of DMSO was added to dissolve until homogeneous solution was obtained. The final concentration of Laninamivir stock solution was 564.34mM and kept in -80°C freezer. This stock solution was used for both IC_{50} and CC_{50} determination.

2.2.2.5 Amantadine stock solution

20 mg of Amantadine hydrochloride was weighted and transferred to 15ml tube. 1ml of DMSO was added to dissolve until homogeneous solution was obtained. The final concentration of Amantadine stock solution was 106.55mM and kept in -80°C freezer. This stock solution was used for both IC_{50} and CC_{50} determination.

2.2.2.6 Methylglyoxal solution (MGO)

MGO 40%H_2O solution, SIGMA® was diluted with MEM containing vitamin to obtain 400μg/ml for IC_{50} and 4mg/ml for CC_{50}.

2.2.3 Virus solution preparation

All virus strains used for this experiment was diluted to obtain 1000$TCID_{50}$/ml. Except A/WSN/33 and B strains, trypsin is required to be added into virus solution for viral infectivity.

2.2.4 $TCID_{50}$ assay

Virus titre in supernatant used in next experiments was determined by the tissue culture infections dose of 50% ($TCID_{50}$) assay. Near confluent monolayers of MDCK cells in 96-well plates were inoculated with 10-fold serial dilutions of each virus culture supernatants. CPE development was scored after 3 days and the 50% end point virus dilution determined using the statistical method by Reed and Muench [88]. The reduction of virus multiplication was calculated as percentage of virus control (MOCK = Uninfected cells).

2.2.5 Fixation and staining

We performed evaluation of antiviral activity and cytotoxicity with 2 different staining method, the WST-1 (water-soluble tetrazolium salt) assay and crystal violet (CV) staining.

For the WST-1 assay, 3-day infected MDCK cells, added 10μl WST-1 solution and shake at 15 second, then kept in 37°C, 5%CO_2 incubator for 1, 2, and 3 hour. Every

1-hour these plates were measured OD value at 450-650 nm using the plate reader. The plates were subsequently fixed and stained with CV and optical density values at 560 nm were determined as described below.

3-days infected MDCK cells with IFV were fixed with 200µl/well of 70%ethanol and left for 5 minutes, then discard 70%ethanol. 200µl/well of 0.5%crystal violet solution was added and left for 5 minutes, then discard it. A stained plate was washed with tap water and lets it dry in room temperature before measured OD value with microplate reader at 560nm.

2.2.5 Cytotoxicity and therapeutic indexes

One of the most important prerequisite for an antiviral agent is safety. To determine cytotoxicity of each commercial anti-influenza drug, 2-fold dilution of each commercial anti IFV drugs was performed. In a 96-well plate for dilution, 120µl/well of E-MEM plus vitamin was added to a 96-well plate except the 2^{nd} line. Next, 240µl of each commercial anti IFV drugs diluted as the below flowchart was added to the 2^{nd} line. 120µl/well of the 2^{nd} line was transferred to the 3^{rd} line using multichannel pipette and pipetting several times to assure homogenous solution will be obtained. This procedure was continuously performed until reach 11^{th} line.

For CC_{50} of Oseltamivir and peramivir, Stock solution of Oseltamivir, 24mM and peramivie 30.5mM were used directly for 2-fold dilution preparation before added to 96-well plates, which contain MDCK cells as final concentration.

For CC_{50} of Zanamivir, Stock solution of Zanamivir, 100mM was pipetted 5µl to 1.5 ml tube containing 995µl of E-MEM plus vitamin to obtain Zanamivir solution at 0.5mM. Next, 0.5mM Zanamivir was pipette 480µl to 1.5 ml tube containing 720µl of E-MEM plus vitamin. The final concentration is 200µM and %DMSO is 0.2%.

For CC_{50} of Laninamivir, Stock solution of Laninamivir, 564.34mM was pipetted 5µl to 1.5 ml tube containing 995µl of E-MEM plus vitamin to obtain Laninamivir solution at 2.82mM. Next, 2.82mM Laninamivir was pipette 144.68µl to 1.5 ml tube containing 1,055.32µl of E-MEM plus vitamin. The final concentration is 340µM and %DMSO is 0.06% (same concentration to that of determination IC_{50}).

For CC_{50} of Amantadine, Stock solution of Amantadine, 106.55mM was pipetted 10µl to 1.5 ml tube containing 990µl of E-MEM plus vitamin to obtain Amantadine solution at 1.0655mM. Next, 1.0655mM Amantadine was pipette 150.17µl to 1.5 ml tube containing 849.83µl of E-MEM plus vitamin. The final concentration is 160µM and %DMSO is 0.15% (same concentration to that of determination IC_{50}).

Cytotoxicity tests use a series of increasing concentrations of each antiviral commercial drug to determine what concentration results in the death of 50 percent of MDCK cells. This value is referred to as the median cellular cytotoxicity concentration and is identified by CC_{50}. The percentage of living MDCK cells was plotted against the concentration of each commercial drug. After 72 hours, MDCK cells morphology was observed under inverted light microscope and cell viability was evaluated using crystal violet staining. The percentage of viable cells was calculated using the following formula;

(ODexp - ODblank)/ (ODcell control- ODblank) X 100%

Where (ODexp), ODblank, and (ODcell control) indicate the absorbencies of test sample, the blank and the cell control, respectively.

2.2.6 Evaluation of anti-influenza activities of commercial anti-influenza drugs

To determine efficacy of each commercial anti-influenza drugs against various influenza strains, 2-fold dilution of each commercial anti IFV drugs was performed. In a 96-well plate for dilution, 120µl/well of E-MEM plus vitamin was added to a 96-well plate except the 2nd line. Next, 240µl of each commercial anti IFV drugs diluted as the below flowchart was added to the 2nd line following the below plate layout (figure 15). 120µl/well of the 2nd line was transferred to the 3rd line using multichannel pipette and pipetting several times to assure homogenous solution will be obtained. This procedure was continuously performed until reach 11th line.

For IC_{50} of Oseltamivir, Stock solution of Oseltamivir, 24mM was pipetted 10µl to 1.5 ml tube containing 990µl of E-MEM plus vitamin to obtain Oseltamivir solution at 0.24mM. Next, 0.24mM Oseltamivir was pipette 83.3µl to 1.5 ml tube containing 991.7µl of E-MEM plus vitamin. The final concentration is 20µM.

For IC_{50} of Zanamivir, Stock solution of Zanamivir, 25mM was pipetted 5µl to 1.5 ml tube containing 995µl of E-MEM plus vitamin to obtain Zanamivir solution at 0.125mM. Next, 0.125mM Zanamivir was pipette 160µl to 1.5 ml tube containing 840µl of E-MEM plus vitamin. The final concentration is 20µM and %DMSO is 0.08%.

For IC_{50} of Laninamivir, Stock solution of Laninamivir, 564.34mM was pipetted 5µl to 1.5 ml tube containing 995µl of E-MEM plus vitamin to obtain Laninamivir

solution at 2.82mM. Next, 2.82mM Laninamivir was pipette 144.68µl to 1.5 ml tube containing 1,055.32µl of E-MEM plus vitamin. The final concentration is 340µM and %DMSO is 0.06%.

For IC_{50} of Peramivir, Stock solution of Peramivir, 30.5mM was pipetted 10µl to 1.5 ml tube containing 990µl of E-MEM plus vitamin to obtain Peramivir solution at 0.305mM. Next, 0.305mM Peramivir was pipette 16.4µl to 1.5 ml tube containing 983.6µl of E-MEM plus vitamin. The final concentration is 5µM.

For IC_{50} of Amantadine, Stock solution of Amantadine, 106.55mM was pipetted 10µl to 1.5 ml tube containing 990µl of E-MEM plus vitamin to obtain Amantadine solution at 1.0655mM. Next, 1.0655mM Amantadine was pipette 150.17µl to 1.5 ml tube containing 849.83µl of E-MEM plus vitamin. The final concentration is 160µM and %DMSO is 0.15%.

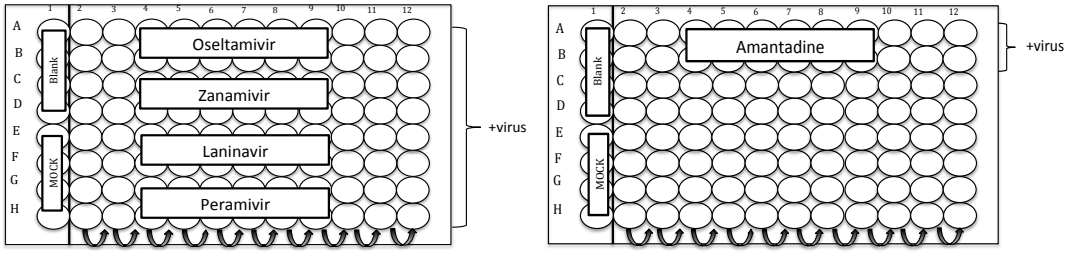

Figure 15 The layout of 96-well plate infected with various influenza virus in order to determine IC_{50}.

MDCK cells were grown in 96-well plates overnight. 2-fold serial dilutions of each commercial anti IFV drugs performed in previous step and equal volume of virus suspension (TCID50/cell=100) were added for 72 h. After 72 h, the virus induced CPE development (CPE reduction assay) was evaluated under microscope. Cell viability was determined using crystal violet staining method. Briefly, the cells were fixed with 200 µL of 70% EtOH for 5 min and then stained with equal amount of 0.5% crystal violet for 6 hours. After washing with water and air drying, the absorbance was measured at

560 nm with Infinite M200 Tecan plate reader. The % protection was calculated by the following formula;

(ODexp - ODblank)/ (ODcell control - ODblank) X 100%

Where (ODexp), (ODblank), and (ODcell control) indicate the absorbencies of test sample, the blank and the cell control, respectively.

The percentage of viable MDCK cells was plotted against the concentration of each commercial drug. The effective concentration is the concentration of product at which virus replication is inhibited by 50 percent (IC_{50}).

2.2.7 Evaluation of IC_{50} and CC_{50} of MGO against various influenza viruses

To evaluate *In vitro* anti-influenza activity and cytotoxicity of MGO, Methylglyoxal 40% in H_2O purchased from Sigma, was diluted with E-MEM plus vitamin to obtain 4mg/ml MGO for CC_{50} determination and 400µg/ml for IC_{50} determination. 2-fold dilution of methylglyoxal was performed. In a 96-well plate for dilution, 120µl/well of E-MEM plus vitamin was added to a 96-well plate except the 2nd line. Next, 240µl of 400µg/ml MGO and 4mg/ml MGO were added to the 2nd line following the below plate layout (figure 16). 120µl/well of the 2nd line was transferred to the 3rd line using multichannel pipette and pipetting several times to assure homogenous solution will be obtained. This procedure was continuously performed until reach 11th line. Finally, the concentration range for IC_{50} determination of MGO was performed of 5.5µM-2.78mM and that of CC_{50} determination was performed of 0.11-6.94mM. The effective concentration is the concentration of product at which virus

replication is inhibited by 50 percent (IC_{50}). The percentage of viable MDCK cells was plotted against the concentration of methylglyoxal (MGO).

This experiment was performed to obtain IC_{50} against each virus strains and also cytotoxicity of MGO as CC_{50}. The result from this experiment was used to evaluation of synergistic effect between commercial anti IFV drugs and MGO. Influenza virus strains used in this experiment included A/WSN/33 (H_1N_1), A/PR8 (H1N1), A/HK/8/68 (H3N2), A/Duck/Pennsylvania/84 (H5N2), and A/Nagasaki/HA-58/2009.

Methylglyoxal 40% in H_2O purchased from Sigma, was diluted with E-MEM plus vitamin to obtain 4mg/ml MGO for CC_{50} determination and 400μg/ml for IC_{50} determination.

Cytotoxicity tests use a series of increasing concentrations of methylglyoxal (MGO) to determine what concentration results in the death of 50 percent of MDCK cells. This value is referred to as the median cellular cytotoxicity concentration and is identified by CC_{50}. The percentage of living MDCK cells was plotted against the concentration of methylglyoxal (MGO).

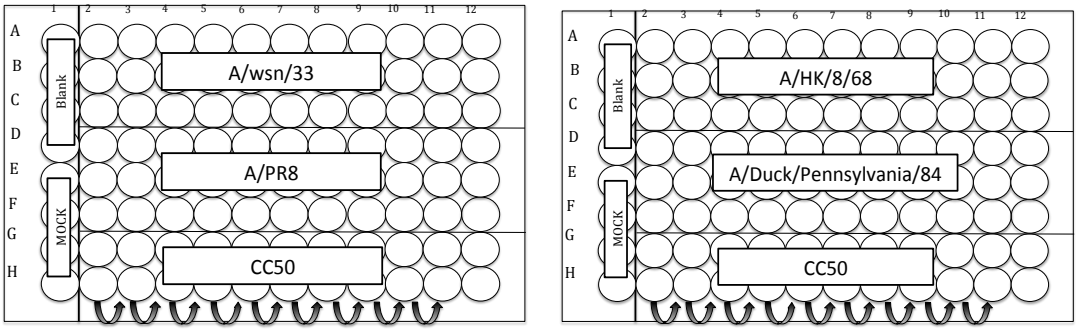

Figure 16 The layout of 96-well plate infected with various influenza virus in order to determine IC_{50} of methylglyoxal (MGO).

To confirm cytotoxicity and therapeutic effect of MGO, we performed experiment again in 24-well plates with various concentration of MGO (170, 340, 700, and 1400 μM). Cell morphology also was evaluated compared to MOCK and treated cell with various concentration of MGO. The viruses supernatant from this experiment also were harvested to further $TCID_{50}$ assay.

Various concentration of MGO were performed in 15-ml tube with MEM + vitamin. MDCK cells seeded in 24-well plates was washed with 1ml MEM (-), and then aspirated. 500 μl of each concentration of MGO was added to MDCK cells (For MOCK, 1ml MEM + vitamin was added instead). At the same time, influenza virus solution (A/WSN) was prepared at concentration of 1200$TCID_{50}$/ml and then added 500 μl diluted virus solution to each well of 24-well plate (600$TCID_{50}$/well). Infected MDCK cells were incubated at 37°C, 5% CO_2 incubator for 3 days.

After 3-day incubation, morphology of MDCK cells was snapped using Axiocam MRm camera microscope. The virus supernatant was collected to 1.5ml tube, then centrifuged at 6,000 rpm, 4°C for 10 minutes. The virus supernatant was used for determination of virus yields using $TCID_{50}$ assay. After that, the WST-1 assay and CV staining were performed respectively.

2.2.8 Determine mode of action of MGO by Plaque Inhibition assay

To determine mode of action of MGO, the plaque inhibitory assay was performed. MDCK cells were seeded in 6-well plates at a density of 1.0×10^6 cells/well (2ml), then kept these plates in 37°C, 5% CO_2 incubator overnight. Zanamivir was selected as a positive control.

Original influenza virus solution was diluted to 10^4 –fold dilution in 1.5-ml tube and always keep on ice. MDCK cells seeded on the previous day were washed with 1ml of MEM (-), and then aspirated. MDCK cells were added with 500μl of 10^4 –fold dilution influenza virus following below chart. After infection of influenza virus, 6-well plates were incubated in 37°C, 5% CO_2 incubator for 1 hour. During 1 hour of incubation, rocking plate every 15 minute was required in order to prevent drying of surface of MDCK cells. Approximately 300 plaque-forming units (pfu) of virus in MEM-vitamin were used for infection. The detailed procedures for each treatment are as follows: (i) Pretreatment of cells; before plaque inhibitory assays, MDCK cells were pretreated with test samples at 37°C for 1 h. After the medium was removed, cells were washed with MEM and infected by adding the viral suspension containing 300 pfu of virus in MEM-vitamin. (ii) Pretreatment of virus; approximately 10^7 pfu/ml of virus stock was preincubated with the test samples at room temperature for 1 h. These mixtures were subsequently diluted in MEM-vitamin to obtain approximately 600 pfu/ml, and 500 μl aliquots of the diluted mixtures (300pfu) were used for infection. (iii) The treatment occurred during infection; 250-μl aliquots of the test samples in MEM-vitamin were added to the MDCK cells, followed by 250 μl of virus suspension (300 pfu). The cells were then incubated for 1 h. (iv) Treatment of cells after viral infection: after viral infection (300 pfu) for 1 h, the cells were overlaid with 3 ml of agarose solution containing the MGO samples and MEM supplemented with 0.8% agarose, 0.1% BSA, and 1% 100× vitamin solution.

During infection period, 2×Maintenance medium was prepared. 25 ml and 4 ml of 2×Maintenance medium was transferred to 50-ml tube and 15-ml tube, respectively. Both be kept in water bath controlled temperature at 37°C. The 2×Maintenance medium

containing in 15-ml tube is used for (iv) Treatment of cells after viral infection. MGO was added to this tube and controlled temperature at 37°C. 1.6%agarose solution was also melted using microwave and kept in water bath controlled temperature at 47°C prior to use.

After 1 hour of incubation, the virus solution was aspirated and MDCK cells were washed with 1ml MEM(-). Then, 25ml of melted agarose gel was transferred to 50-ml tube containing 2×Maintenance medium. Gently mixing was required before added 3 ml of 8%agarose/MM mixture to each well of 6-well plate for (i) Pretreatment of cells, (ii) Pretreatment of virus, and (iii) The treatment occurred during infection. As the same way, equal amount of 1.6%agarose gel (4ml) was transferred to 15-ml tube containing 4ml 2MM, then added to 6-well plate for (iv) Treatment of cells after viral infection. The 6-well plates overlaid with agarose solution were placed at room temperature until solidification was completed, then incubated in 37°C, 5% CO_2 incubator for 3 days.

After 3-day incubation, fixation process was performed. 1ml Ethanol and 1ml acetic acid were added to each well and stood for 1 hour at room temperature. After 1 hour, gel was gentle removed and carefully wash with tab water. 2ml 0.5% amido black was added to each well for staining and left for 1 hour at room temperature. Amido black was returned to a bottle and 6-well plates were washed with tab water, dried at room temperature, then plaques were counted.

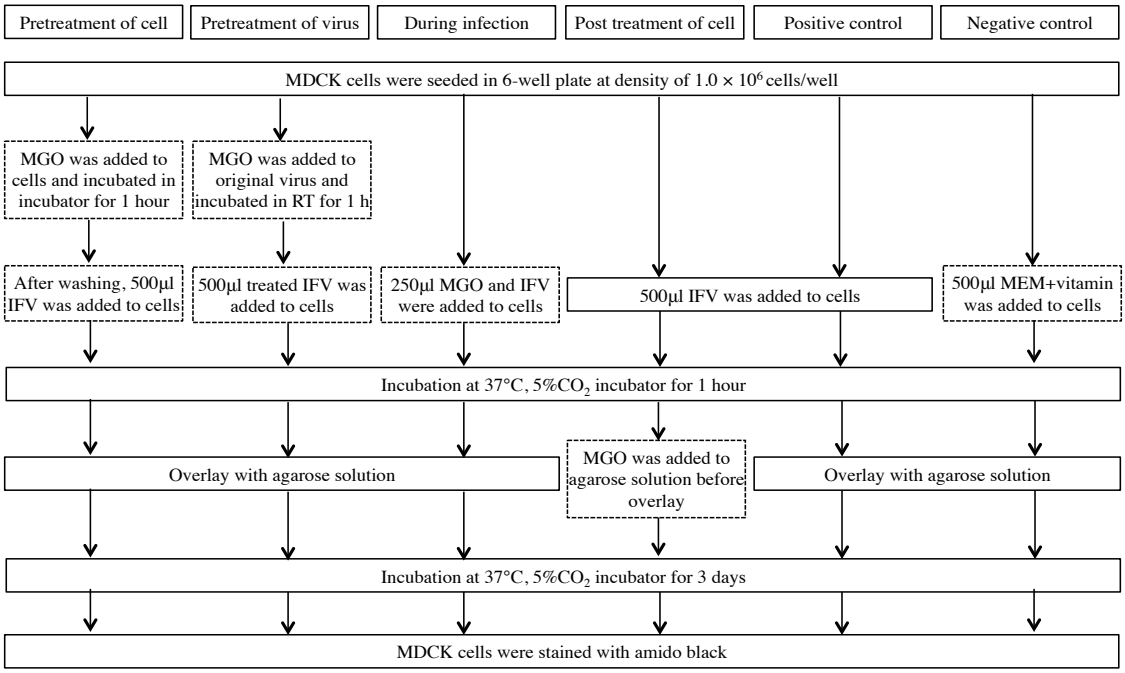

Figure 17 The flowchart of determination of mode of action of MGO

2.2.9 Evaluation of synergistic effect between commercial anti IFV drugs and MGO

The most important requirement of development anti IFV drugs is to obtain anti IFV drug in high efficacy with low cytotoxicity. MGO having anti IFV activity was selected to augment anti IFV activity of commercial anti IFV drugs.

The IC_{50} of commercial anti IFV drugs obtaining form previous experiments were used to settle optimal concentration of each commercial drug added together with MGO in order to increase anti IFV activity in lower concentration compared to using anti IFV drug alone.

2-fold dilution of MGO was prepared in horizontal axis while 2-fold dilution of each commercial drug was performed in vertical axis.

For 2-fold dilution of MGO, 120µl/well of E-MEM plus vitamin was added to row B to row H, then 240µl/well of 400µg/ml /MGO was added to row A. 120µl/well of the row A was transferred to the row B using multichannel pipette and pipetting several times to assure homogenous solution will be obtained. This procedure was continuously performed until reach row H.

For 2-fold dilution of commercial anti IFV drugs, the same procedure as previous experiment was performed. However, the concentration of each sample was slightly changed as shown as below procedure.

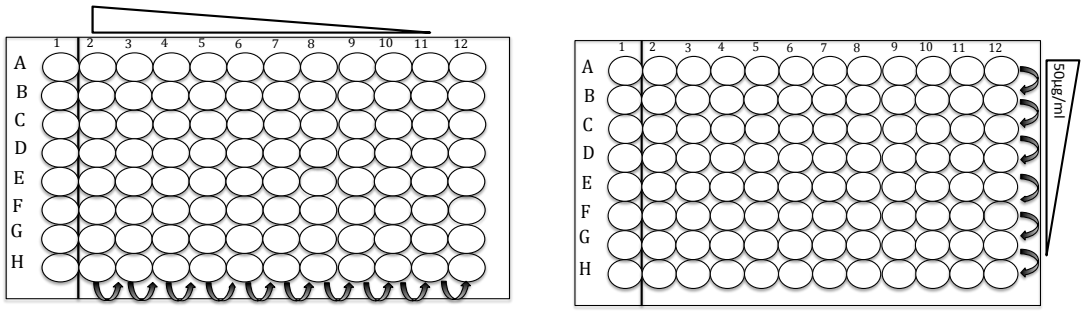

Figure 18 (left) Show the direction of preparation for 2-fold dilution of commercial drug and (right) show the direction of preparation for 2-fold dilution of MGO.

For oseltamivir, Stock solution of oseltamivir, 24mM was pipetted 10µl to 1.5 ml tube containing 990µl of E-MEM plus vitamin to obtain oseltamivir solution at 0.24mM. Next, 0.24mM oseltamivir was pipette 166.67µl to 1.5 ml tube containing 833.33µl of E-MEM plus vitamin. The final concentration is 40µM.

For zanamivir, Stock solution of zanamivir, 25mM was pipetted 5µl to 1.5 ml tube containing 995µl of E-MEM plus vitamin to obtain zanamivir solution at 0.125mM. Next, 0.125mM zanamivir was pipette 16µl to 1.5 ml tube containing 984µl of E-MEM plus vitamin. The final concentration is 2µM and %DMSO is 0.008%.

For laninamivir, Stock solution of laninamivir, 564.34mM was pipetted 5µl to 1.5 ml tube containing 995µl of E-MEM plus vitamin to obtain laninamivir solution at

2.82mM. Next, 2.82mM laninamivir was pipette 7.1µl to 1.5 ml tube containing 992.9µl of E-MEM plus vitamin. The final concentration is 20µM and %DMSO is 0.0035%.

For peramivir, Stock solution of peramivir, 30.5mM was pipetted 10µl to 1.5 ml tube containing 990µl of E-MEM plus vitamin to obtain peramivir solution at 0.305mM. Next, 0.305mM peramivir was pipette 10µl to 1.5 ml tube containing 990µl of E-MEM plus vitamin at 3.05µM. After that, 3.05µM was pipette 105µl to 1.5 ml tube containing 895µl of E-MEM plus vitamin. The final concentration is 0.32µM.

Since pandemic influenza virus outbreaks are serious public health concerns worldwide that cause considerable mortality and morbidity, we also examined the synergistic effect of MGO and oseltamivir against osetamivir-resistant pandemic influenza virus, A/Nagasaki/HA-58/2009. The 2-fold dilution of MGO and oseltamivir were prepared as described above with modification of plate layout.

For Oseltamivir, Stock solution of Oseltamivir, 24mM was pipetted 667µl to 15 ml tube containing 15ml of E-MEM plus vitamin to obtain Oseltamivir solution at final concentration as 1mM.

For 2-fold dilution of oseltamivir, 96-well plate was used. 120µl/well of E-MEM plus vitamin was added to 96-well plate except line 12^{th}, then 240µl/well of 1mM oseltamivir was added to line 12^{th}. 120µl/well oseltamivir of the line 12^{th} was transferred to the line 11^{th} using multichannel pipette and pipetting several times to assure homogenous solution will be obtained. This procedure was continuously performed until reach the line 3^{rd}. Discard 120µl/well oseltamivir from the line 3^{rd}. Finally, every well of 96-well plate contained 120µl/well.

Methylglyoxal 40% in H_2O purchased from Sigma, was diluted with E-MEM plus vitamin to obtain 2mg/ml MGO designed as initial concentration. 2-fold dilution of MGO was prepared in 50-ml tube. The first group started with addition of 720µl MGO at concentration of 2mg/ml into 50-ml tube containing 10ml E-MEM + vitamin to obtain 144µg/ml or 2000µM, then transferred 5ml of this concentration to next 50-ml tube containing 5ml E-MEM + vitamin to obtain 72µg/ml or 1000µM, then transferred 5ml of this concentration to next 50-ml tube containing 5ml E-MEM + vitamin to obtain 36µg/ml or 500µM. These concentrations of this group provided the final concentration of MGO at of 125, 250, and 500µM. The second group started with addition of 144µl MGO at concentration of 2mg/ml into 50-ml tube containing 10ml E-MEM + vitamin to obtain 28.8µg/ml or 400µM, then transferred 5ml of this concentration to next 50-ml tube containing 5ml E-MEM + vitamin to obtain 14.4µg/ml or 200µM, then transferred 5ml of this concentration to next 50-ml tube containing 5ml E-MEM + vitamin to obtain 7.2µg/ml or 100µM. These concentrations of this group provided the final concentration of MGO at of 25, 50, and 100 µM.

In 96-well plate containing serial 2-fold dilution of oseltamivir, 120µl/well of E-MEM plus vitamin was added to row A and B of both plates. The 120µl/well of serial 2-fold dilution of MGO also was transferred to 96-well plate containing serial 2-fold dilution of oseltamivir following the plate layout below

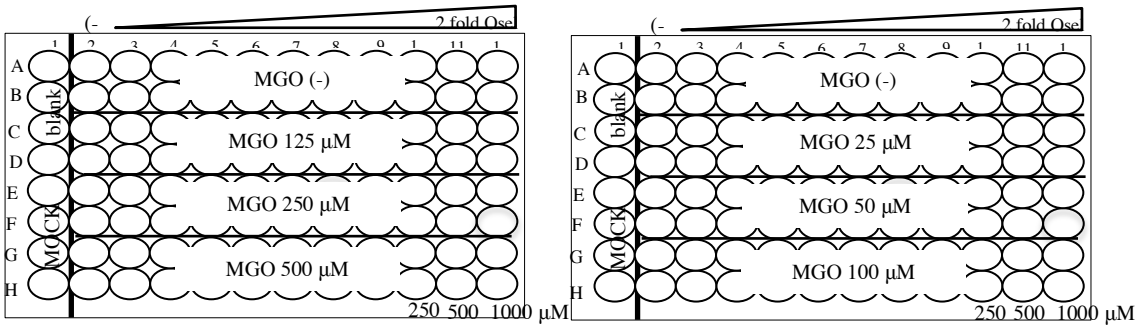

The evaluation of synergistic effect of MGO and oseltamivir against oseltamivir-resistant influenza strain was performed with different infectious dose of oseltamivir-resistant influenza virus. Trypsin also was required for influenza infectivity so 5μg/ml of trypsin would be prepared as final concentration in virus solution before infection. The A/Nagasaki/HA-58/2009 influenza virus was diluted to obtain a concentration of 1000, 62.5, and 31.25$TCID_{50}$/ml providing infectious dose at 100, 6.25, and 3.125$TCID_{50}$/well

CHAPTER 3: RESULTS

3.1 Cytotoxicity of commercial anti-influenza drugs

MDCK cells seeded in a 96-well plate on the previous day at a density of 3×10^4cells/well were washed with 100µl/well of MEM (-) and treated with 100µl/well of 2-fold diluted sample. The 96-well plate was shaken by Microplate genie for 30 seconds and then incubated in 37°C, 5%CO_2 incubator for 3 days.

The relative effectiveness of commercial drugs in inhibiting viral replication compared to inducing cell death is defined as selectivity index (SI). The selectivity index (SI) was calculated by dividing the CC_{50} by the IC_{50} (CC_{50}/IC_{50}). It is desirable to have a high therapeutic index giving maximum antiviral activity with minimal cell toxicity.

As shown in figure 19, (A) oseltamivir (0.02-12mM) showed CC_{50} of 1.78mM with cytotoxicity being observed in concentrations greater than this. (B) The serial dilution of zanamivir (0.2-100µM) added to MDCK cells lacked cytotoxicity on the cell. The solvent used for dissolve zanamivir is DMSO having cytotoxicity to MDCK cells when the percentage of DMSO is greater than 0.1% (data not shown). From this reason, increasing of concentration of zanamivir adding to MDCK cells could not be performed. Thus CC_{50} of zanamivir was defined as >100µM in this experiment condition. (C) The serial dilution of laninamivir (0.33-170µM) added to MDCK cells lacked cytotoxicity on the cell so CC_{50} of laninamivir was defined as >170µM. (D) The serial dilution of peramivir (0.03-15.25mM) added to MDCK cells lacked cytotoxicity on the cell so CC_{50} of peramivir was defined as >15.25mM. (E) The serial dilution of amantadine (0.16-80µM) added to MDCK cells lacked cytotoxicity on the cell so CC_{50} of

amantadine was defined as >80μM.

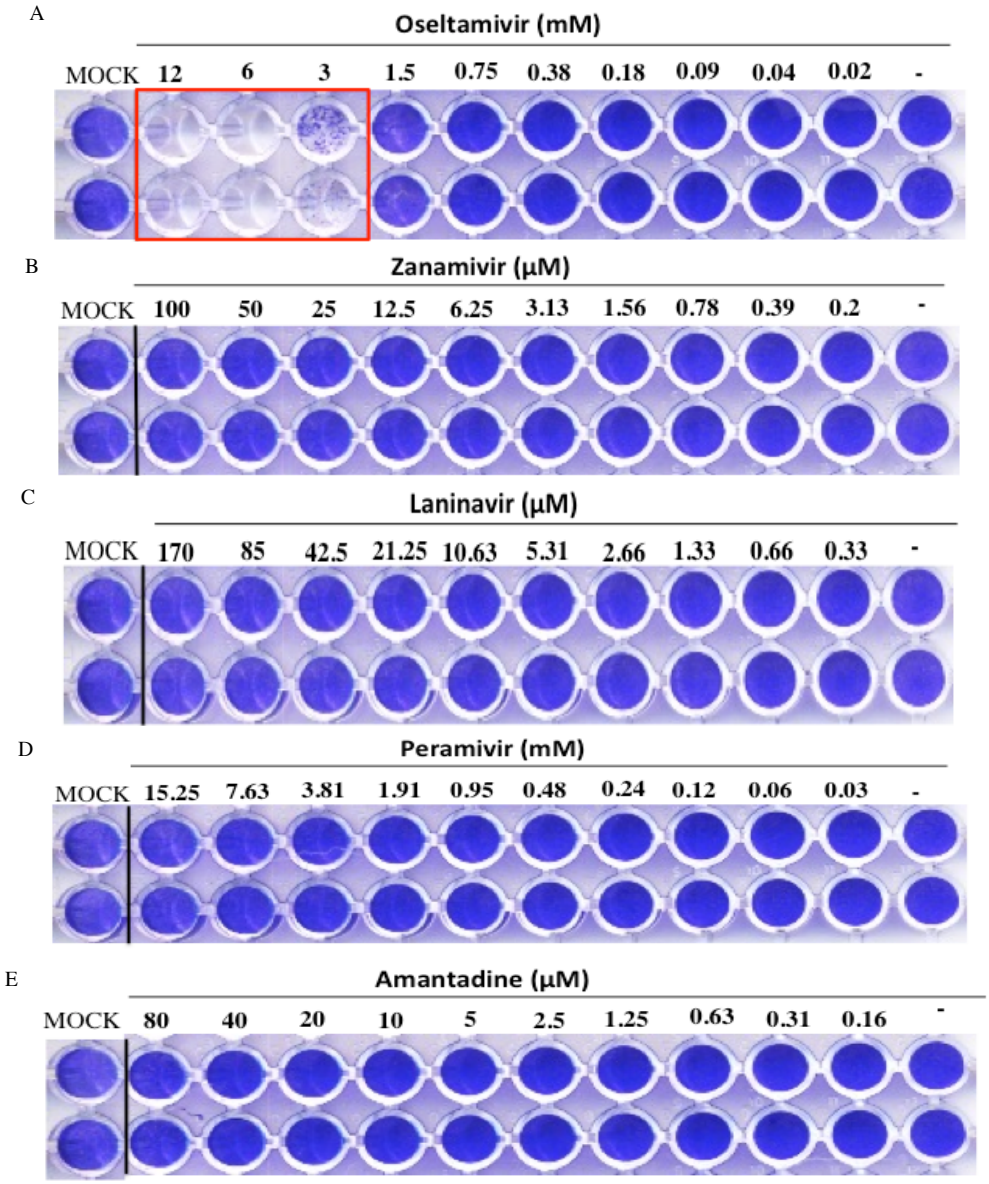

Figure 19 Toxicity of each commercial drug on uninfected MDCK cells. 2-fold serial dilution was added into MDCK cells (3×10^4cells/well) in a 96-well plate at 37°C for 72h. (A) A representative data obtained by CV staining. Red line is used to depict wells were cytotoxicity occurred due to high concentrations of oseltamivir. (B), (C), (D), and (E) A representative data obtained by CV staining for cytotoxicity of zanamivir, laninamivir, peramivir, and amantadine, respectively.

CC_{50} (μM)	oseltamivir	zanamivir	laninamivir	peramivir	amantadine
	1.78 mM	>100 μM	>170 μM	>15.25 mM	>80 μm

Table 4 The summarize CC_{50} of commercial anti influenza drugs

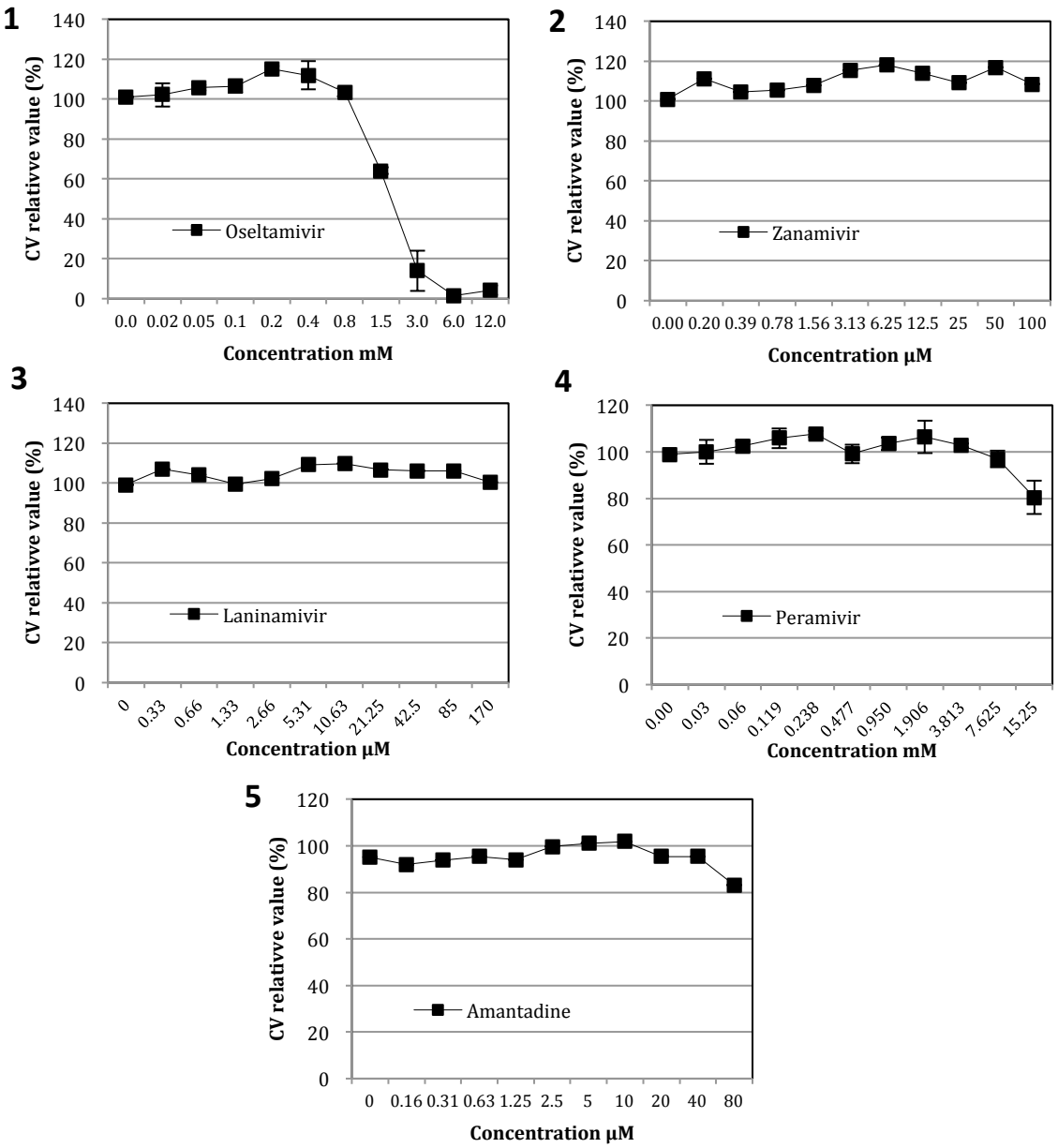

Figure 20 The Graphs show cytotoxicity of each commercial drugs to MDCK cell

3.2 Efficacy of various commercial drugs on various influenza virus A strains

MDCK cells seeded in a 96-well plate on the day before infection at a density of 3×10^4cells/well were treated with 100µl/well of 2-fold diluted sample and then infected with 100$TCID_{50}$/well of influenza virus solution in case of A/PR8, A/HK/8/68, A/Duck/Pennsylvania/84, and A/Nagasaki/HA-58/2009 (a oseltamivir-resistant IFV, trypsin is required for virus infection so 5µg/ml of trypsin would be prepared as final

concentration in virus solution before infection). The 96-well plate infected by various strains of influenza virus was shaken by Microplate genie for 30 seconds and then incubated in 37°C, 5%CO_2 incubator for 3 days. After 72 hours, MDCK cells morphology was observed under inverted light microscope and the virus induced CPE development (CPE reduction assay) was evaluated using crystal violet staining.

As shown in figure 21, 22, efficacy of each commercial anti-influenza drug against A/WSN/33 influenza strain was observed by staining with crystal violet. (A1) The inhibitory efficacy against A/WSN/33 influenza strain of oseltamivir and zanamivir were determined. 2-fold serial dilution of each drug (0.02-10μM) was added into MDCK cells infected with A/WSN/33. Oseltamivir showed IC_{50} against A/WSN/33 of 2.46μM while that of zanamivir was observed of 0.11μM. (A2) The representation of inhibitory against A/WSN/33 of laninamivir was shown. 2-fold serial dilution (0.33-170μM) was added into MDCK cells infected by A/WSN/33. The half maximal inhibitory concentration of laninamivir was defined of 1.22 μM. (A3) The representation of inhibitory against A/WSN/33 of peramivir was shown. 2-fold serial dilution (0.005-2.5μM) was added into MDCK cells infected by A/WSN/33. The IC_{50} of peramivir against A/WSN/33 was determined of 0.0132μM. (A4) The representation of inhibitory against A/WSN/33 of amantadine was shown. 2-fold serial dilution (0.16-80μM) was added into MDCK cells infected by A/WSN/33. The half maximal inhibitory concentration of amantadine was defined of 61.4μM (Table 5).

Virus strain	IC_{50} (μM)				
	oseltamivir	zanamivir	laninamivir	peramivir	amantadine
A/WSN/33	2.46	0.11	1.22	0.0132	61.4

Table 5 The summary IC_{50} of anti-influenza drugs against A/WSN/33

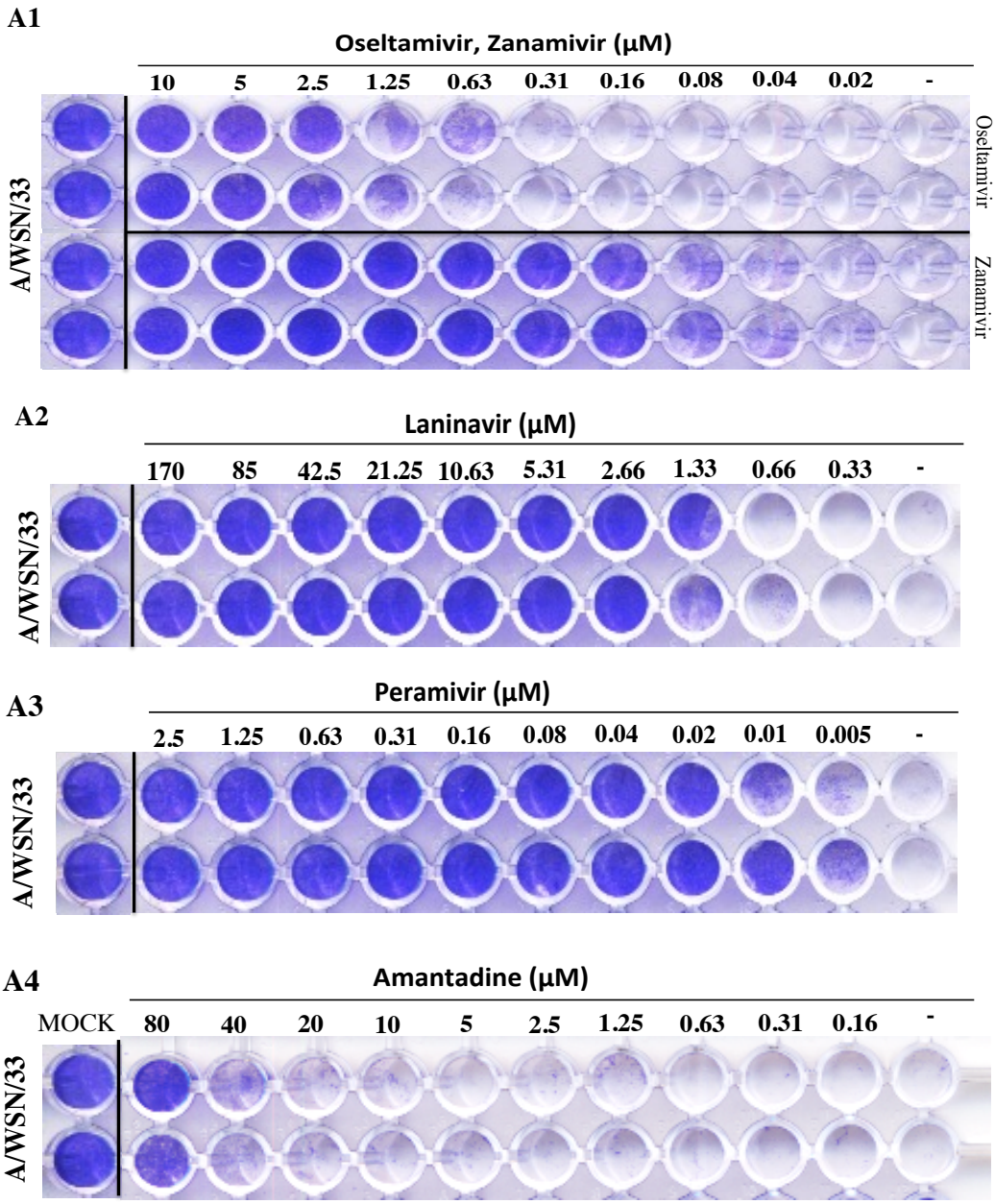

Figure 21 Efficiency of each commercial drug on infected MDCK cells by A/WSN/33 strain. 2-fold serial dilution was added into MDCK cells (3×10^4cells/well) in a 96-well plate at 37°C for 72h. (A1) A representative data obtained by CV staining to show the half maximal inhibitory concentration of oseltamivir and zanamivir in inhibiting virus growth defined as IC_{50}. (A2), (A3), and (A4) A representative data obtained by CV staining for the half maximal inhibitory concentration of laninamivir, peramivir, and amantadine, respectively.

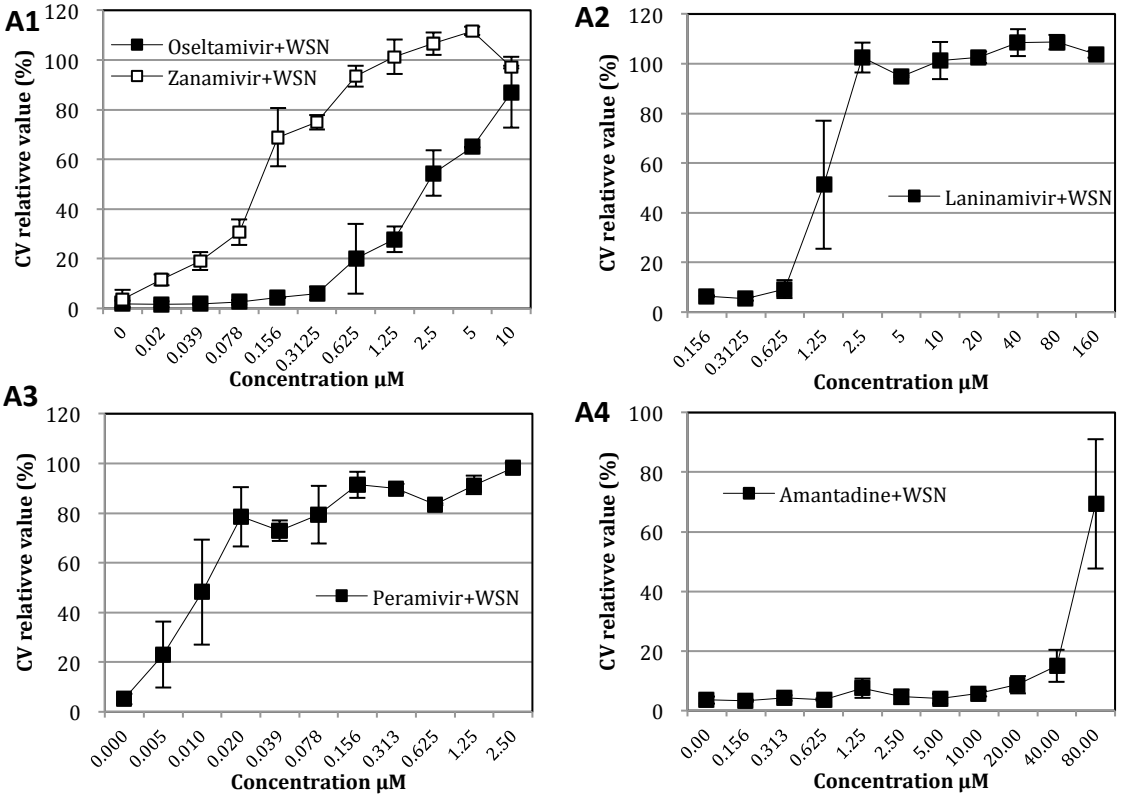

Figure 22 After infected with 100TCID$_{50}$/well A/WSN/33 influenza virus, viable MDCK cells were obtained by CV staining. The graph plotted between CV relative value (%) of viable MDCK cells and concentration of each drug (μM) was shown.

The efficiency of commercial anti-influenza drugs inhibiting viral growth of A/PR/8 strain was shown in figure 23, 24. The efficacy of each commercial anti-influenza drug against A/PR/8 influenza strain was observed by staining with crystal violet. (B1) The inhibitory efficacy against A/PR/8 influenza strain of oseltamivir and zanamivir were determined. 2-fold serial dilution of each drug (0.02-10μM) was added into MDCK cells infected with A/PR/8. Oseltamivir showed IC_{50} against A/PR/8 of 9.43μM while that of zanamivir was observed of 0.024μM. (B2) The representation of inhibitory against A/PR/8 of laninamivir was shown. 2-fold serial dilution (0.33-170μM) was added into MDCK cells infected by A/PR/8. The half maximal inhibitory concentration of laninamivir was defined of 1.62μM. (B3) The representation of inhibitory against

A/PR/8 of peramivir was shown. 2-fold serial dilution (0.005-2.5μM) was added into MDCK cells infected by A/PR/8. The IC_{50} of peramivir against A/PR/8 was determined of 0.06μM. (B4) The representation of inhibitory against A/PR/8 of amantadine was shown. 2-fold serial dilution (0.16-80μM) was added into MDCK cells infected by A/PR/8. However, amantadine could not inhibit CPE development in cells incubated with A/PR/8 (Table 6). A/PR/8 is apparently amantadine-resistant.

Virus strain	**IC_{50} (μM)**				
	oseltamivir	zanamivir	laninamivir	peramivir	amantadine
A/PR/8	9.43	0.024	1.62	0.06	>80

Table 6 The summary IC_{50} of anti-influenza drugs against A/PR/8

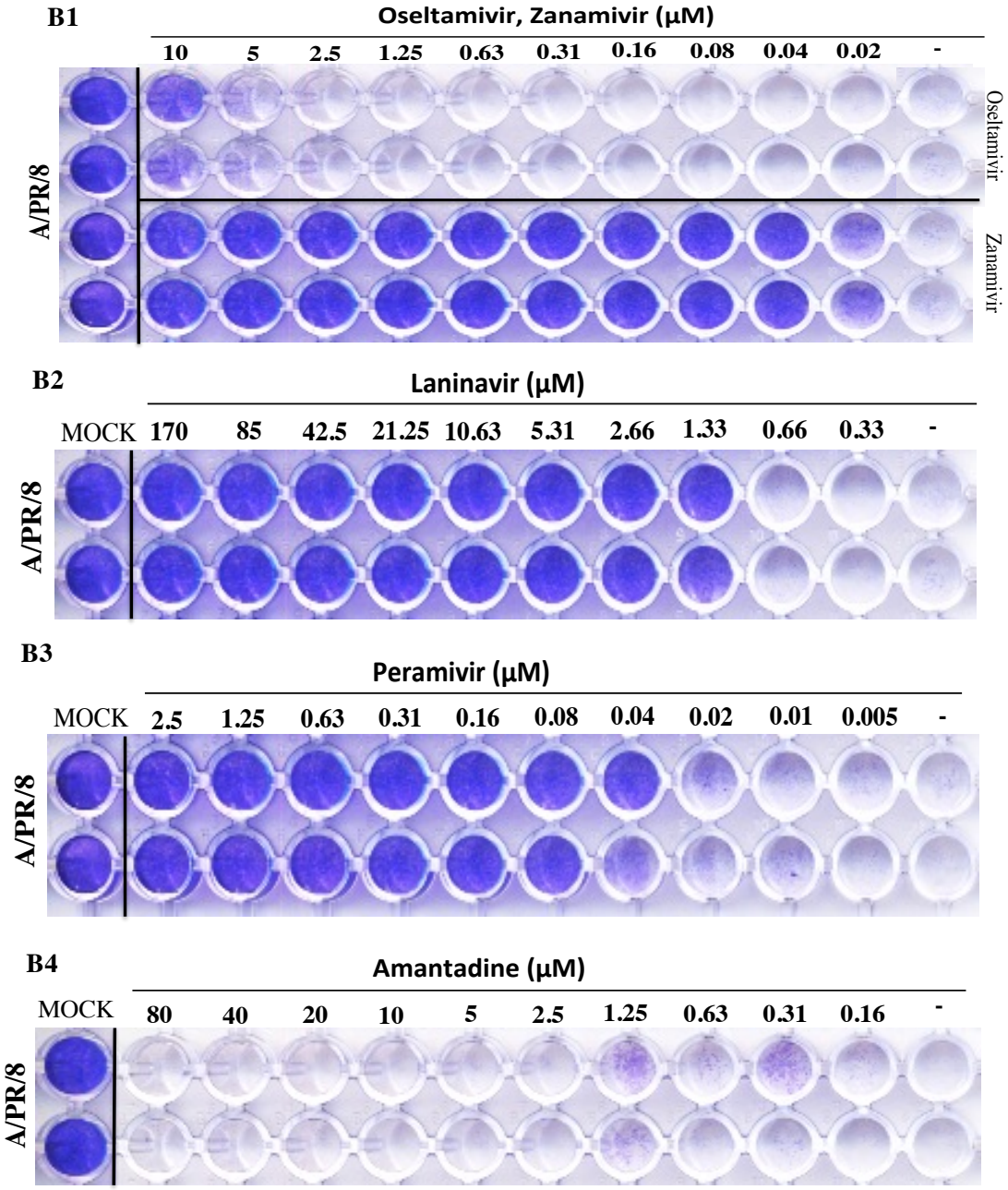

Figure 23 Efficiency of each commercial drug on infected MDCK cells by A/PR/8 strain. 2-fold serial dilution was added into MDCK cells (3×10^4cells/well) in a 96-well plate at 37°C for 72h. (B1) A representative data obtained by CV staining to show the half maximal inhibitory concentration of oseltamivir and zanamivir in inhibiting virus growth defined as IC_{50}. (B2), (B3), and (B4) A representative data obtained by CV staining for the half maximal inhibitory concentration of laninamivir, peramivir, and amantadine, respectively.

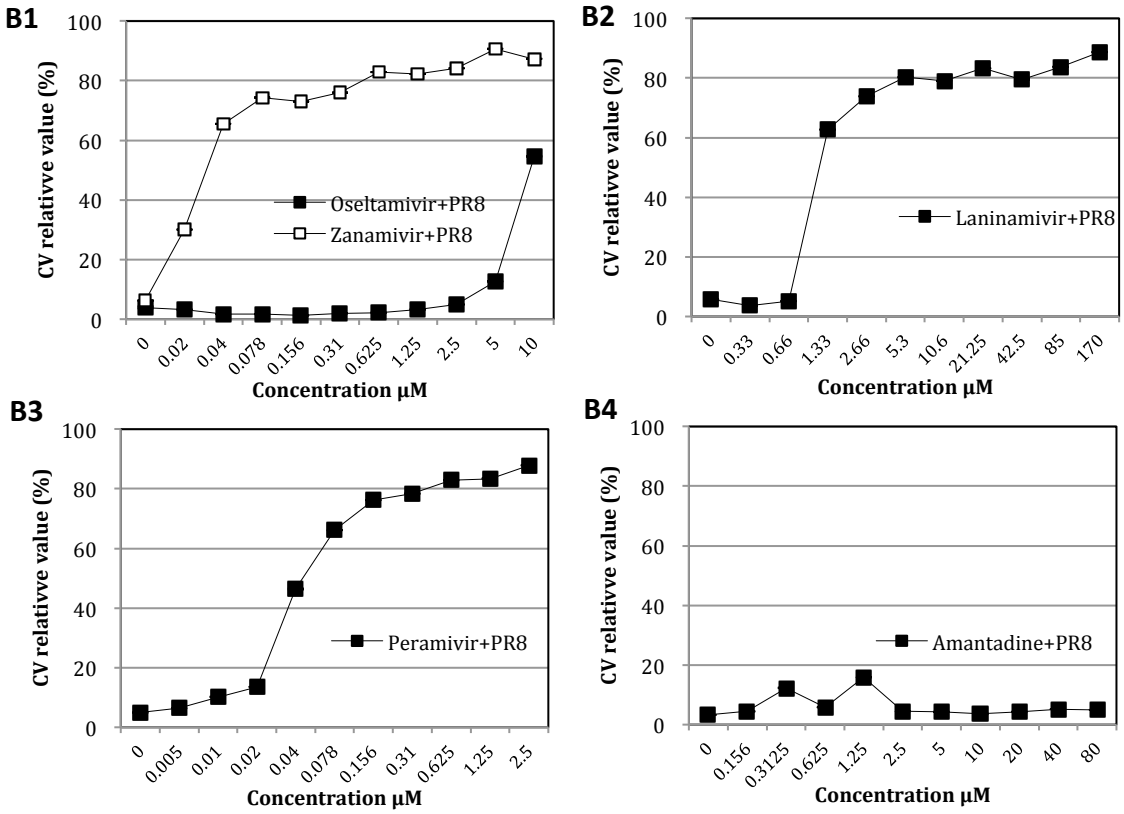

Figure 24 After infected with 100$TCID_{50}$/well A/PR/8 influenza virus, viable MDCK cells were obtained by CV staining. The graph plotted between CV relative value (%) of viable MDCK cells and concentration of each drug (μM) was shown.

Next, the half maximal inhibitory concentration of each commercial anti-influenza drug against A/HK/8/68 was evaluated as figure 25, 26. The efficacy of each drug against A/HK/8/68 influenza strain was observed by staining with crystal violet. (C1) The inhibitory efficacy against A/HK/8/68 influenza strain of oseltamivir and zanamivir were determined. 2-fold serial dilution of each drug (0.02-10μM) was added into MDCK cells infected with A/HK/8/68. Oseltamivir showed IC_{50} against A/HK/8/68 of 0.71μM while that of zanamivir was observed of 0.11μM. (C2) The representation of inhibitory against A/HK/8/68 of laninamivir was shown. 2-fold serial dilution (0.33-170μM) was added into MDCK cells infected by A/HK/8/68. The half maximal inhibitory concentration of laninamivir was defined of 2.95μM. (C3) The representation

of inhibitory against A/HK/8/68 of peramivir was shown. 2-fold serial dilution (0.005-2.5μM) was added into MDCK cells infected by A/HK/8/68. In spite of addition of the lowest concentration of peramivir, CPE development in cell was suppressed so IC_{50} of peramivir against A/HK/8/68 was determined of <0.005μM. (C4) The representation of inhibitory against A/HK/8/68 of amantadine was shown. 2-fold serial dilution (0.16-80μM) was added into MDCK cells infected by A/HK/8/68. The IC_{50} of amantadine was defined of 1.28μM (Table 7).

Virus strain	**IC_{50} (μM)**				
	oseltamivir	zanamivir	laninamivir	peramivir	amantadine
A/HK/68	0.71	0.11	2.95	<0.005	1.28

Table 7 The summary IC_{50} of anti-influenza drugs against A/HK/68

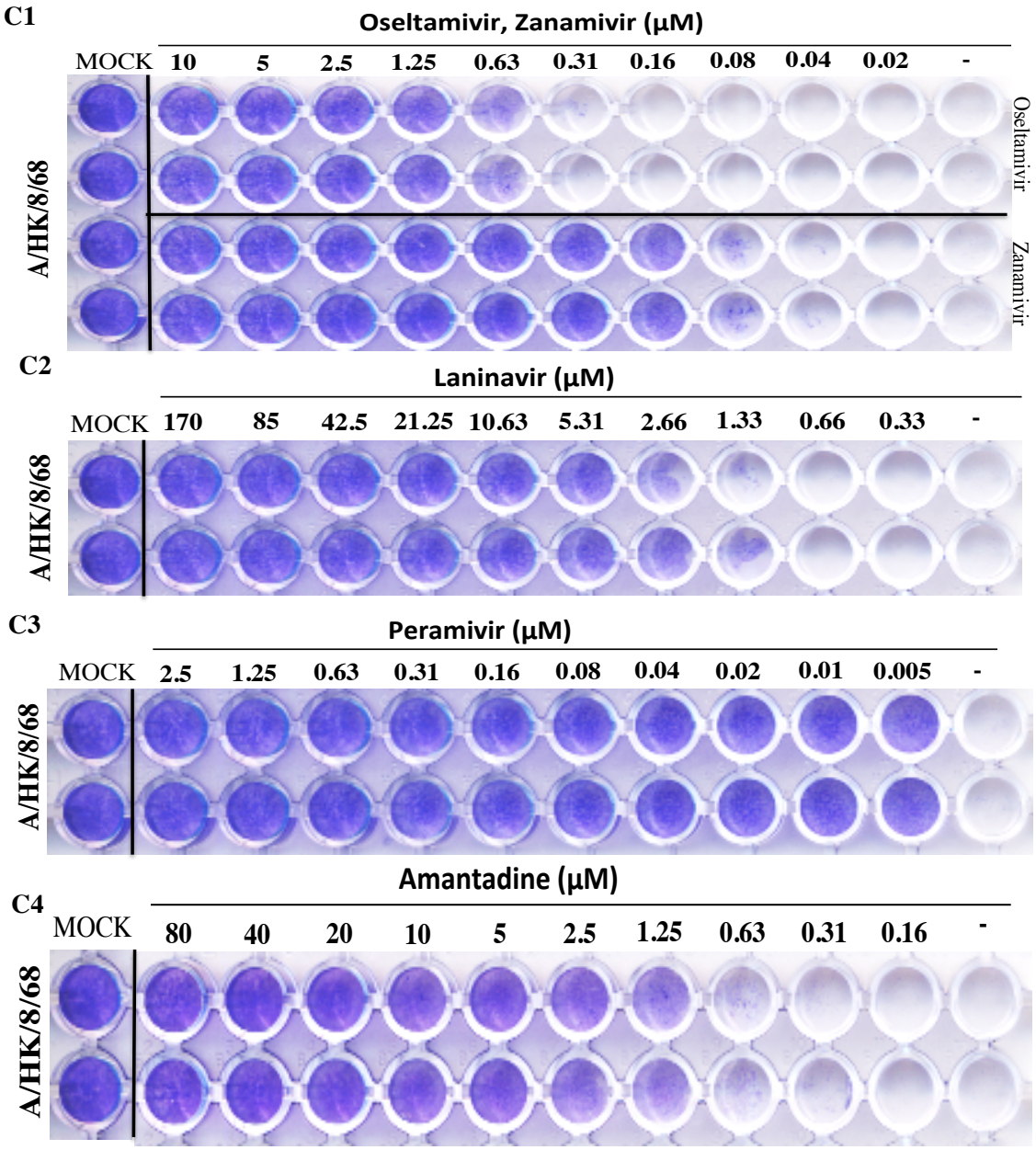

Figure 25 Efficiency of each commercial drug on infected MDCK cells by A/HK/8/68 strain. 2-fold serial dilution was added into MDCK cells (3×10^4cells/well) in a 96-well plate at 37°C for 72h. (C1) A representative data obtained by CV staining to show the half maximal inhibitory concentration of oseltamivir and zanamivir in inhibiting virus growth defined as IC_{50}. (C2), (C3), and (C4) show a representative data obtained by CV staining for the half maximal inhibitory concentration of laninamivir, peramivir, and amantadine, respectively.

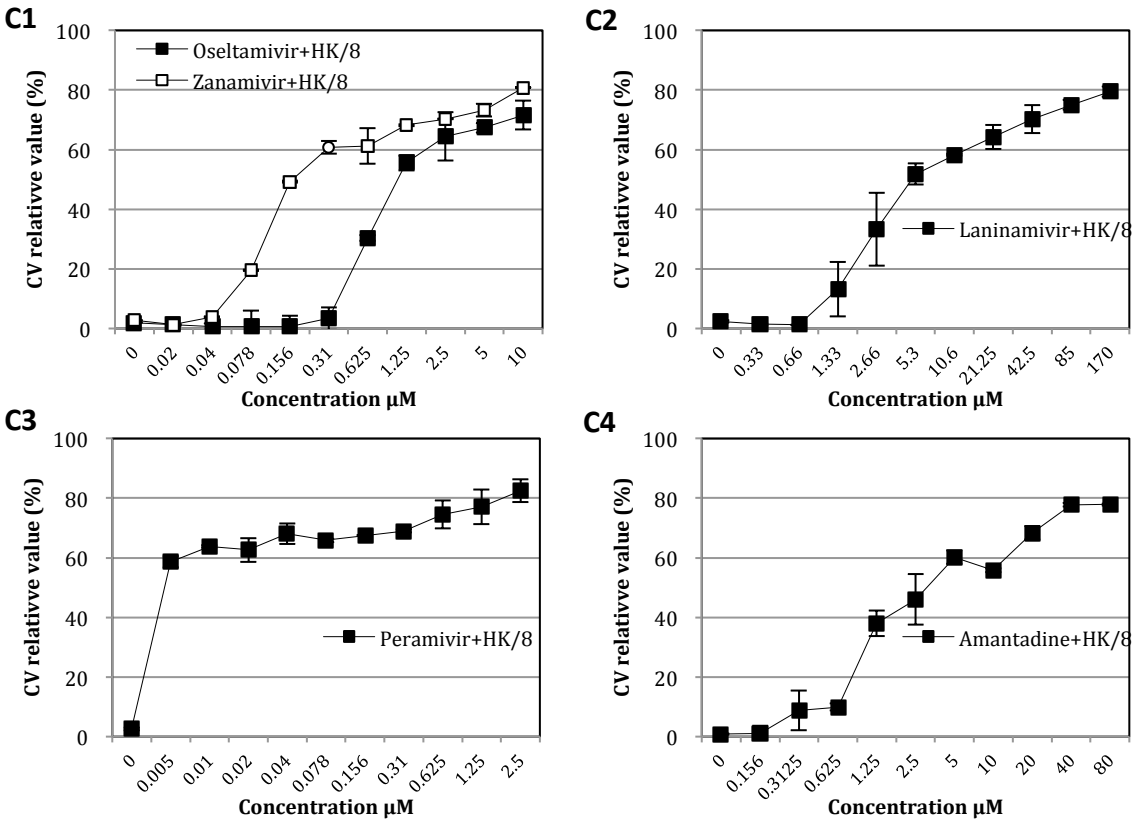

Figure 26 After infected with 100$TCID_{50}$/well A/HK/8/68 influenza virus, viable MDCK cells were obtained by CV staining. The graph plotted between CV relative value (%) of viable MDCK cells and concentration of each drug (µM) was shown

The other influenza strain, A/Duck/Pennsylvania/84, also was evaluated against serial dilution of various commercial drugs to obtain the half maximal inhibitory concentration. The efficacy of each drug against A/Duck/Pennsylvania84 influenza strain was observed by staining with crystal violet. The results were shown as figure 27, 28 (D1) The inhibitory efficacy against A/Duck/Pennsylvania84 influenza strain of oseltamivir was determined. 2-fold serial dilution of oseltamivir (0.04-20µM) was added into MDCK cells infected with A/Duck/Pennsylvania84. Oseltamivir showed IC_{50} against A/Duck/Pennsylvania84 of 7.9µM while (D2) that of zanamivir adding into MDCK cells at concentration range of 0.02-10µM was observed of 1.14µM. (D3) The representation of inhibitory against A/Duck/Pennsylvania84 of laninamivir was shown. 2-fold serial dilution (0.33-170µM) was added into MDCK cells infected by

A/Duck/Pennsylvania84. The half maximal inhibitory concentration of laninamivir was defined of 44.6μM. (D4) The representation of inhibitory against A/Duck/Pennsylvania84 of peramivir was shown. 2-fold serial dilution (0.005-2.5μM) was added into MDCK cells infected by A/Duck/Pennsylvania84. The IC_{50} of peramivir against A/Duck/Pennsylvania84 was found of 4nM. (D5) The representation of inhibitory against A/Duck/Pennsylvania84 of amantadine was shown. 2-fold serial dilution (0.16-80μM) was added into MDCK cells infected by A/Duck/Pennsylvania84. The IC_{50} of amantadine was defined of 14.9μM (Table 8).

Virus strain	**IC_{50} (μM)**				
	oseltamivir	zanamivir	laninamivir	peramivir	amantadine
A/DP/84	7.9	1.14	44.6	0.004	14.9

Table 8 The summary IC_{50} of anti-influenza drugs against A/DP/84

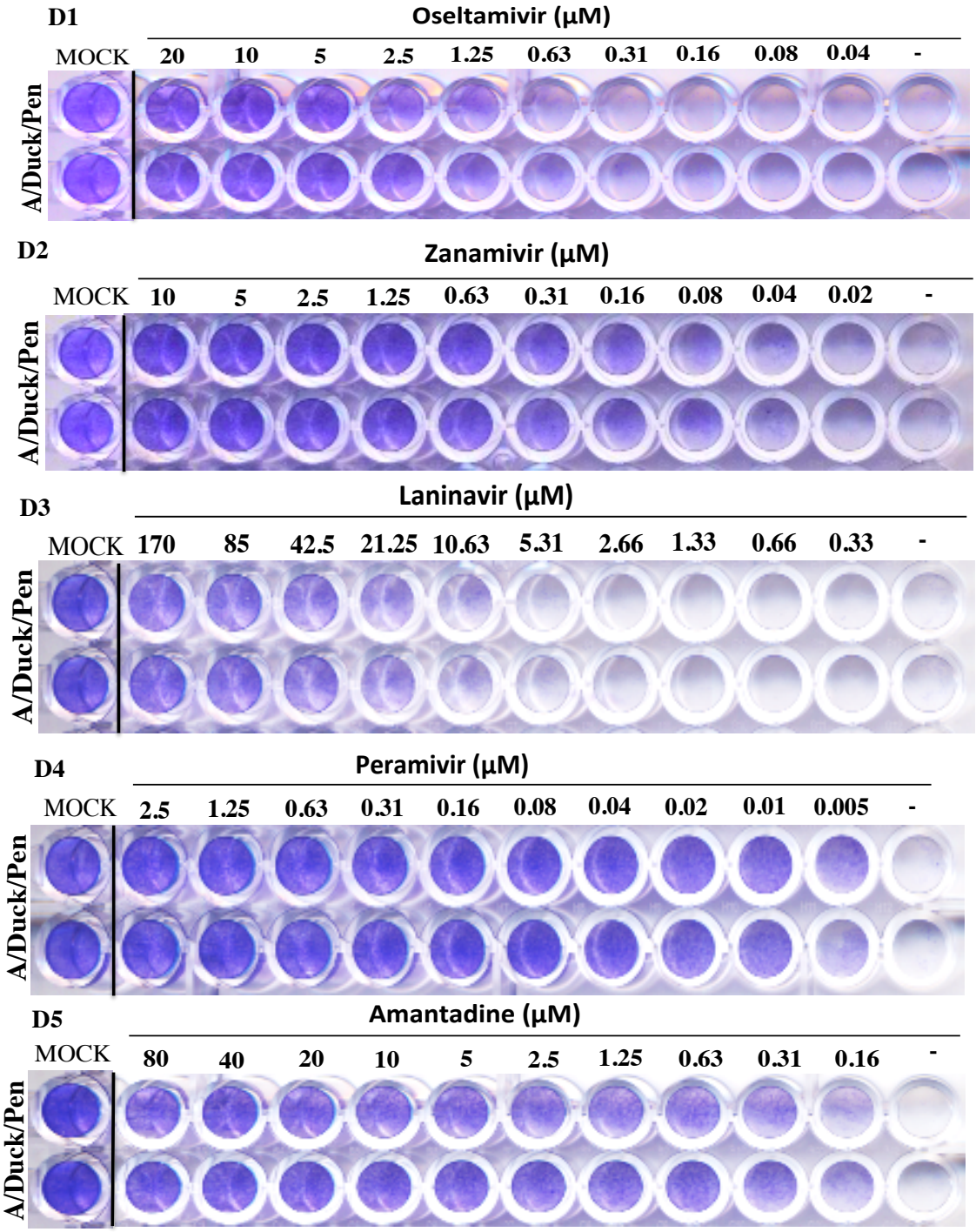

Figure 27 Efficiency of each commercial drug on infected MDCK cells by A/Duck/Pennsylvania/84 strain. 2-fold serial dilution was added into MDCK cells (3×10^4cells/well) in a 96-well plate at 37°C for 72h. (D1) A representative data obtained by CV staining to show the half maximal inhibitory concentration of oseltamivir in inhibiting virus growth defined as IC_{50}. (D2), (D3), (D4) and (D5) show a representative data obtained by CV staining for the half maximal inhibitory concentration of zanamivir, laninamivir, peramivir, and amantadine, respectively.

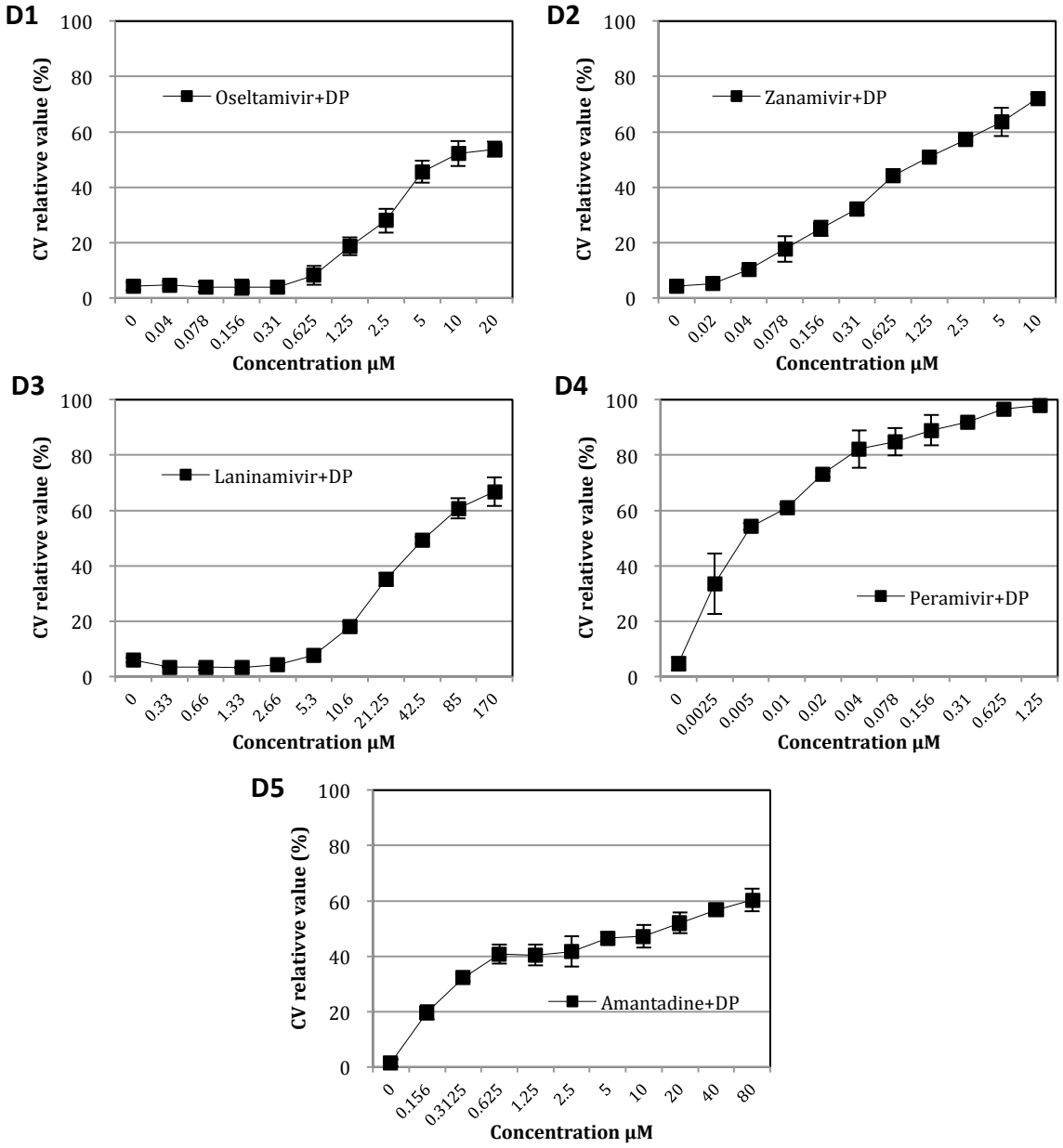

Figure 28 After infected with 100TCID$_{50}$/well A/duck/Pennsylvania/84 influenza virus, viable MDCK cells were obtained by CV staining. The graph plotted between CV relative value (%) of viable MDCK cells and concentration of each drug (μM) was shown

The oseltamivir-resistant influenza virus strain, A/Nagasaki/HA-58/2009 also was evaluated against serial dilution of various commercial drugs to obtain the half maximal inhibitory concentration. The efficacy of each drug against A/Nagasaki/HA-58/2009 influenza strain was observed by staining with crystal violet. The results were shown as figure 29. The inhibitory efficacy against A/Nagasaki/HA-58/2009 influenza strain of oseltamivir was determined. 2-fold serial dilution of oseltamivir (1.95-1000μM) was added into MDCK cells infected with A/Nagasaki/HA-58/2009. Oseltamivir did not provide IC_{50} against A/Nagasaki/HA-58/2009 due to resistant to oseltamivir of this virus strain (>870μM) (E1). Previously, we determined partial sequence of NA gene of this strain and we found that it contains H257Y mutation gene. (E2) Zanamivir adding into MDCK cells at concentration range of 0.02-10μM was observed of 0.11μM. (E3) The representation of inhibitory against A/Nagasaki/HA-58/2009 of laninamivir was shown. 2-fold serial dilution (0.33-170μM) was added into MDCK cells and infected by A/Nagasaki/HA-58/2009. The half maximal inhibitory concentration of laninamivir was defined of 3.2μM. (E4) The representation of inhibitory against A/Nagasaki/HA-58/2009 of peramivir was shown. 2-fold serial dilution (0.005-2.5μM) was added into MDCK cells, and infected with A/Nagasaki/HA-58/2009. As expected, A/Nagasaki/HA-58/2009 was resistant to peramivir (>2.5 μM) due to cross-resistace between oseltamivir as reported previously[89].

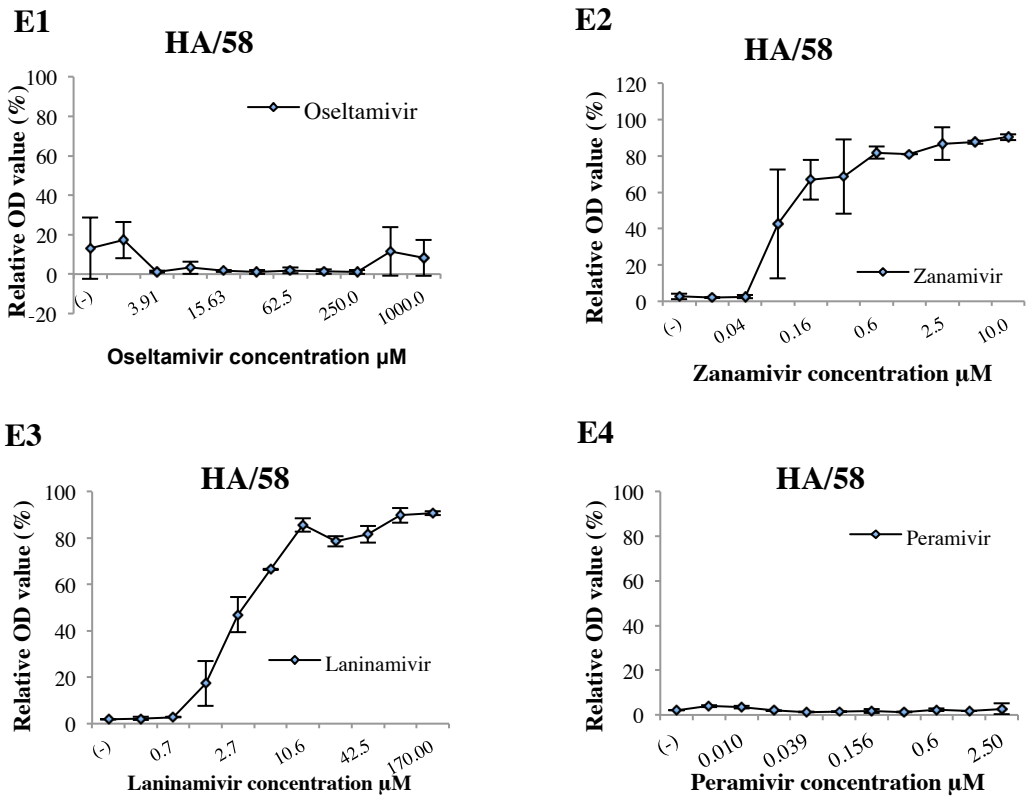

Figure 29 After infected with 100TCID$_{50}$/well A/Nagasaki/HA-58/2009 influenza virus, viable MDCK cells were obtained by CV staining. The graph plotted between CV relative value (%) of viable MDCK cells and concentration of each drug (μM) was shown

Virus strain	IC_{50} (μM)			
	oseltamivir	zanamivir	laninamivir	peramivir
A/HA/58	>870	0.11	3.2	>2.5

Table 9 The summary IC_{50} of anti-influenza drugs against A/HA-58

From above experiment, IC_{50} of each commercial drug against various influenza strains and CC_{50} of each commercial drug were obtained and selective index (SI) of each commercial drugs were calculated. It is desirable to have a high therapeutic index giving maximum antiviral activity with minimal cell toxicity. The summary of *In vitro* anti-influenza activity and cytotoxicity of commercial drugs against various influenza A strains was represented in Table 10.

3.3 Evaluation of IC_{50} and CC_{50} of MGO against various influenza A viruses

Preliminarily, MDCK cells seeded in a 96-well plate on the day before infection at a density of 3×10^4cells/well were treated with 2-fold diluted MGO and infected with 100$TCID_{50}$/well of influenza virus solution. In case of A/PR8, A/HK/8/68 and A/Duck/Pennsylvania/84, trypsin is required for virus infection so 5μg/ml of trypsin would be prepared as final concentration in virus solution before infection. The 96-well plate infected by various strains of influenza virus was shaken by Microplate genie for 30 seconds and then incubated in 37°C, 5%CO_2 incubator for 3 days. After 72 hours, MDCK cells morphology was observed under inverted light microscope and the virus induced CPE development (CPE reduction assay) was evaluated using crystal violet staining. The percentage of protection was calculated using same formula with the previous experiment;

As shown in figure 30, MDCK cells of 3.0×10^4/well treated with serial dilution of MGO before infected by various influenza strains were incubated for 72h in 37°C, 5%CO_2 incubator. CV staining was used for determination viable MDCK cells. (A) The IC_{50} of MGO against A/WSN/33 strain was obtains of 0.13μM while (B) show IC_{50} of MGO against A/PR/8 of 0.27μM. (C), (D) IC_{50} of MGO against A/HK/8/68 and A/Duck/Pennsylvania/84 were evaluated of 0.32μM and 0.16μM, respectively. (E) The graph plotted between CV relative viable MDCK (%)against concentration of MGO (μM) was illustrated.

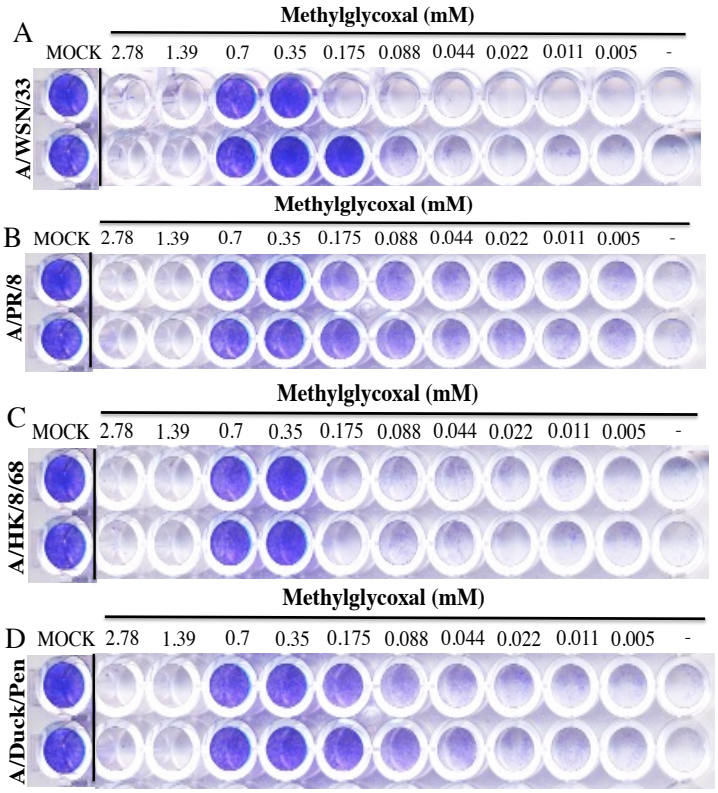

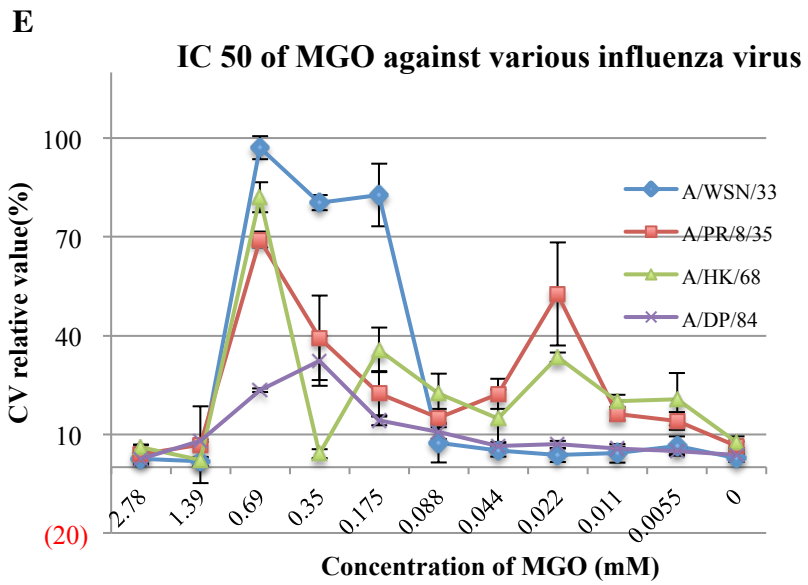

Figure 30 (A)(B)(C)(D) A representative data obtained by CV staining to show IC_{50} of MGO against A/WSN/33, A/PR/8, A/HK/8/68, and A/Duck/Pennsylvania/84, respectively. (E) All of representative data was shown together in graph plotted between CV relative viable MDCK (%) against concentration of MGO (μM).

We confirmed cytotoxicity of MGO using the WST-1 assay, which provides a sensitive and accurate method to measure activity of mitochondria and this method is often used to show cellular activity. Moreover, morphology of MDCK cells treated with various concentration of MGO was taken by camera microscope compared to normal MDCK cells. As shown in Figure 31A CC_{50} valued evaluated by the WST-1 assay and CC staining was similar (1.6 ± 0.4 mM vs. 1.4 ± 0.4 mM, respectively). Cell morphology (Figure 31B) seem to be correlated to the relative OD values observed in Figure 31C. We decided to select the CV staining method for further evaluation. We next evaluated anti-influenza viral activity of MGO using MDCK cells (Figure 31C, D, and Table 10). The viral cytopathic effect (CPE) was suppressed in the presence of MGO in a dose-dependent manner for all influenza virus strains. The IC_{50} of MGO (previous result from preliminarily experiment also was calculated) against A/WSN/33 was 240 ± 190 μM (Figure 31C and Table 10), yielding an SI value (CC_{50}/IC_{50}) of 5.8. In the absence and the presence of 700 μM MGO, the virus yield was $5.9 \times 10^5 \pm 3.3 \times 10^5$ $TCID_{50}$/mL and undetectable. The anti-influenza viral activity of MGO against different influenza virus A strains was evaluated and compared to that of commercial NA inhibitors (Table 10). While NA inhibitors drastically differentially suppressed viral replication depending on the infecting strain, MGO showed only slight differential activity against all strains, including an oseltamivir-resistant A/Nagasaki/HA-58/2009 clinical isolate, which carries the H275Y mutation in the NA gene [2]. Cell morphology (Figure 31D) seems to be correlated to the relative OD value observed in Figure 31C. These results suggest that MGO suppressed influenza virus replication.

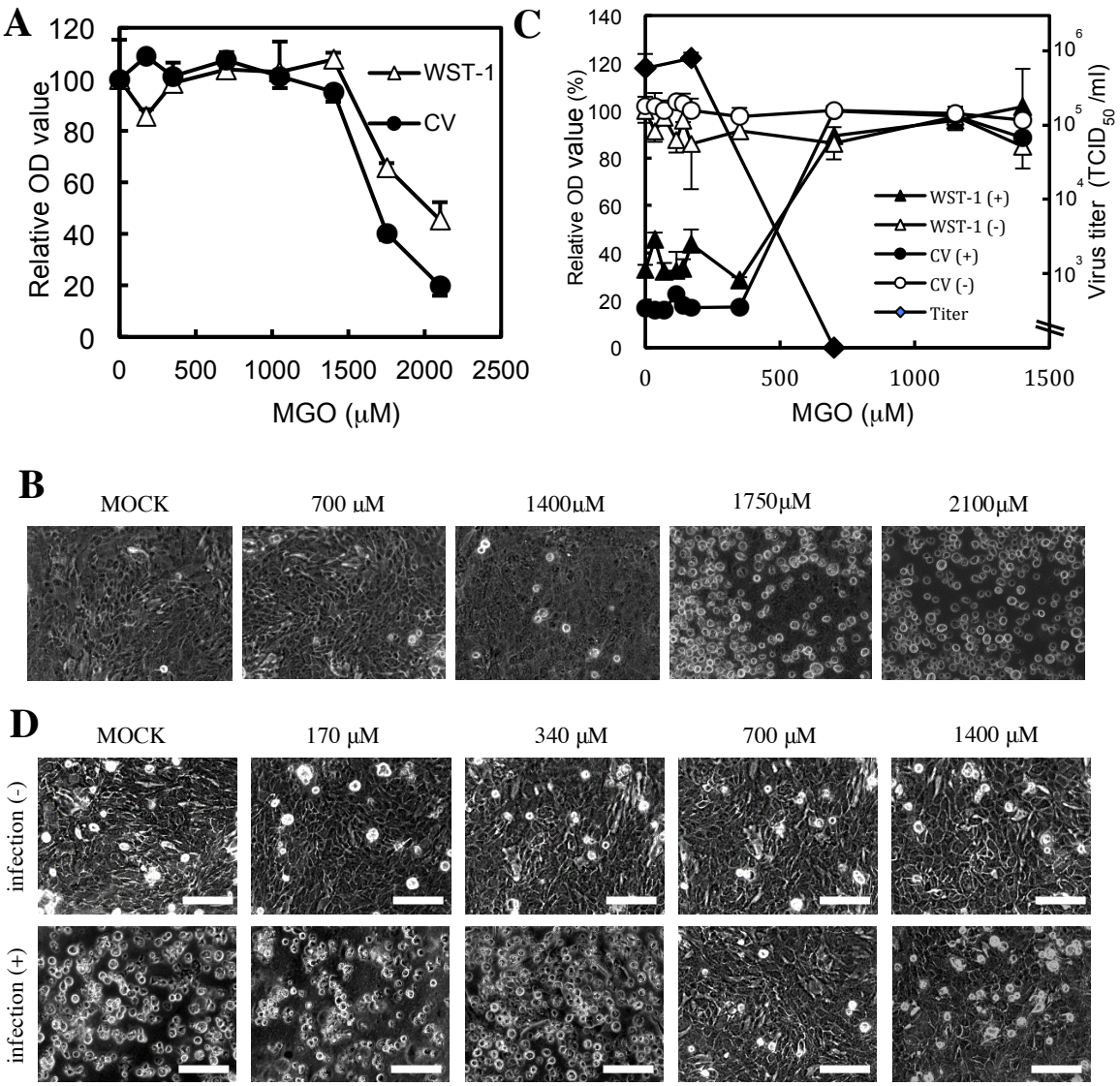

Figure 31 Anti-influenza activity of MGO Evaluation of the cytotoxicity and anti-influenza activity of MGO was performed as described in Methodology section. (A) Cytotoxicity of MGO. MDCK cells grown in 24-well plates were treated with serial dilution of MGO and left uninfected. Three days after infection, cytotoxicity was measured by the WST-1 assay (open triangles) or CV staining (close circles). Relative OD value (%) are expressed as the percentage of cells without MGO treatment. (B) Cell morphology of infected MDCK cells treated with increasing concentrations of MGO shown in (A) was compared with those of untreated cell Bar = 100μM. (C) Anti-influenza viral activity of MGO. MDCK cells grown in 24-well plates were treated with (close symbols) or without (open symbols) 600 $TCID_{50}$ of A/WSN/33 virus in the presence of MGO. Three days after infection, antiviral activity was measured using the WST-1 assay (triangles) and CV staining (circles). Relative OD value (%) are expressed as the percentage of uninfected cell (open symbols) without MGO treatment. Virus yields in the supernatant were also determined and represented (closed diamonds). (D) Cell morphology of infected MDCK cells treated with increasing concentration of MGO shown in (C) was compared with those of uninfected cells. Bar = 100μM. The data are representative of three independent experiments.

Table 10. Efficacy of NA inhibitors and MGO against various strains of influenza A virus

Compound	CC_{50}[a] (μM)	Virus	Subtype	IC_{50}[a](μM)	SI[b]
MGO	$1.4\times10^3 \pm 400$	WSN[c]	H1N1	240 ± 190	5.8
		PR8[d]	H1N1	360 ± 130	3.9
		HK[e]	H3N2	420 ± 140	3.3
		Duck Pen[f]	H5N2	180 ± 20	7.8
		HA-58[g]	H1N1	250 ± 140	5.6
Oseltamivir	$1.8\times10^3 \pm 30$	WSN	H1N1	2.5 ± 0.5	740
		PR8	H1N1	9.4 ± 0.9	190
		HK	H3N2	0.71 ± 0.03	2.6×10^3
		Duck Pen	H5N2	7.9 ± 4.9	230
		HA-58[g]	H1N1	>870	<2.1
Zanamivir	>100	WSN	H1N1	0.11 ± 0.02	>890
		PR8	H1N1	0.024 ± 0.001	$>4.1\times10^3$
		HK	H3N2	0.11 ± 0.03	>890
		Duck Pen	H5N2	1.1 ± 0.02	>88
		HA-58[g]	H1N1	0.11 ± 0.02	>910
Laninamivir	>170	WSN	H1N1	1.2 ± 0.3	>140
		PR8	H1N1	1.6 ± 0.1	>100
		HK	H3N2	3.0 ± 0.8	>58
		Duck Pen	H5N2	45 ± 4	>3.8
		HA-58[g]	H1N1	3.2 ± 0.3	>53
Peramivir	$>1.5\times10^4$	WSN	H1N1	0.011 ± 0.004	$>1.4\times10^6$
		PR8	H1N1	0.061 ± 0.020	$>2.5\times10^5$
		HK	H3N2	<0.0050	$>3.1\times10^6$
		Duck Pen	H5N2	0.0040 ± 0.0004	$>3.5\times10^6$
		HA-58[g]	H1N1	>2.5	N/A

[a] IC_{50}: 50% inhibitory concentration, CC_{50}: 50% cytotoxic concentration
[b] SI: selective index = CC_{50}/IC_{50}
[c] A/WSN/33
[d] A/Puerto Rico/8/34
[e] A/Hong Kong/8/68
[f] A/duck/Pennsylvania/1/84
[g] A/Nagasaki/HA-58/2009

3.4 Efficacy of various commercial drugs on various influenza virus B strains

Next, we evaluated inhibitory effect of commercial NA inhibitors against various influenza B strains to determine the susceptibility to each drug of several strains of influenza B viruses. The susceptibilities of NAIs have been considered to be dependent on the B lineage in the same manner as observed for different influenza A neuraminidase subtypes [62]. The criteria recommended by the World Health Organization (WHO) Antiviral Working Group for data interpretation of resistant phenotypes are related to fold changes in IC_{50} values compared with those of the susceptible viruses, and the criteria for influenza B viruses are different from that of influenza A viruses. Influenza B was described as having 'normal inhibition' (<five-fold higher IC_{50} than that of the reference susceptible virus), 'reduced inhibition, RI' (five-50-fold higher IC_{50} than that of the reference susceptible virus) or 'highly reduced inhibition, HRI' (>50-fold higher IC_{50} than that of the reference susceptible virus) [90].

Our results also revealed that the mean IC_{50} of oseltamivir against laboratory B strains (B/Lee/40 and B/Brisbane/60/2008) increased approximately ten-fold relative to the IC_{50} values against laboratory A strains (A/WSN/33, A/PR/8, A/HK), as shown in Figures 32A and 32B.

On the other hand, the efficacy of oseltamivir was not significantly different among the drug-sensitive clinical strains of A and B influenza viruses. For example, the IC_{50} value of oseltamivir against drug-sensitive clinical influenza A viruses (A/2009/no.6 and A/2009/no.33) ranged from 36–39 μM, which was not much different from that of oseltamivir against drug-sensitive clinical influenza B viruses (B/2014/6 and B/2014/8), which ranged from 11–33 μM (Figures 32C, 32D and Table 11). The IC_{50} of oseltamivir against drug-resistant influenza B viruses was also >500 μM.

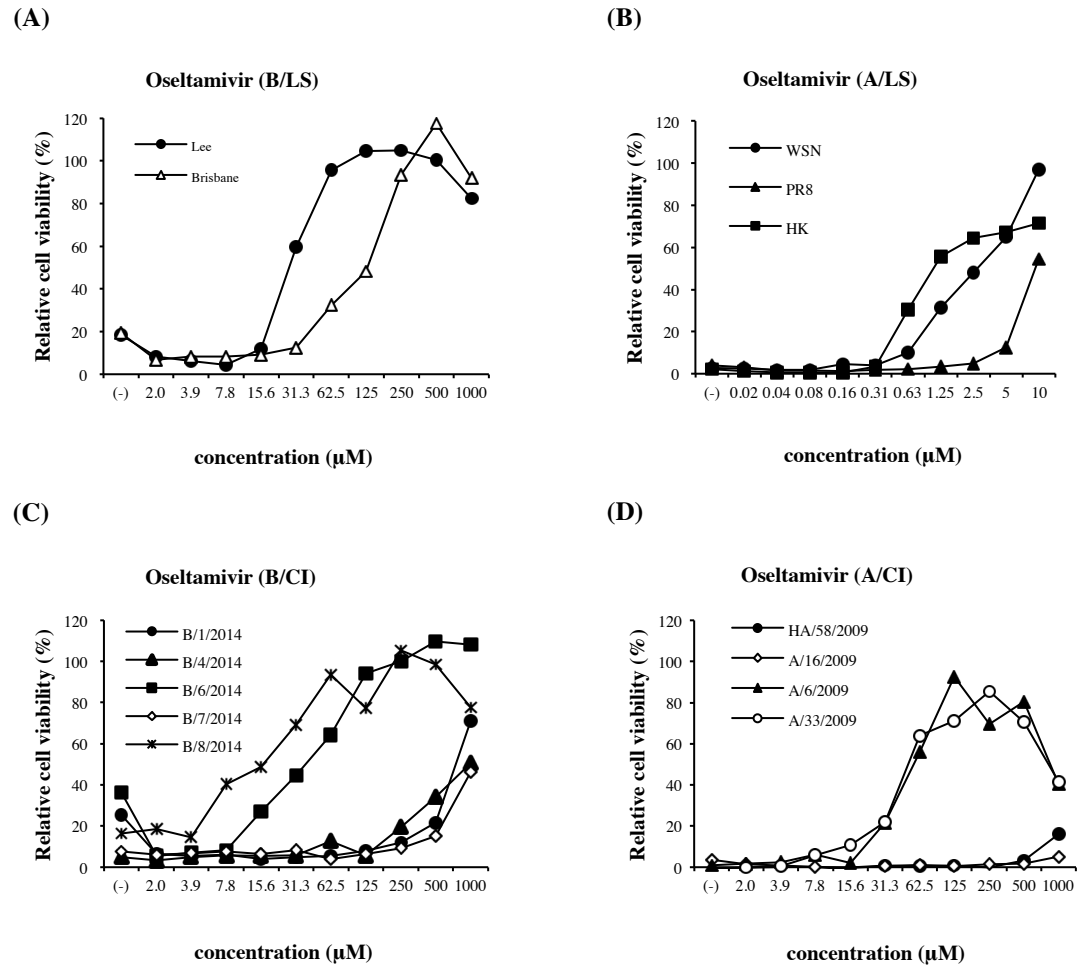

Figure 32 Anti-influenza viral activity of oseltamivir. Evaluation of the anti-influenza viral activity of oseltamivir was performed as described in the methods section. MDCK cells grown in 96-well plates were treated with serial dilutions of oseltamivir and then infected with various strains of influenza viruses. Three days after infection, cells were fixed and stained with CV, and absorbance was measured using a plate reader. A graph was plotted showing relative CV staining (%), expressed as a percentage of uninfected cells and concentration of oseltamivir (μM). (A), (B), (C), and (D) show the susceptibilities of oseltamivir to influenza B laboratory strains, influenza A laboratory strains, influenza B clinically isolated strains, and influenza A clinically isolated strains, respectively.

Resistance to zanamivir in influenza B was not detected in either laboratory strains or clinical strains (Figure 33A and 33C); however, the susceptibilities of some clinically isolated influenza B viruses decreased relative to those of the influenza A viruses (Figure 33B, 33D) (Table 11). Interestingly, emergence of influenza B viruses with

resistance to oseltamivir (Figure 32C) tended also to be resistant to laninamivir (Figure 34C) and peramivir (Figure 35C) (Table11)

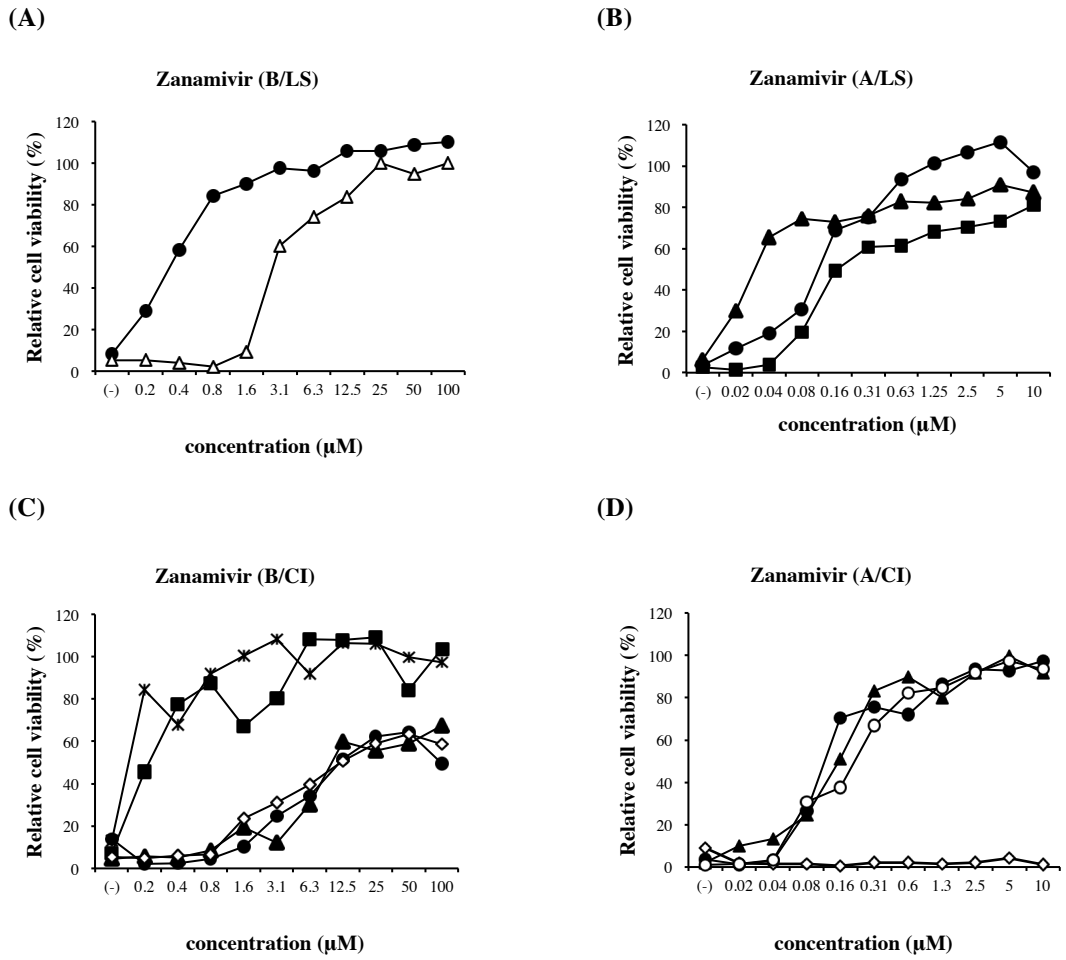

Figure 33 Anti-influenza viral activity of zanamivir. Evaluation of the anti-influenza viral activity of zanamivir was performed as described in the methods section. MDCK cells grown in 96-well plates were treated with serial dilutions of zanamivir and then infected with various strains of influenza viruses. Three days after infection, cells were fixed and stained with CV, and absorbance was measured using a plate reader. A graph was plotted showing relative CV staining (%), expressed as a percentage of uninfected cells and concentration of zanamivir (μM). (A), (B), (C), and (D) show the susceptibilities of zanamivir to influenza B laboratory strains, influenza A laboratory strains, influenza B clinically isolated strains, and influenza A clinically isolated strains, respectively.

Resistance of oseltamivir has also been shown to be cross-resistant to peramivir [89]. We also demonstrated correlations between the drug resistance of oseltamivir and peramivir not just for influenza A viruses (Figures 32D and 35D) but also for influenza

B viruses (Figures 32C and 35C). The susceptibility to peramivir of influenza B viruses dramatically decreased, as shown by the 20-fold and almost 70-fold increases in the mean IC_{50} values for laboratory strains and drug-sensitive clinical strains, respectively (Table 11). On the basis of the criteria recommended by WHO, influenza B was determined to show reduced inhibition and highly reduced inhibition to peramivir for laboratory strains and drug-sensitive clinical strains, respectively.

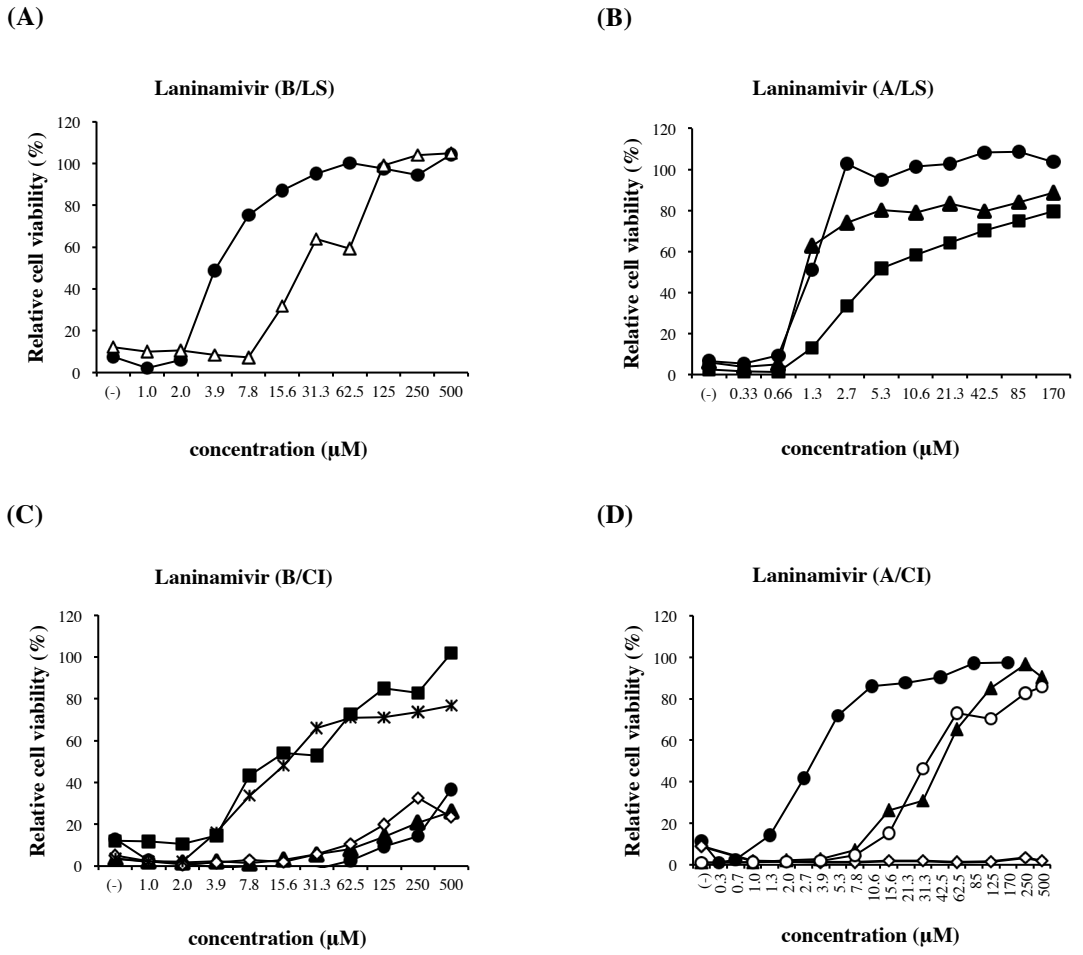

Figure 34 Anti-influenza viral activity of laninamivir. Evaluation of the anti-influenza viral activity of laninamivir was performed as described in the methods section. MDCK cells grown in 96-well plates were treated with serial dilutions of laninamivir and then infected with various strains of influenza viruses. Three days after infection, cells were fixed and stained with CV, and absorbance was measured using a plate reader. A graph was plotted showing relative CV staining (%), expressed as a percentage of uninfected cells and concentration of laninamivir (μM). (A), (B), (C), and (D) show the susceptibilities of laninamivir to influenza B laboratory strains, influenza A laboratory strains, influenza B clinically isolated strains, and influenza A clinically isolated strains, respectively.

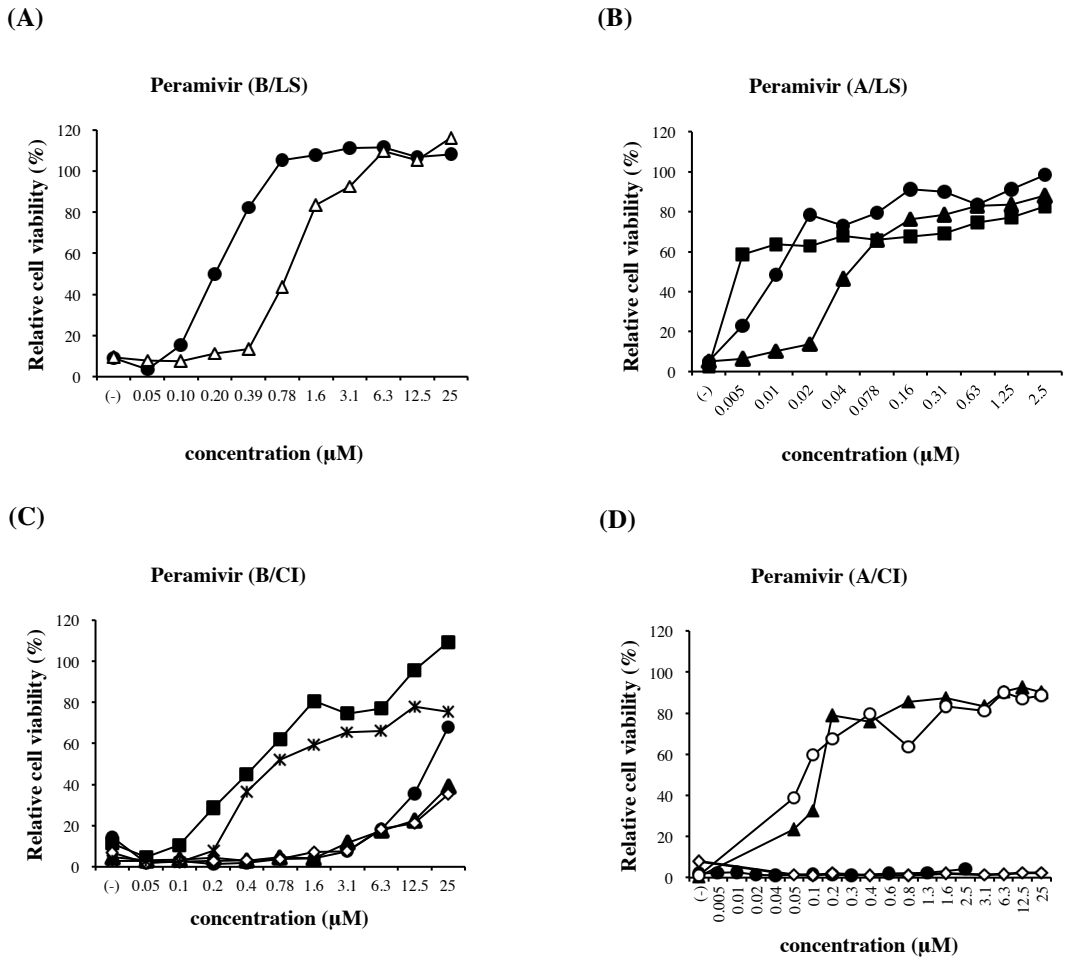

.Figure 35 Anti-influenza viral activity of peramivir. Evaluation of the anti-influenza viral activity of peramivir was performed as described in the methods section. MDCK cells grown in 96-well plates were treated with serial dilutions of peramivir and then infected with various strains of influenza viruses. Three days after infection, cells were fixed and stained with CV, and absorbance was measured using a plate reader. A graph was plotted showing relative CV staining (%), expressed as a percentage of uninfected cells and concentration of peramivir (μM). (A), (B), (C), and (D) show the susceptibilities of peramivir to influenza B laboratory strains, influenza A laboratory strains, influenza B clinically isolated strains, and influenza A clinically isolated strains, respectively.

Table 11 Efficacy of NA inhibitors and MGO against various strains of influenza viruses

Compound	Virus strain		[a]IC_{50} (μM)			Ave. (relative)		Virus strain		IC_{50} (μM)			Ave. (relative)	
Oseltamivir	B/Lee/40	[b]LS	23	±	3.50	49 (11.7)	S	A/WSN (H1N1)	LS	2.5	±	0.50	4.2 (1.0)	S
	B/Brisbane	LS	75	±	48.00		S	A/PR/8 (H1N1)	LS	9.4	±	0.90		S
	B/2014/6	[c]CI	33	±	6.50	22 (5.2)	S	A/HK (H3N2)	LS	0.7	±	0.03		S
	B/2014/8	CI	11				S	A/no.6 (2009)	CI	36	±	28.00	37.5 (8.9)	S
	B/2014/1	CI >	810	±	270.00		R	A/no.33 (2009)	CI	39	±	16.00		S
	B/2014/4	CI	970			>926.7 (220.6)	R	A/HA-58 (2009)	CI	870			>935 (222.6)	R
	B/2014/7	CI >	1000				R	A/no.16 (2009)	CI >	1000				R
Zanamivir	B/Lee/40	LS	0.32	±	0.06	1.51 (10.1)	S	A/WSN (H1N1)	LS	0.11	±	0.02	0.15 (1.0)	S
	B/Brisbane	LS	2.7	±	5.20		S	A/PR/8 (H1N1)	LS	0.24	±	0.00		S
	B/2014/6	CI	0.2				S	A/HK (H3N2)	LS	0.11	±	0.03		S
	B/2014/8	CI <	0.2				S	A/no.6 (2009)	CI	1.7	±	0.80	1.34 (8.9)	S
	B/2014/1	CI	11.7			6.2 (41.3)	S	A/no.33 (2009)	CI	2.2	±	0.50		S
	B/2014/4	CI	9.9				S	A/HA-58 (2009)	CI	0.11	±	0.02		S
	B/2014/7	CI	9.0				S	A/no.16 (2009)	CI >	100			>100 (666.7)	R
Laninamivir	B/Lee/40	LS	4.0	±	0.21	13.5 (7.0)	S	A/WSN (H1N1)	LS	1.2	±	0.30	1.93 (1.0)	S
	B/Brisbane	LS	23	±	3.30		S	A/PR/8 (H1N1)	LS	1.6	±	0.10		S
	B/20 1 4/6	CI	12	±	4.50	14.5 (7.5)	S	A/HK (H3N2)	LS	3.0	±	0.80		S
	B/2014/8	CI	17				S	A/no.6 (2009)	CI	48	±	13.00		S
	B/2014/1	CI >	500				R	A/no.33 (2009)	CI	35	±	5.30	28.73 (14.9)	S
	B/2014/4	CI >	500			>500 (259.1)	R	A/HA-58 (2009)	CI	3.2	±	0.30		S
	B/2014/7	CI >	500				R	A/no.16 (2009)	CI >	500			>500 (259.1)	R
Peramivir	B/Lee/40	LS	0.2	±	0.06	0.52 (20)	S	A/WSN (H1N1)	LS	0.011	±	0.00	0.26 (1.0)	S
	B/Brisbane	LS	0.84	±	0.04		S	A/PR/8 (H1N1)	LS	0.061	±	0.00		S
	B/2014/6	CI	2.8	±	0.10	1.75 (67.3)	S	A/HK (H3N2)	LS <	0.005				S
	B/2014/8	CI	0.7				S	A/no.6 (2009)	CI	0.12	±	0.03	0.95 (3.6)	S
	B/2014/1	CI	17	±	3.50		R	A/no.33 (2009)	CI <	0.07	±	0.03		S
	B/2014/4	CI >	25			>22.3 (859)	R	A/HA-58 (2009)	CI >	2.5			>13.75 (528.8)	R
	B/2014/7	CI >	25				R	A/no.16 (2009)	CI >	25				R
MGO	B/Lee/40	LS	39	±	10.00	31 (0.09)	S	A/WSN (H1N1)	LS	240	±	190.00	340 (1.0)	S
	B/Brisbane	LS	23	±	6.90		S	A/PR/8 (H1N1)	LS	360	±	130.00		S
	B/2014/6	CI	48	±	29.00		S	A/HK (H3N2)	LS	420	±	140.00		S
	B/2014/8	CI	140	±	19.00		S	A/no.6 (2009)	CI	195	±	79.00		S
	B/2014/1	CI	110	±	5.70	89 (0.26)	S	A/no.33 (2009)	CI	246	±	2.00	234.5 (0.7)	S
	B/2014/4	CI	59				S	A/HA-58 (2009)	CI	250	±	140.00		S
	B/2014/7	CI	88				S	A/no.16 (2009)	CI	247	±	3.70		S

3.5 Evaluation of effect of MGO against various influenza B viruses

Previous experiment, we established evaluation method of the cytotoxicity of MGO and antiviral activity of MGO against influenza A viruses by using MDCK cells. We first determined the cytotoxicity of MGO with cell-based system and determined a CC_{50} value of 1.4 ± 0.4mM. We also first reported that MGO obviously inhibited influenza A virus replication in a strain-independent manner. However, the activity of MGO against influenza B virus replication has not yet been evaluated. We first evaluated the inhibitory effect of MGO against influenza B viruses by using the same experimental method used for evaluation of influenza A viruses to compare the anti-influenza viral activity of MGO between influenza types A and B, as shown in Figure 36. The viral replication was suppressed in the presence of MGO in a dose-dependent manner for all influenza virus B strains, not only laboratory strains (Figure 36A), B/Lee/40 and B/Brisbane/60/2008, but also clinical strains (Figure 36C), B/2014/1, B/2014/4, B/2014/6, B/2014/7 and B/2014/8. The IC_{50} value of MGO against various influenza B strains was measured as 39 ± 10 and 23 ± 6.9 for B/Lee/40 and B/Brisbane grouped as influenza B laboratory strain, respectively. IC_{50} value of MGO against clinically isolated B strains also were shown as 48 ± 29, 140 ±19, 110 ± 5.7, 59, and 88 for B/2014/6, B/2014/8, B/2014/1, B/2014/4, and B/2014/7, respectively. Briefly, the IC_{50} values of MGO ranged from 23–140 μM against influenza B virus and from 195–420 μM against influenza A viruses (Table 11), which indicated greater sensitivity of the influenza B viruses than the influenza A viruses (Figures 36B and 36D). Median IC_{50} values of MGO against influenza B were 0.09-fold and 0.26-fold lower than those of influenza A viruses for laboratory strains and clinical strains, respectively.

Interestingly, MGO also inhibited viral replication of B/2014/1, B/2014/4, and B/2014/7, which were observed resistant to oseltamivir, laninamivir, and peramivir.

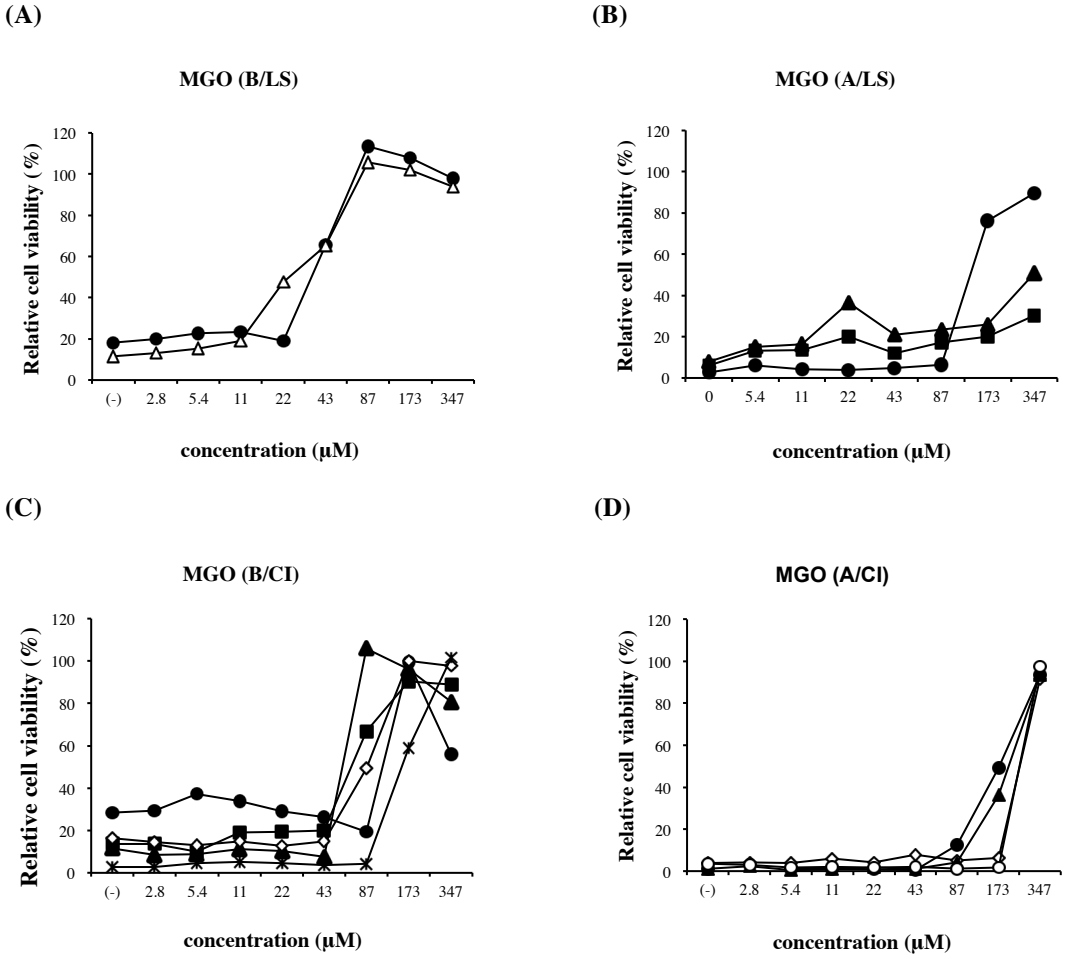

Figure 36 Anti-influenza viral activity of MGO. Evaluation of the anti-influenza viral activity of MGO was performed as described in the methods section. MDCK cells grown in 96-well plates were treated with serial dilutions of MGO and then infected with various strains of influenza viruses. Three days after infection, cells were fixed and stained with CV, and absorbance was measured using a plate reader. A graph was plotted showing relative CV staining (%), expressed as a percentage of uninfected cells and concentration of MGO (μM). (A), (B), (C), and (D) show the susceptibilities of MGO to influenza B laboratory strains, influenza A laboratory strains, influenza B clinically isolated strains, and influenza A clinically isolated strains, respectively.

3.6 Mode of action of MGO

Plaque inhibitory assays were performed to determine whether MGO affects influenza virus growth (Figure 37). For these experiments, MGO was either (i) added to the cells for 1 h and subsequently washed out before viral infection ("pretreatment of cell"), (ii) mixed with influenza virus solution for 1 h before viral infection ("pretreatment of virus"), (iii) added during viral adsorption for 1 h and subsequently washed out ("during infection only"), or (iv) added to the agarose gels that overlaid infected cells ("after infection"). Pretreatment of cells with MGO had slight effect on relative plaque numbers (170 μM, 86.5% ± 2.6%; Figure 37B). In contrast, plaque formation was completely inhibited when the virus was treated with 170 μM MGO before infection (Figure 37B), suggesting that MGO exhibited potent virucidal activity. Moreover, moderate reductions in plaque numbers were obtained by treating MDCK cells with MGO during (170 μM, 24.8% ± 2.0%; Figure 37B) and after infection (170 μM, 72% ± 10%; Figure 37B). As a positive control, the commercial anti-influenza viral drug zanamivir was added after infection (100 nM) and caused a decrease in plaque numbers (29% ± 3.8%; Figure 37B). Moreover, 170 μM MGO incubated with influenza virus for 1 hour completely reduced their infectivity (Figure 37C). Taken together, these data suggest that MGO has strong virucidal activity.

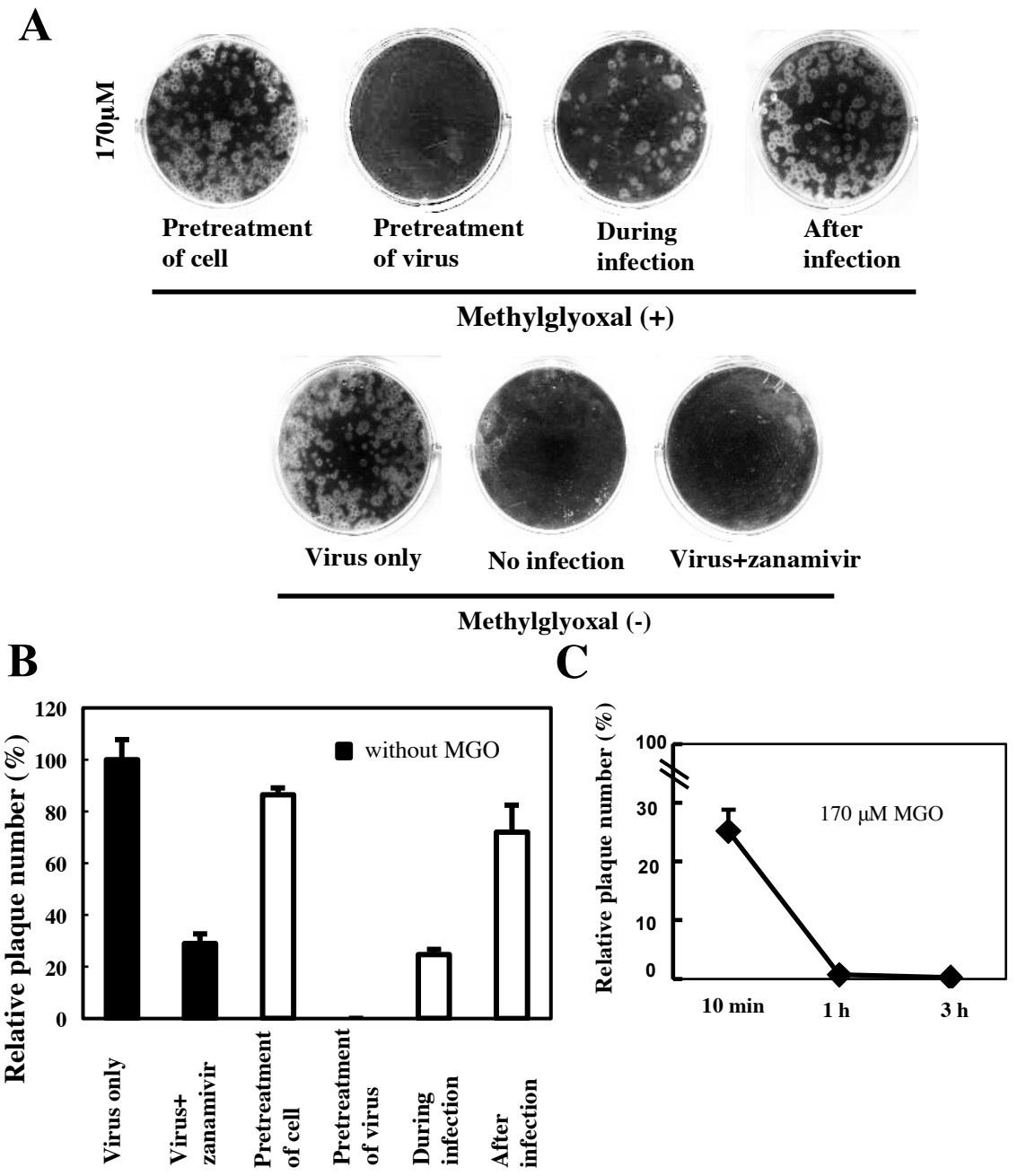

Figure 37 Virucidal activity of MGO. (A) Plaque formation in the presence of MGO. Confluent monolayers of MDCK cells were grown in 6-well plates and infected with dilutions of virus that produced approximately 300 plaques per well. After 1 h, the virus solution was removed, cells were washed and overlaid with an agarose solution (0.8% agarose in MEM), and plaques were counted after 3 days. For the "pretreatment of cells" experiment, MGO was added to the cells 1 h before infection. For the "pretreatment of virus" experiment, virus and MGO were mixed at room temperature 1 h before addition to the cells. For the "during infection" experiment, MGO/virus solution was added at the beginning of the 1-h infection period. For the "after infection" experiment, MGO was mixed with the agarose solution that was laid over the infected cells. As a control, zanamivir (100 nM) was mixed with the agarose solution (virus + zanamivir). Representative data from duplicate independent experiments are presented. (B) Effect of MGO on plaque numbers. Plaques in (A) were counted and the percentage of plaque

inhibition relative to infected controls (virus only) was determined for each drug concentration. Open bar, 170 μM MGO; closed bar, 700 μM MGO; gray bar, without MGO. Means of duplicate samples are shown as relative plaque numbers. Data are presented as the mean ± SD. (C) Time-dependent virucidal activity of MGO. Samples were mixed with virus preparations to final concentrations of 170 μM and 700 μM and incubated at room temperature for the indicated time periods. The mixtures were subsequently diluted and plaque assays were immediately performed. Plaque numbers are expressed as a percentage of the number of plaques obtained in the absence of MGO. Data are presented as the mean ± SD of duplicate measurements.

3.7 Evaluation of synergistic effect between NA inhibitor drugs and MGO

As MGO shows virucidal effect, we examined synergistic effect of MGO and NA inhibitors. MDCK cells seeded in a 96-well plate on the day before infection at a density of 3×10^4cells/well were washed with 100μl/well of MEM (-) and then discarded. The 2-fold diluted MGO were added to 96-well plate containing MDCK cells at 50μl/well in horizontal direction together with 50μl/well of 2-fold diluted commercial drug in vertical direction.

The A/WSN/33 influenza virus was diluted to make a 1000$TCID_{50}$/ml of influenza solution. 100μl/well of diluted virus solution was added to 96-well plate containing MDCK cells. The final concentration of influenza virus is 100$TCID_{50}$/well. 96-well plate infected with influenza virus was shaken using Microplate genie for 30 seconds before incubated in 37°C, 5%CO_2 incubator for 72 hours. After 72 hours, MDCK cells morphology was observed under inverted light microscope and the virus induced CPE development (CPE reduction assay) was evaluated using crystal violet staining. The percentage of protection was calculated using the same formula with the previous experiment.

The inhibitory effect of all NA inhibitors used in this experiment against influenza virus (A/WSN/33) significantly increased in the presence of MGO as indicated by the decrease of IC_{50} value of NA inhibitors. Significantly, the combination

use of NA inhibitors and MGO tended to decrease IC_{50} of NA inhibitors when the concentration of MGO increased. The IC_{50} of NA inhibitors against A/WSN/33 influenza virus when combined with various concentration of MGO are shown in Table 12. When 170 μM MGO was combined together with various NA inhibitors, the IC_{50} decreased to ~1/100, 1/300, 1/30, and 1/200th of those values for oseltamivir, zanamivir, laninamivir, and peramivir, respectively. In addition, the SI value of each NA inhibitors remarkably increased when the concentration of MGO in the co-treatment increased as shown in Table 13.

Conc, of MGO (μM)	oseltamivir		zanamivir		laninamivir		peramivir	
	IC_{50} (μM)	Relative ratio	IC_{50} (μM)	Relative ratio	IC_{50} (μM)	Relative ratio	IC_{50} (μM)	Relative ratio
0	1.8 ± 0.08	1.0	0.30 ± 0.19	1.0	0.25 ± 0.01	1.0	0.028 ± 0.015	1.0
5.4	2.0 ± 0.31	1.1	0.37 ± 0.25	1.2	0.22 ± 0.03	0.86	0.0055 ± 0.001	0.20
22	0.58 ± 0.22	0.32	0.046 ± 0.02	0.15	0.14 ± 0.07	0.53	0.0033 ± 0.0020	0.12
170	<0.020	<0.011	<0.0010	<0.0033	<0.010	<0.04	0.0033 ± 0.0020	<0.0054

Table 12 The synergistic effect of combination of MGO and NA inhibitors against A/WSN/33

NA inhibitor	SI value		
	NA inhibitor only	Combination	Increasing ratio
Oseltamivir	780	9.0×10^4	115
Zanamivir	>890	$>1.0 \times 10^5$	112
Laninamivir	>140	$>1.7 \times 10^4$	121
Peramivir	$>1.4 \times 10^6$	$>1.0 \times 10^8$	71

Table 13 The combination of MGO and NA inhibitors increases SI value

Finally, we tested the synergistic effect of MGO and oseltamivir against the oseltamivir-resistant pandemic influenza virus, A/Nagasaki/HA-58/2009. As expected, oseltamivir could not inhibit viral replication exhibited as the IC_{50} of oseltamivir was >1000μM, 200μM at 100 and 6.25 $TCID_{50}$/well, respectively. The combination of oseltamivir and MGO tends to reduce IC_{50} value of oseltamivir in the same as infection with influenza laboratory strain, A/WSN/33. When 100μM of MGO was administered

with oseltamivir, the IC_{50} value of oseltamivir decreased to ~1/30th at 6.25$TCID_{50}$/well. A similar synergistic effect was observed at 100$TCID_{50}$/well (Table 14). Moreover, we also investigated the cytotoxicity of oseltamivir in the presence of 125-500μM MGO and the cytotoxicity was not observed (>1000μM; data not shown).

Concentration of MGO (μM)	6.25 $TCID_{50}$		100 $TCID_{50}$	
	IC_{50} of oseltamivir (μM)	Relative ratio	IC_{50} of oseltamivir (μM)	Relative ratio
0	200	1	>1000	1
25	110	0.55	ND	N/A
100	7.7	0.038	ND	N/A
125	<3.9	<0.019	448	<0.45
250	<3.9	<0.019	46	<0.046

Table 14 The synergistic effect of combination of MGO and oseltamivir against oseltamivir-resistant pandemic virus, A/Nagasaki/HA-58/2009.

(ND = not determined; N/A = not applicable)

CHAPTER 4: DISCUSSION

Nowadays, infectious diseases caused by influenza viruses are seriously public health problem worldwide that many people are suffered from influenza infection every year. Because of RNA virus lack of proofreading mechanism, mutation of influenza easily occurred. Thus, there is an urgent requirement for the development of novel anti-influenza compounds including finding from natural sources. Natural products, such as microbial metabolites and medicinal plants, are promising as potentially effective and novel antiviral drugs. So far, several agents isolated from these natural products have been reported. Natural products contain a variety of polyphenols, flavonoids, and alkaloids known as anti-influenza compounds. For example, polyphenols pentagalloylglucose (PGG) from *phyllanthus emblica* L. [91], (-)-Epigallocatechin-3-gallate (EGCG) from Green tea [92], polyketide leptomycin B from *Streptomyces* spp. [93], and alkaloid (-)-thalimonine from *Thalictrum simplex* L. [94] exhibited anti-influenza activity by interaction with HA, inhibition of viral NA, inhibiting nuclear export of vRNP, and inhibition of viral protein synthesis. It was also reported that valtrate and 1'-acetoxychavicol acetate derived from Valerianae Radix and the roots of *Alpinia galanga*, respectively inhibit influenza virus replication by preventing the nuclear export of vRNPs [95]. Moreover, it was reported that *Alchemilla mollis* extracts inhibit the replication of influenza virus due to its virucidal activity [96]

Previously, C.A. de Bock et al. [75] reported the anti-influenza virus activity of MGO, which is a component in honey. However, MGO itself is not enough to inhibit virus replication compared with commercial available anti-influenza drugs. However, mode of action of MGO is different from these drugs. Thus, in this experiment we evaluate the synergistic effect of combination between commercial anti IFV drugs. As

be shown in HIV treatment, drug monotherapies frequently led to treatment failure because HIV virus promptly developed resistant to the single drug. The combination therapy is a critical key of successful treatment outcomes. The rational of combining anti HIV drugs is to provide more efficacy of viral suppression, to decrease the emergence of drug resistant virus during chronic virus replication, and to provide more effective antiretroviral treatment even when mixture of drug-resistant and drug-sensitive virus occur [97, 98]. In addition, several guidelines for HIV treatment regiment also recommend that an initiate antiretroviral regiment should consist of two drugs from nucleoside/nucleotide reverse transcriptase inhibitors (NRTIs) plus other antiviral drugs from one of following drug groups; nonnucleoside reverse transcriptase inhibitors (NNRTIs), protease inhibitors (PI; boosted with ritronavir), or integrase strand transfer inhibitor (INSTI).

One of important initial step in evaluating combination therapy is to determine whether the combined agents inhibited IFV replication synergistically or not. First, IC_{50} of each commercial drug against various IFV was determined. As shown in Table 10, peramivir was observed as the highest effective drug against A/WSN/33, A/HK/8/68, and A/Duck/Pennsylvania /84 of 13.2nM, <5nM, and 4nM, respectively. Efficiency of zanamivir against A/WSN/33, A/PR/8, A/HK/8/68, and A/Duck/Pennsylvania/84 IFV viruses was found of 0.11μM, 24nM, 0.11μM, and 1.14μM, respectively. Oseltamivir showed the most effective when against A/HK/8/68 strain of 0.71μM and concentration used for against IFV was increased in order to inhibit viral growth of A/WSN/33, A/PR/8 and A/Duck/Pennsylvania/84 of 2.46μM, 9.43μM, and 7.9μM, respectively. IC_{50} of laninamivir against A/WSN/33, A/PR/8, A/HK/8/68, and A/Duck/Pennsylvania/84 were reported of 1.22μM, 1.62μM, 2.95μM, and 44.6μM,

respectively. *In vitro* cytotoxicity was performed to support toxicity data of each drug. Based on IC_{50} and CC_{50}, selective index (SI) was calculated by divided CC_{50} with IC_{50}. The higher selective index is preferable to the lower one because it implied that much higher taking dose was observed cytotoxicity effect when compared to taking dose that elicit the therapeutic effect. The results from this experiment indicated that peramivir is the best anti IFV drug when concerned both effectiveness and cytotoxicity aspects.

Although *In vitro* study of NA inhibitors was obtained promising result to inhibit viral releasing, NA inhibitor also has some limitations that could not treat in late stage of infection. Treatment with NA inhibitor can protect only neighbouring cells from secondary infection; therefore, if all or most cells are initially infected with virus, the effect of the drugs may be underestimated. Some literature suggested that NA inhibitors would give the most effective when they were administered within 24 hours after virus infection. The most effective of NA inhibitors might be not achieved in human.

In addition, the emergence of influenza viruses with reduced susceptibility to NAIs has also been a critical issue recently, especially for influenza A and B viruses. The high rates of resistance to oseltamivir of influenza A viruses were reported in clinical samples worldwide during the 2007–2008 influenza season. NA mutations of oseltamivir were observed at a higher rate than the rate for NA mutations of zanamivir. This phenomenon is because zanamivir is more similar to Neu5ac than is oseltamivir, so the binding of zanamivir to the NA active site is similar to natural substrate binding. Moreover, the rate of use of zanamivir is clinically lower than that of oseltamivir [99]. Recently, the possibility of laninamivir resistance *in vitro* was investigated and the susceptibility profile was similar to that of zanamivir [100]. Laninamivir is a long-

acting derivative of zanamivir, which is administered as a single inhaled dose. The advantages of laninamivir are that it not only resides in the lung for many days [101] but also has slower dissociation than that of other NA inhibitors [56]. Mutations at the location affecting the laninamivir dissociation rate can confer a dramatic resistance to laninamivir [102]. Some studies have reported that mutations conferring zanamivir resistance also induce resistance to laninamivir with the loss of slow binding and/or faster dissociation [102], also relevant to our results (Table 10). The first emergence of peramivir resistant clinical isolates was reported during the 2009 pandemic, following prophylaxis or treatment with oseltamivir [103, 104]. The emergence of NAI-resistance influenza B viruses is also a serious public health concern worldwide. The emergence of NAI-resistant influenza B virus information is not well-understood, and concerns are often underestimated relative to those of influenza A viruses, although both viruses are regarded to cause significant disease burdens to a similar degree. In Japan, the rate of NAIs used for clinical treatment have been found to be much higher than anywhere else in the world, and the use of NAIs has caused the spread of influenza B viruses with reduced susceptibility to NA inhibitors [64]. Our studies exhibit that influenza A viruses are more susceptible to NAIs than influenza B viruses. The patterns observed for drug susceptibility were similar to those previous published [105]. One possible explanation is that the binding affinities of HA protein of influenza B viruses and the sialic acid moiety are weaker than those of influenza A viruses [105, 106]. The problem of wild type influenza B viruses already having reduced susceptibility to NAIs relative to that of influenza A viruses is a seriously concern because any further increase in IC_{50} values due to mutations may induce complete loss of drug effectiveness in influenza B treatment or prophylaxis. Although the similarity of the amino acid composition of NAs

between influenza A and B viruses is only 30% [107], the 19 amino acids at the catalytic site are highly conserved among all known influenza A and B NAs [108]. Several clinical studies have reported that the locations of NA mutations differs among the NAIs used [109], and the locations of NA substitutions confer different levels of resistance among the NAIs used [105, 110, 111].

Although our results do not show any resistance of influenza B viruses to zanamivir, the median IC_{50} of zanamivir against clinical strains resistant to other NA inhibitors (B/2014/1, B/2014/4, B/2014/7) was approximately 50-fold greater than those of clinical strains sensitive to other NA inhibitors (B/2014/6, B/2014/8). On the basis of the criteria recommend by WHO, B/2014/1, B/2014/4, and B/2014/7 were classified as showing highly reduced susceptibility to inhibition by zanamivir and all NAIs. Peramivir contains a guanidino group, as does zanamivir, and a hydrophobic group, as does oseltamivir; consequently, mutations affecting the activities of oseltamivir and zanamivir can also confer resistance to peramivir [104], supported by our results.

In consideration of the findings of a previous report using embryonated chicken eggs [75] and those of our previous report regarding the anti-influenza viral activity of manuka honey [70], we hypothesized that MGO is effective to suppress influenza A virus replication, including the pandemic 2009 H1N1 virus as evaluated in the present study using MDCK cells. The presented data shows that MGO has anti-influenza viral activity (Figure 31 and Table 10), which is most likely due to a virucidal effect, as suggested by the plaque inhibitory assay (Figure 37). Furthermore, MGO showed promising activity against multiple influenza virus strains (Table 10, 11) in addition to demonstrating a synergistic effect when co-treated with NA inhibitors as demonstrated by the drastic increase in their SI (Table 13).

We found that the IC_{50} of MGO alone was 180–420 μM (Table 10). This is comparable with previous reports that demonstrated its inhibitory effects against the proliferation of malaria parasites (IC_{50} approximately 200 μM) [112] and *Escherichia coli* and *Staphylococcus aureus* (IC_{50} approximately 1.1 mM for each bacteria) [69]. Previous reports have shown that α-ketoaldehydes, including MGO, had antiviral activity against influenza virus [75]. They observed that inhibition of hemagglutination occurs in the presence of MGO (4 mM) during an extended incubation period (24–54 h). We observed that a 10-min incubation in the presence of 700 μM MGO is sufficient for its virucidal activity (Figure 37C); thus, magnifying the outcome of the previous finding. Our results exhibit that MGO inhibit viral replication of various influenza virus, including H1N1, H3N2, H5N2, and oseltamivir-resistant H1N1, suggesting that MGO has a broad spectrum of anti-influenza viral activity. Although we did not test the virucidal activity of MGO against clinical isolates, highly pathogenic H5N1 and H7N9 viruses, it is possible that MGO is also effective against them. A previous study reported that MGO demonstrated a hemagglutination inhibition effect [75]. Thus, MGO may directly interact on the virus surface and interfere with the interaction between viruses and host cells.

Based on the finding of our study regarding the anti-influenza A viral activity of MGO [113], we hypothesised that MGO would also be effective against influenza B viruses in MDCK cells. As expected, MGO has antiviral activity against influenza B viruses, including influenza B virus with reduced susceptibility to NAIs (Figure 32-36 and Table 11). Interestingly, the susceptibility of MGO against influenza B viruses was higher than that against influenza A viruses, as suggested by the ten-fold and 3.8-fold reduced IC_{50} values for laboratory strains and clinical strains, respectively (Table 11).

Since MGO shows anti-influenza activity in a strain-independent manner and can inhibit replication of influenza viruses with reduced susceptibility to NA inhibitors, the mechanism of MGO may not be related to interactions of HA or NA, in which mutation easily occurs. Some studies have reported that MGO showed antiviral activity against foot-and-mouse disease [73] and Newcastle disease virus [74] via interaction with viral RNA. The infectiousness of RNA isolated from MGO-treated virus was not infectious in subcutaneous inoculation of mice [73]. The influenza virus polymerase does not possess a proof-reading function, so the virus rapidly adapts to certain selection pressures, thereby generating resistant viruses, especially if a viral protein is a drug target, such as an NAI. Recently, the cellular cofactors that are necessary during influenza virus infection could be new targets for drug development. Several studies have reported that during infection, influenza viruses activate the Raf/MEK/ERK-cascade and the transcription factor nuclear factor kappa B (NF-κB) [114-117]. The Raf/MEK/ERK-cascade is activated by influenza virus to support viral propagation, if this cascade is inhibited, the function of the nuclear export protein also impairs, which results in accumulation of ribonucleoprotein complexes (RNPs) in the nucleus [118, 119]. Like the Raf/MEK/ERK-cascade, NF-κB is activated by influenza infection, then induces caspases, which subsequently supports the replication of influenza virus by enhancing RNP export [115, 120]. Molecules interfering with the NF-κB pathway, such as acetylsalicylic acid (ASA) [120], have been reported to have antiviral activity [116]. Inhibition of cellular signalling of antiviral activity may be a novel function of new anti-influenza agents that target host-cell functions. Most importantly, no resistant virus variants have been shown to emerge in the presence of cellular pathway inhibitors,

which suggests that influenza viruses cannot easily adapt to missing crucial cellular functions [119, 120].

MGO has been reported to suppress tumour necrosis factor-α–induced NF-κB activation by inhibition of NF-κB DNA-binding and NF-κB–dependent reporter gene expression in a concentration-dependent manner [121], which is consistent with our data showing that MGO can inhibit influenza replication in a dose-dependent manner. Similar to ASA that blocks influenza virus by inhibiting NF-κB activity, MGO may inhibit influenza virus replication by interfering with NF-κB activation. Therefore, MGO can suppress influenza viral replication in a strain-independent manner.

Mechanism of MGO was supposed that it would block at early stage of virus infection (prevention of absorption or penetration) while that of NA was found that interrupt an established infection at a late stage by inhibiting the release of virions from infected cells. Thus, two classes of inhibitors act by different mechanisms and at different stages of the virus replication cycle. It is generally accepted that two classes of inhibitors that act by different mechanisms exhibit synergistic effects and reduce the rate of drug resistance [122, 123]. Accordingly, it is reasonable that MGO enhances the efficacy of NA inhibitors. Our data indicated that the combination of MGO and NA inhibitors markedly increased antiviral activity compared to that of either drug alone for the laboratory strain A/WSN/33 and the 2009 pandemic strain A/Nagasaki/HA-58/2009.

Moreover, synergistic combination can reduce amount of taken dose that could inhibit viral growth [86, 124]. In addition, as mentioned in introduction part, zanamivir and laninamivir are an oral inhalation dosage form, which difficult controlled how much NA blockers were absorbed. The amount of drug administered was related to the ability

of patients to use this delivery system. An improper technique using this apparatus was concerned to be related to low or undetectable serum concentrations [125]. For some patients, such as children treated with combination of MGO and zanamivir or laninamivir, even if insufficient dose of zanamivir or laninamivir were taken, MGO could boost anti IFV activity to inhibit viral growth and reduce incident of drug resistant due to insufficient drug uptake.

Although influenza A and B viruses belong to the family of Orthomyxoviridae, they possess distinct characteristics that are grouped into different types. Currently, several researchers are interested in influenza virus–host interactions. The transcription mechanisms of influenza A and B viruses enabled influenza B polymerase to recognise the cap structure in a manner different from that of influenza A polymerase, and the growth of influenza B viruses was more sensitive to the amount of cellular mRNA than was growth of influenza A viruses [126]. These phenomena may explain our finding that MGO was more sensitive to influenza B viruses than to influenza A viruses and had a synergistic effect with NAIs only on influenza A viruses and not on influenza B viruses (data not shown).

Overall, we supposed that using combination of NA inhibitor and MGO may provide several advantages over single-agent treatment, such as greater potency, superior clinical efficacy, reduction of drug dosage needed, reduction of toxicity and side effects, and greater cost-effectiveness. Our result supports the idea that an appearance of CPE can be synergistically reduced by combination therapy with have different mechanism of action. However, studied with animal models are needed to determine the advantages of the drug combination tested here.

REFERENCES

[1] Claas EC, Osterhaus AD, van Beek R, De Jong JC, Rimmelzwaan GF, Senne DA, et al. Human influenza A H5N1 virus related to a highly pathogenic avian influenza virus. Lancet. 1998;351:472-7.

[2] Kawano H, Haruyama T, Hayashi Y, Sinoda Y, Sonoda M, Kobayashi N. Genetic Analysis and Phylogenetic Characterization of Pandemic (H1N1) 2009 influenza viruses that found in Nagasaki, Japan. Jpn J Infect Dis. 2011;64:195-203.

[3] Watanabe T, Kiso M, Fukuyama S, Nakajima N, Imai M, Yamada S, et al. Characterization of H7N9 influenza A viruses isolated from humans. Nature. 2013;501:551-5.

[4] Taubenberger JK, Kash JC. Influenza virus evolution, host adaptation, and pandemic formation. Cell Host Microbe. 2010;7:440-51.

[5] Simon-Loriere E, Holmes EC. Why do RNA viruses recombine? Nat Rev Microbiol. 2011;9:617-26.

[6] Silvennoinen H, Huusko T, Vuorinen T, Heikkinen T. Comparative burden of influenza A/H1N1, A/H3N2, and B infections in children treated as outpatients. Pediatr Infect Dis J. 2015;34:1081-5.

[7] Gutiérrez-Pizarraya A, Pérez-Romero P, Alvarez R, Aydillo TA, Osorio-Gómez G, Milara-Ibáñez C, et al. Unexpected severity of cases of influenza B infection in patients that required hospitalization during the first postpandemic wave. J Infect. 2012;65:423-30.

[8] Aebi T, Weisser M, Bucher E, Hirsch HH, Marsch S, Siegemund M. Co-infection of Influenza B and Streptococci causing severe pneumonia and septic shock in healthy women. BMC Infect Dis. 2010;10:308.

[9] Paddock CD, Liu L, Denison AM, Bartlett JH, Holman RC, Deleon-Carnes M, et al. Myocardial injury and bacterial pneumonia contribute to the pathogenesis of fatal influenza B virus infection. J Infect Dis. 2012;205:895-905.

[10] McCullers JA, Hayden FG. Fatal influenza B infections: time to reexamine influenza research priorities. J Infect Dis. 2012;205:870-2.

[11] Goenka A, Michael BD, Ledger E, Hart IJ, Absoud M, Chow G, et al. Neurological manifestations of influenza infection in children and adults: results of a National British Surveillance Study. Clin Infect Dis. 2014;58:775-84.

[12] Hatta M, Kawaoka Y. The NB protein of influenza B virus is not necessary for virus replication in vitro. J Virol. 2003;77:6050-4.

[13] Chen R, Holmes EC. The evolutionary dynamics of human influenza B virus. J Mol Evol. 2008;66:655-63.

[14] Das K, Aramini JM, Ma LC, Krug RM, Arnold E. Structures of influenza A proteins and insights into antiviral drug targets. Nat Struct Mol Biol. 2010;17:530-8.

[15] Samji T. Influenza A: understanding the viral life cycle. Yale J Biol Med. 2009;82:153-9.

[16] Lakadamyali M, Rust MJ, Zhuang X. Endocytosis of influenza viruses. Microbes Infect. 2004;6:929-36.

[17] Edinger TO, Pohl MO, Stertz S. Entry of influenza A virus: host factors and antiviral targets. J Gen Virol. 2014;95:263-77.

[18] Maxfield FR, Yamashiro DJ. Endosome acidification and the pathways of receptor-mediated endocytosis. Adv Exp Med Biol. 1987;225:189-98.

[19] Lee KK. Architecture of a nascent viral fusion pore. EMBO J. 2010;29:1299-311.

[20] Hu YB, Dammer EB, Ren RJ, Wang G. The endosomal-lysosomal system: from acidification and cargo sorting to neurodegeneration. Transl Neurodegener. 2015;4:18.

[21] Cross KJ, Langley WA, Russell RJ, Skehel JJ, Steinhauer DA. Composition and functions of the influenza fusion peptide. Protein Pept Lett. 2009;16:766-78.

[22] Palmeri D, Malim MH. Importin beta can mediate the nuclear import of an arginine-rich nuclear localization signal in the absence of importin alpha. Mol Cell Biol. 1999;19:1218-25.

[23] Lange A, Mills RE, Lange CJ, Stewart M, Devine SE, Corbett AH. Classical nuclear localization signals: definition, function, and interaction with importin alpha. J Biol Chem. 2007;282:5101-5.

[24] Shimizu T, Takizawa N, Watanabe K, Nagata K, Kobayashi N. Crucial role of the influenza virus NS2 (NEP) C-terminal domain in M1 binding and nuclear export of vRNP. FEBS Lett. 2011;585:41-6.

[25] Watanabe K, Fuse T, Asano I, Tsukahara F, Maru Y, Nagata K, et al. Identification of Hsc70 as an influenza virus matrix protein (M1) binding factor involved in the virus life cycle. FEBS Lett. 2006;580:5785-90.

[26] Cao S, Liu X, Yu M, Li J, Jia X, Bi Y, et al. A nuclear export signal in the matrix protein of Influenza A virus is required for efficient virus replication. J Virol. 2012;86:4883-91.

[27] Paterson D, Fodor E. Emerging roles for the influenza A virus nuclear export protein (NEP). PLoS Pathog. 2012;8:e1003019.

[28] Francis T. A NEW TYPE OF VIRUS FROM EPIDEMIC INFLUENZA. Science. 1940;92:405-8.

[29] DAVIES WL, GRUNERT RR, HAFF RF, MCGAHEN JW, NEUMAYER EM, PAULSHOCK M, et al. ANTIVIRAL ACTIVITY OF 1-ADAMANTANAMINE (AMANTADINE). Science. 1964;144:862-3.

[30] Nobusawa E, Sato K. Comparison of the mutation rates of human influenza A and B viruses. J Virol. 2006;80:3675-8.

[31] Gong J, Xu W, Zhang J. Structure and functions of influenza virus neuraminidase. Curr Med Chem. 2007;14:113-22.

[32] Sriwilaijaroen N, Suzuki Y. Molecular basis of the structure and function of H1 hemagglutinin of influenza virus. Proc Jpn Acad Ser B Phys Biol Sci. 2012;88:226-49.

[33] Huang Q, Sivaramakrishna RP, Ludwig K, Korte T, Böttcher C, Herrmann A. Early steps of the conformational change of influenza virus hemagglutinin to a fusion active state: stability and energetics of the hemagglutinin. Biochim Biophys Acta. 2003;1614:3-13.

[34] Bartesaghi A, Merk A, Borgnia MJ, Milne JL, Subramaniam S. Prefusion structure of trimeric HIV-1 envelope glycoprotein determined by cryo-electron microscopy. Nat Struct Mol Biol. 2013;20:1352-7.

[35] Skehel JJ, Wiley DC. Receptor binding and membrane fusion in virus entry: the influenza hemagglutinin. Annu Rev Biochem. 2000;69:531-69.

[36] Noma K, Kiyotani K, Kouchi H, Fujii Y, Egi Y, Tanaka K, et al. Endogenous protease-dependent replication of human influenza viruses in two MDCK cell lines. Arch Virol. 1998;143:1893-909.

[37] Lawrence H P, Robert A L. The M2 Proton Channels of Influenza A and B Viruses. J Biol Chem. 2006;281:8997-9000.

[38] da Silva DV, Nordholm J, Dou D, Wang H, Rossman JS, Daniels R. The influenza virus neuraminidase protein transmembrane and head domains have coevolved. J Virol. 2015;89:1094-104.

[39] Wohlbold TJ, Krammer F. In the shadow of hemagglutinin: a growing interest in influenza viral neuraminidase and its role as a vaccine antigen. Viruses. 2014;6:2465-94.

[40] Matrosovich MN, Matrosovich TY, Gray T, Roberts NA, Klenk HD. Neuraminidase is important for the initiation of influenza virus infection in human airway epithelium. J Virol. 2004;78:12665-7.

[41] Dawson J. Neuraminidase inhibitor and amantadine. Lancet. 2000;355:2254.

[42] Marcelin G, Sandbulte MR, Webby RJ. Contribution of antibody production against neuraminidase to the protection afforded by influenza vaccines. Rev Med Virol. 2012;22:267-79.

[43] Wang C, Takeuchi K, Pinto LH, Lamb RA. Ion channel activity of influenza A virus M2 protein: characterization of the amantadine block. J Virol. 1993;67:5585-94.

[44] Pinto LH, Holsinger LJ, Lamb RA. Influenza virus M2 protein has ion channel activity. Cell. 1992;69:517-28.

[45] Hay AJ, Wolstenholme AJ, Skehel JJ, Smith MH. The molecular basis of the specific anti-influenza action of amantadine. EMBO J. 1985;4:3021-4.

[46] Kato N, Eggers HJ. Inhibition of uncoating of fowl plague virus by l-adamantanamine hydrochloride. Virology. 1969;37:632-41.

[47] Skehel JJ, Hay AJ, Armstrong JA. On the mechanism of inhibition of influenza virus replication by amantadine hydrochloride. J Gen Virol. 1978;38:97-110.

[48] Gubareva LV, Kaiser L, Hayden FG. Influenza virus neuraminidase inhibitors. Lancet. 2000;355:827-35.

[49] Wagner R, Matrosovich M, Klenk HD. Functional balance between haemagglutinin and neuraminidase in influenza virus infections. Rev Med Virol. 2002;12:159-66.

[50] Burmeister WP, Baudin F, Cusack S, Ruigrok RW. Comparison of structure and sequence of influenza B/Yamagata and B/Beijing neuraminidases shows a conserved "head" but much greater variability in the "stalk" and NB protein. Virology. 1993;192:683-6.

[51] Varghese JN, Smith PW, Sollis SL, Blick TJ, Sahasrabudhe A, McKimm-Breschkin JL, et al. Drug design against a shifting target: a structural basis for resistance to inhibitors in a variant of influenza virus neuraminidase. Structure. 1998;6:735-46.

[52] von Itzstein M, Wu WY, Kok GB, Pegg MS, Dyason JC, Jin B, et al. Rational design of potent sialidase-based inhibitors of influenza virus replication. Nature. 1993;363:418-23.

[53] Meindl P, Bodo G, Palese P, Schulman J, Tuppy H. Inhibition of neuraminidase activity by derivatives of 2-deoxy-2,3-dehydro-N-acetylneuraminic acid. Virology. 1974;58:457-63.

[54] Alymova IV, Taylor G, Portner A. Neuraminidase inhibitors as antiviral agents. Curr Drug Targets Infect Disord. 2005;5:401-9.

[55] Storms AD, Gubareva LV, Su S, Wheeling JT, Okomo-Adhiambo M, Pan CY, et al. Oseltamivir-resistant pandemic (H1N1) 2009 virus infections, United States, 2010-11. Emerg Infect Dis. 2012;18:308-11.

[56] Kubo S, Tomozawa T, Kakuta M, Tokumitsu A, Yamashita M. Laninamivir prodrug CS-8958, a long-acting neuraminidase inhibitor, shows superior anti-influenza virus activity after a single administration. Antimicrob Agents Chemother. 2010;54:1256-64.

[57] Yamashita M, Tomozawa T, Kakuta M, Tokumitsu A, Nasu H, Kubo S. CS-8958, a prodrug of the new neuraminidase inhibitor R-125489, shows long-acting anti-influenza virus activity. Antimicrob Agents Chemother. 2009;53:186-92.

[58] Kashiwagi S, Yoshida S, Yamaguchi H, Niwa S, Mitsui N, Tanigawa M, et al. Safety of the long-acting neuraminidase inhibitor laninamivir octanoate hydrate in post-marketing surveillance. Int J Antimicrob Agents. 2012;40:381-8.

[59] Sidwell RW, Smee DF. Peramivir (BCX-1812, RWJ-270201): potential new therapy for influenza. Expert Opin Investig Drugs. 2002;11:859-69.

[60] Hikita T, Hikita H, Hikita F, Hikita N, Hikita S. Clinical effectiveness of peramivir in comparison with other neuraminidase inhibitors in pediatric influenza patients. Int J Pediatr. 2012;2012:834181.

[61] von Itzstein M. The war against influenza: discovery and development of sialidase inhibitors. Nat Rev Drug Discov. 2007;6:967-74.

[62] Farrukee R, Leang SK, Butler J, Lee RT, Maurer-Stroh S, Tilmanis D, et al. Influenza viruses with B/Yamagata- and B/Victoria-like neuraminidases are differentially affected by mutations that alter antiviral susceptibility. J Antimicrob Chemother. 2015;70:2004-12.

[63] Sheu TG, Deyde VM, Okomo-Adhiambo M, Garten RJ, Xu X, Bright RA, et al. Surveillance for neuraminidase inhibitor resistance among human influenza A and B viruses circulating worldwide from 2004 to 2008. Antimicrob Agents Chemother. 2008;52:3284-92.

[64] Hatakeyama S, Sugaya N, Ito M, Yamazaki M, Ichikawa M, Kimura K, et al. Emergence of influenza B viruses with reduced sensitivity to neuraminidase inhibitors. JAMA. 2007;297:1435-42.

[65] McKimm-Breschkin J, Trivedi T, Hampson A, Hay A, Klimov A, Tashiro M, et al. Neuraminidase sequence analysis and susceptibilities of influenza virus clinical isolates to zanamivir and oseltamivir. Antimicrob Agents Chemother. 2003;47:2264-72.

[66] Oakley AJ, Barrett S, Peat TS, Newman J, Streltsov VA, Waddington L, et al. Structural and functional basis of resistance to neuraminidase inhibitors of influenza B viruses. J Med Chem. 2010;53:6421-31.

[67] Furuta Y, Gowen BB, Takahashi K, Shiraki K, Smee DF, Barnard DL. Favipiravir (T-705), a novel viral RNA polymerase inhibitor. Antiviral Res. 2013;100:446-54.

[68] Wallace A, Eady S, Miles M, Martin H, McLachlan A, Rodier M, et al. Demonstrating the safety of manuka honey UMF 20+in a human clinical trial with healthy individuals. Br J Nutr. 2010;103:1023-8.

[69] Mavric E, Wittmann S, Barth G, Henle T. Identification and quantification of methylglyoxal as the dominant antibacterial constituent of Manuka (Leptospermum scoparium) honeys from New Zealand. Mol Nutr Food Res. 2008;52:483-9.

[70] Watanabe K, Rahmasari R, Matsunaga A, Haruyama T, Kobayashi N. Anti-influenza Viral Effects of Honey In Vitro: Potent High Activity of Manuka Honey. Arch Med Res. 2014.

[71] Schneider M, Coyle S, Warnock M, Gow I, Fyfe L. Anti-microbial activity and composition of manuka and portobello honey. Phytother Res. 2013;27:1162-8.

[72] Kilty SJ, Duval M, Chan FT, Ferris W, Slinger R. Methylglyoxal: (active agent of manuka honey) in vitro activity against bacterial biofilms. Int Forum Allergy Rhinol. 2011;1:348-50.

[73] Ghizatullina NK. Effect of methyl glyoxal on infectivity and antigenicity of foot-and-mouth disease virus. Acta Virol. 1976;20:380-6.

[74] Tiffany BD, Wright JB, Moffett RB, Heinzelmspergren BD, Lincoin EH, White JH. Antiviral compound. Aliphalic Glyoxals, α-hydroxyaldehydes and related compounds. J Am Chem Soc. 1957;79:1682-7.

[75] DE BOCK CA, BRUG J, WALOP JN. Antiviral activity of glyoxals. Nature. 1957;179:706-7.

[76] Bardiya N, Bae JH. Influenza vaccines: recent advances in production technologies. Appl Microbiol Biotechnol. 2005;67:299-305.

[77] Kang SM, Song JM, Compans RW. Novel vaccines against influenza viruses. Virus Res. 2011;162:31-8.

[78] Caton AJ, Brownlee GG, Yewdell JW, Gerhard W. The antigenic structure of the influenza virus A/PR/8/34 hemagglutinin (H1 subtype). Cell. 1982;31:417-27.

[79] Plotkin JB, Dushoff J. Codon bias and frequency-dependent selection on the hemagglutinin epitopes of influenza A virus. Proc Natl Acad Sci U S A. 2003;100:7152-7.

[80] Berlanda Scorza F, Tsvetnitsky V, Donnelly JJ. Universal influenza vaccines: Shifting to better vaccines. Vaccine. 2016;34:2926-33.

[81] Ekiert DC, Bhabha G, Elsliger MA, Friesen RH, Jongeneelen M, Throsby M, et al. Antibody recognition of a highly conserved influenza virus epitope. Science. 2009;324:246-51.

[82] Throsby M, van den Brink E, Jongeneelen M, Poon LL, Alard P, Cornelissen L, et al. Heterosubtypic neutralizing monoclonal antibodies cross-protective against H5N1 and H1N1 recovered from human IgM+ memory B cells. PLoS One. 2008;3:e3942.

[83] Fiers W, De Filette M, El Bakkouri K, Schepens B, Roose K, Schotsaert M, et al. M2e-based universal influenza A vaccine. Vaccine. 2009;27:6280-3.

[84] Wiersma LC, Rimmelzwaan GF, de Vries RD. Developing Universal Influenza Vaccines: Hitting the Nail, Not Just on the Head. Vaccines (Basel). 2015;3:239-62.

[85] Du L, Zhou Y, Jiang S. Research and development of universal influenza vaccines. Microbes Infect. 2010;12:280-6.

[86] Govorkova EA, Fang HB, Tan M, Webster RG. Neuraminidase inhibitor-rimantadine combinations exert additive and synergistic anti-influenza virus effects in MDCK cells. Antimicrob Agents Chemother. 2004;48:4855-63.

[87] Freshney Rl. Culture of Animal Cells: A Manual of Basic Technique. Chapter 13 Subculture and cell lines2005.

[88] Reed LJ, Muench H. A simple method of estimating fifty percent endpoints. Am J Epidemiol. 1938;27:493-7.

[89] Ikematsu H, Kawai N, Kashiwagi S. In vitro neuraminidase inhibitory activities of four neuraminidase inhibitors against influenza viruses isolated in the 2010-2011 season in Japan. J Infect Chemother. 2012;18:529-33.

[90] Meetings of the WHO working group on surveillance of influenza antiviral susceptibility – Geneva, November 2011 and June 2012. Wkly Epidemiol Rec. 2012;87:369-74.

[91] Liu G, Xiong S, Xiang YF, Guo CW, Ge F, Yang CR, et al. Antiviral activity and possible mechanisms of action of pentagalloylglucose (PGG) against influenza A virus. Arch Virol. 2011;156:1359-69.

[92] Kim M, Kim SY, Lee HW, Shin JS, Kim P, Jung YS, et al. Inhibition of influenza virus internalization by (-)-epigallocatechin-3-gallate. Antiviral Res. 2013;100:460-72.

[93] Elton D, Simpson-Holley M, Archer K, Medcalf L, Hallam R, McCauley J, et al. Interaction of the influenza virus nucleoprotein with the cellular CRM1-mediated nuclear export pathway. J Virol. 2001;75:408-19.

[94] Serkedjieva J, Velcheva M. In vitro anti-influenza virus activity of the pavine alkaloid (-)-thalimonine isolated from Thalictrum simplex L. Antivir Chem Chemother. 2003;14:75-80.

[95] Watanabe K, Takatsuki H, Sonoda M, Tamura S, Murakami N, Kobayashi N. Anti-influenza viral effects of novel nuclear export inhibitors from Valerianae Radix and Alpinia galanga. Drug Discov Ther. 2011;5:26-31.

[96] Makau JN, Watanabe K, Kobayashi N. Anti-influenza activity of Alchemilla mollis extract: possible virucidal activity against influenza virus particles. Drug Discov Ther. 2013;7:189-95.

[97] Johnson VA. Combination therapy: more effective control of HIV type 1? AIDS Res Hum Retroviruses. 1994;10:907-12.

[98] Pirrone V, Thakkar N, Jacobson JM, Wigdahl B, Krebs FC. Combinatorial approaches to the prevention and treatment of HIV-1 infection. Antimicrob Agents Chemother. 2011;55:1831-42.

[99] Ferraris O, Lina B. Mutations of neuraminidase implicated in neuraminidase inhibitors resistance. J Clin Virol. 2008;41:13-9.

[100] Samson M, Abed Y, Desrochers FM, Hamilton S, Luttick A, Tucker SP, et al. Characterization of drug-resistant influenza A(H1N1) and A(H3N2) variants selected in vitro with laninamivir. Antimicrob Agents Chemother. 2014.

[101] Kakuta M, Kubo S, Tanaka M, Tobiume S, Tomozawa T, Yamashita M. Efficacy of a single intravenous administration of laninamivir (an active metabolite of laninamivir octanoate) in an influenza virus infection mouse model. Antiviral Res. 2013;100:190-5.

[102] McKimm-Breschkin JL, Barrett S. Neuraminidase mutations conferring resistance to laninamivir lead to faster drug binding and dissociation. Antiviral Res. 2015;114:62-6.

[103] Leang SK, Kwok S, Sullivan SG, Maurer-Stroh S, Kelso A, Barr IG, et al. Peramivir and laninamivir susceptibility of circulating influenza A and B viruses. Influenza Other Respir Viruses. 2014;8:135-9.

[104] Samson M, Pizzorno A, Abed Y, Boivin G. Influenza virus resistance to neuraminidase inhibitors. Antiviral Res. 2013;98:174-85.

[105] Burnham AJ, Baranovich T, Marathe BM, Armstrong J, Webster RG, Govorkova EA. Fitness costs for Influenza B viruses carrying neuraminidase inhibitor-resistant substitutions: underscoring the importance of E119A and H274Y. Antimicrob Agents Chemother. 2014;58:2718-30.

[106] Wang Q, Tian X, Chen X, Ma J. Structural basis for receptor specificity of influenza B virus hemagglutinin. Proc Natl Acad Sci U S A. 2007;104:16874-9.

[107] Colman PM. Influenza virus neuraminidase: structure, antibodies, and inhibitors. Protein Sci. 1994;3:1687-96.

[108] Colman PM, Hoyne PA, Lawrence MC. Sequence and structure alignment of paramyxovirus hemagglutinin-neuraminidase with influenza virus neuraminidase. J Virol. 1993;67:2972-80.

[109] Burnham AJ, Baranovich T, Govorkova EA. Neuraminidase inhibitors for influenza B virus infection: efficacy and resistance. Antiviral Res. 2013;100:520-34.

[110] Fujisaki S, Takashita E, Yokoyama M, Taniwaki T, Xu H, Kishida N, et al. A single E105K mutation far from the active site of influenza B virus neuraminidase contributes to reduced susceptibility to multiple neuraminidase-inhibitor drugs. Biochem Biophys Res Commun. 2012;429:51-6.

[111] Cheam AL, Barr IG, Hampson AW, Mosse J, Hurt AC. In vitro generation and characterisation of an influenza B variant with reduced sensitivity to neuraminidase inhibitors. Antiviral Res. 2004;63:177-81.

[112] Pavlovic-Djuranovic S, Kun JF, Schultz JE, Beitz E. Dihydroxyacetone and methylglyoxal as permeants of the Plasmodium aquaglyceroporin inhibit parasite proliferation. Biochim Biophys Acta. 2006;1758:1012-7.

[113] Charyasriwong S, Watanabe K, Rahmasari R, Matsunaga A, Haruyama T, Kobayashi N. In vitro evaluation of synergistic inhibitory effects of neuraminidase inhibitors and methylglyoxal against influenza virus infection. Arch Med Res. 2015;46:8-16.

[114] Julkunen I, Sareneva T, Pirhonen J, Ronni T, Melén K, Matikainen S. Molecular pathogenesis of influenza A virus infection and virus-induced regulation of cytokine gene expression. Cytokine Growth Factor Rev. 2001;12:171-80.

[115] Nimmerjahn F, Dudziak D, Dirmeier U, Hobom G, Riedel A, Schlee M, et al. Active NF-kappaB signalling is a prerequisite for influenza virus infection. J Gen Virol. 2004;85:2347-56.

[116] Santoro MG, Rossi A, Amici C. NF-kappaB and virus infection: who controls whom. EMBO J. 2003;22:2552-60.

[117] Pinto R, Herold S, Cakarova L, Hoegner K, Lohmeyer J, Planz O, et al. Inhibition of influenza virus-induced NF-kappaB and Raf/MEK/ERK activation can reduce both virus titers and cytokine expression simultaneously in vitro and in vivo. Antiviral Res. 2011;92:45-56.

[118] Pleschka S, Wolff T, Ehrhardt C, Hobom G, Planz O, Rapp UR, et al. Influenza virus propagation is impaired by inhibition of the Raf/MEK/ERK signalling cascade. Nat Cell Biol. 2001;3:301-5.

[119] Ludwig S, Wolff T, Ehrhardt C, Wurzer WJ, Reinhardt J, Planz O, et al. MEK inhibition impairs influenza B virus propagation without emergence of resistant variants. FEBS Lett. 2004;561:37-43.

[120] Mazur I, Wurzer WJ, Ehrhardt C, Pleschka S, Puthavathana P, Silberzahn T, et al. Acetylsalicylic acid (ASA) blocks influenza virus propagation via its NF-kappaB-inhibiting activity. Cell Microbiol. 2007;9:1683-94.

[121] Laga M, Cottyn A, Van Herreweghe F, Vanden Berghe W, Haegeman G, Van Oostveldt P, et al. Methylglyoxal suppresses TNF-alpha-induced NF-kappaB activation by inhibiting NF-kappaB DNA-binding. Biochem Pharmacol. 2007;74:579-89.

[122] Haidari M, Ali M, Ward Casscells S, Madjid M. Pomegranate (Punica granatum) purified polyphenol extract inhibits influenza virus and has a synergistic effect with oseltamivir. Phytomedicine. 2009;16:1127-36.

[123] Nguyen JT, Hoopes JD, Smee DF, Prichard MN, Driebe EM, Engelthaler DM, et al. Triple combination of oseltamivir, amantadine, and ribavirin displays synergistic activity against multiple influenza virus strains in vitro. Antimicrob Agents Chemother. 2009;53:4115-26.

[124] Shigeta S, Mori S, Watanabe J, Soeda S, Takahashi K, Yamase T. Synergistic anti-influenza virus A (H1N1) activities of PM-523 (polyoxometalate) and ribavirin in vitro and in vivo. Antimicrob Agents Chemother. 1997;41:1423-7.

[125] us.gsk.com: Medicine and products information (accessed 17 january 2014).

[126] Wakai C, Iwama M, Mizumoto K, Nagata K. Recognition of cap structure by influenza B virus RNA polymerase is less dependent on the methyl residue than recognition by influenza A virus polymerase. J Virol. 2011;85:7504-12.

ACKNOWLEDGEMENT

First and foremost, I would like to express my sincere gratitude to Professor Nobuyuki Kobayashi for accepting me in his laboratory and his patience, motivation, enthusiasm, and immense knowledge. His guidance helped me in all the time of research and writing of this thesis. I could not have imagined having a better advisor and mentor for my master study. This thesis would not have been possible without his indefatigable supervision and invaluable scientific insight.

Ever since I started in my lab it was Dr. Hiroaki Kawano who patiently taught and introduced me to all techniques that is necessary in molecular field and shared his knowledge with me. I am greatly indebted to him for shaping my nascent scientific career. I would also like to show my gratitude to Dr. Ken Watanabe for his worthy suggestions and help both before and after I came here.

Moreover, I would like to express my special gratitude to Dr. Haruyama takahiro who carefully introduced me to basic cell culture techniques and virology principles that I found them valuable to the test of time. Through discussions with him, I learned to appreciate the aspect of attention to detail (keenness), one that is mandatory to any discovery in science. I am greatly indebted to him for shaping my budding scientific career and giving me confidence.

Special recognition to the government pharmaceutical organization, GPO, Thailand, especially Dr. Witit Artavatkun, my previous managing director for awarding me a scholarship to pursue my postgraduate degree in Japan and for a first-hand exposure to Japanese culture.